

Towards vertex renormalization in 4d Spin Foams

by

Andrzej Banburski

A thesis
presented to the University of Waterloo
in fulfillment of the
thesis requirement for the degree of
Doctor of Philosophy
in
Physics

Waterloo, Ontario, Canada, 2017

© Andrzej Banburski 2017

Examining Committee Membership

The following served on the Examining Committee for this thesis. The decision of the Examining Committee is by majority vote.

External Examiner	Jesus Fernando Barbero Gonzalez Prof.
Supervisor	Lee Smolin Prof.
Co-supervisor	Laurent Freidel Prof.
Internal Member	Niayesh Afshordi Prof.
Committee Member	Bianca Dittrich Prof.
Internal-external Examiner	Eduardo Martin-Martinez Prof.

This thesis consists of material all of which I authored or co-authored: see Statement of Contributions included in the thesis. This is a true copy of the thesis, including any required final revisions, as accepted by my examiners.

I understand that my thesis may be made electronically available to the public.

Statement of Contributions

Sections 3.1, 3.2, 5.1, 5.2 together with Chapters 4 and 6 are in big parts based on work [1] in collaboration with Lin-Qing Chen and Jeff Hnybida, which was supervised by Laurent Freidel. The section 3.4 is based on work [2] in collaboration with Lin-Qing Chen.

The rest of the original results are based solely on my own work.

Abstract

A long-standing open problem in 4-dimensional Spin Foam models of Quantum Gravity has been the behavior of the amplitudes under coarse graining. In this thesis, we attempt to study this question by using the recent reformulation of Spin Foam amplitudes in terms of spinors. We define a new model by imposing the holomorphic simplicity constraints in an alternative way, which facilitates greatly simplified calculations. We show that the simplification does not come at the cost of loss of the correct semi-classical limit, as the model has the same asymptotic behavior as the usual approach. Using the power of the holomorphic integration techniques, and with the introduction of two new tools: the homogeneity map and the loop identity, for the first time we give the analytic expressions for the behavior of the Spin Foam amplitudes under 4-dimensional Pachner moves. We show that the coarse-graining 5–1 move generates non-geometrical couplings, but we find a natural truncation scheme that restricts the flow to the space of 4-simplices. Under this truncation scheme, the 3–3 Pachner move is only invariant for symmetric configurations, while the 4–2 and 5–1 moves are invariant up to an overall possibly divergent factor depending on boundary spins. The study of the divergences shows that there is a range of parameter space for which the 4–2 move is finite while the 5–1 move diverges, which distinguishes the model from the topological case. We then show that the amplitude after the 5–1 move cannot be written as a symmetric local product of renormalized edge propagators, but instead has to be written in terms of a vertex amplitude. The study of the additional nonlocal function of the boundary spins shows a transition, at which the spin dependence is very slow, suggesting the existence of an approximate notion of a vertex translation symmetry. We conclude with a proposal for an amplitude, where iterated 5–1 Pachner moves only renormalize this nonlocal function at a vertex, and in which all the divergences can be absorbed by a single coupling constant.

Acknowledgements

I would like to thank my supervisors, Lee Smolin and Laurent Freidel for the many inspiring discussions and giving me free rein to pursue my interests, while providing invaluable guidance. It has been a pleasure to be your student. I would also like to thank Jaron Lanier, my dear mentor in my explorations of the virtual world, for being so encouraging and inspirational.

I would like to also express my undying gratitude to my fiancée and collaborator, Lin-Qing Chen, with whom I have explored Quantum Gravity and who supported me in difficult situations. I am indebted also to my other collaborator, Jeff Hnybida, who has taught me most of what I know about coherent states in Spin Foams and Muay Thai. Big thanks go out also to my committee members: Bianca Dittrich, Niayesh Afshordi and Florian Girelli.

Finally, I want to also thank all the people who work so hard at the Perimeter Institute to make it such a welcoming place, particularly Debbie Guenther, Dan Lynch and Dawn Bombay.

This thesis was partially fueled by Monster Energy™.

To those who dream.

Table of Contents

List of Figures	xi
1 Introduction	1
1.1 Why Quantum Gravity?	1
1.2 Problem of renormalizability	3
1.3 Outline of the thesis	6
2 Loopy review	9
2.1 Loop Quantum Gravity	9
2.2 Discretized gravity and Ponzano-Regge model	16
2.3 Gravity and BF theory	18
2.4 Quantized BF theory	19
2.5 The Spin Foam program	22
2.6 The Holomorphic Representation of $SU(2)$	26
2.7 Holomorphic Simplicity Constraints	29
3 Two spinorial models	32
3.1 Imposing constraints	32
3.1.1 DL prescription	33
3.1.2 Constrained projector	34
3.2 The Homogeneity Map	38

3.3	Comparing the two models	40
3.4	Asymptotics	42
3.4.1	The dihedral angle	42
3.4.2	The asymptotics of DL model	43
3.4.3	The asymptotics of constrained propagator model	45
4	Lessons from 3d quantum gravity	49
4.1	Definition of Pachner Moves	49
4.2	Fixing the gauge	51
4.3	The Loop Identity	52
4.4	Alternative method	52
4.5	Invariance under Pachner moves and symmetry	54
5	Loop identity with constraints	57
5.1	Toy Loop	57
5.2	The Constrained Loop Identity	59
5.3	The Loop Identity for the DL model	62
5.4	Exact results in 2d	65
6	Evaluating 4d Pachner moves	68
6.1	Computing Pachner Moves with Simplicity Constraints	68
6.1.1	3–3 move	69
6.1.2	4–2 move	72
6.1.3	5–1 move	75
6.2	Necessity for truncation	80
6.3	Truncation of the loop identity	81
6.4	Counting the degree of divergence	85
6.5	Truncated Pachner moves	90

7	Towards vertex renormalization	92
7.1	Current state of Spin Foam renormalization	92
7.2	Non-locality with spinors	95
7.3	4-simplex amplitude in terms of spins	98
7.4	Renormalizing the 15j symbol	100
7.5	Proposal for a new amplitude	107
8	Summary & Concluding remarks	110
	Bibliography	114
	APPENDICES	124
A	Appendix	125
A.1	Gaussian Integration Techniques	125
A.2	Mapping $SU(2)$ to spinors	126
A.3	Group averaging the $SU(2)$ projector	127
A.4	Proof of Lemma (4.4.1)	128
A.5	The 4-simplex amplitude for the constrained propagator model	129
A.6	Explicit calculation of the Constrained Loop Identity	130
A.7	Mixing of spins in DL model	132
A.8	Arbitrary face weight in DL model	133
A.9	Justification for the nonlocality	133

List of Figures

2.1	Example spin network state	15
3.1	Graph for the 4-simplex amplitude in the DL model. The contractions inside correspond to two copies of BF 20j symbols, constrained on the boundary.	33
3.2	Left: behavior of $F_\rho(J)$ at fixed ρ as a function of spin J . Right: at fixed spin, $F_\rho(J)$ is rapidly increasing as $\rho \rightarrow 1$	35
3.3	The expression (3.10) is an excellent approximation to $F_\rho(J)$ even at small spins. Plotted at $\rho = \frac{1}{2}$	36
3.4	Left: for small spins (3.12) is a rather poor approximation. Right: as we increase spin however, we rapidly converge. Plotted at $\rho = \frac{1}{2}$	37
3.5	Graph for the amplitude of contraction of two 4-simplices. Propagators P_ρ^1 and P_ρ^2 belong to the same edge but two different 4-simplices. The spinors belonging on the same strand but belonging to different propagators are contracted according to the strand orientation. For example, spinors $w_i^1 = \tilde{z}_i^2$	38
3.6	DL projector. Red strands correspond to $SU(2)_L$, blue strands to $SU(2)_R$. Simplicity constraints are imposed on spinors $ z_i\rangle$, which are integrated over.	41
4.1	Two dimensional Pachner moves: a) 3–1 move, in which three triangles are merged into one by removing a vertex inside; b) 2–2 move, in which two triangles exchange the edge, along which they are glued.	50
4.2	Three dimensional Pachner moves: a) 3–2 move, in which three tetrahedra are changed into two tetrahedra by removing a common edge; b) 4–1 move, in which four tetrahedra are combined into one by removing a common vertex.	50
4.3	a) Cable diagram for the 3-2 move. The internal loop is colored. b) After gauge-fixing projectors 7 and 9 and performing loop identity on projector 8, the diagram reduces to gluing of two tetrahedral graphs.	55

4.4	a) Cable diagram for the 4–1 move. The 4 different loops are colored. b) After applying three loop identities we are left with a tetrahedral cable graph with an insertion of one loop.	56
5.1	Loop identity with for the constrained projector with two extra gauge fixed projectors	60
5.2	Loop identity for the DL propagator with two extra gauge fixed ones.	63
6.1	Triangulations for the 3–3 move.	69
6.2	Cable diagram for the 3–3 move $ABCdef \rightarrow abcDEF$	70
6.3	Zoomed in part of the cable diagram for the 3–3 move with some of the labels and contractions of spinors explicitly written down.	71
6.4	For 4-d BF theory, after integrating out the middle loops in the 3–3 move, the rest of the strands are combinatorially equivalent.	72
6.5	Triangulations for the 4–2 move.	73
6.6	Cable diagram for the 4–2 move with gauge fixing along BC, AC, CD	74
6.7	Performing the calculation we get a configuration of two 4-simplices with a nonlocal gluing.	75
6.8	Triangulations for the 5–1 Pachner move.	76
6.9	Cable diagram for the 5–1 move. The loops inside are colored.	77
6.10	Gauge-fixing 4 strands allows to apply loop identities 6 times, leaving the 4 colored loops.	78
6.11	Performing the calculation we get a 4-simplex with an insertion of a nonlocal operator.	79
6.12	Logarithmic plots for the coefficient N when $J = A = B = 100$ and face weight scaling is $\eta = 1$. The blue, red, yellow lines correspond to $J' = 0, 1, 2$ respectively.	82
6.13	Plots of the ratio between $N(J' = 0)$ and the sum of subleading coefficients $\sum_{J'=1}^{10} N(J')$ with $J = A = B = 100$ and face weight scaling $\eta = 1$	83
6.14	Logarithmic plots for the coefficient N when $J = 7, A = 6, B = 5$, and $J = 30, A = 17, B = 10$. The blue, red, yellow lines correspond to $J' = 0, 1, 2$ respectively.	84

6.15	Partial sum of $\sum_{J'=1}^k N$ for $J = A = B = 50$ and $\rho = 1$. The $J' = 0$ term is dominant with $N(J' = 0) \approx 7.1 \times 10^{31}$. The subdominant terms converge very rapidly.	84
6.16	Plots of the dependence of the ratio between $N(J' = 0)$ and the sum of subleading coefficients with face weight η when $J = 7, A = 6, B = 5$ and ρ is close to 1.	85
6.17	X_{4-2} has an obvious dependence on η on a logarithmic plot. The sum diverges a lot faster with increasing η	86
6.18	X_{4-2} gets suppressed with increasing ρ , with $\rho = 0$ being the limit of SU(2) BF divergence. The sum is even more suppressed with increasing ρ	87
6.19	For small values of η , X_{4-2} gets suppressed with increasing spin. There seems to be a transition in the behavior around $\eta = 5$	87
6.20	X_{5-1} is suppressed with increasing ρ for all values of η and spin. This plot is evaluated at $2j = 100$ and $\eta = 1$	89
6.21	For small values of η , X_{5-1} gets suppressed with increasing spin. There seems to be a transition in the behavior for $\eta = 3.2$, but the overall the summation is divergent for $\eta \geq 2.8$	89
7.1	Moving the τ s onto edges after the 4-1 Pachner move. The open circles denote gauge-fixed contributions to the nonlocal factor, while dots denote the un-gauge-fixed ones.	96
7.2	Spin labels in a $20j$ symbol, together with ordering of strands for each vertex.	101
7.3	Plot of $\frac{\mathcal{N}_{5-1}(j)}{\mathcal{N}_{5-1}(0)}$ at $\eta = 3$, where the 5-1 move has Λ^2 divergence.	106
7.4	Plot of $\frac{\mathcal{N}_{5-1}(j)}{\mathcal{N}_{5-1}(0)}$ for 3 different values of η around the transition point.	107
A.1	Cable diagram with all the labels for the constrained loop identity.	131

Chapter 1

Introduction

It appeared that way, Lawrence, but this raised the question of was mathematics really true or was it just a game played with symbols? In other words – are we discovering Truth, or just wanking?

Neal Stephenson
Cryptonomicon

1.1 Why Quantum Gravity?

The search for a theory of Quantum Gravity is the culmination of the quest that started when the first intelligent humans looked up at the night sky and wondered where it all came from and how do we fit in this Universe. Various proposals for answering these questions have been put forward throughout the ages, but it was only with the advent of natural philosophy that we started approaching the answers in a systematic manner. The search for the elusive Truth led eventually to the two great discoveries of early 20th century – Quantum Mechanics and General Theory of Relativity. We now believe that the answers about the origin of the Universe and its ultimate fate lie on the intersection of these two theories. Since we now know that we are really made from stardust, the search for Quantum Gravity is fundamentally about the Universe trying to understand itself.

As we are faced with the curious situation, where the theoretical considerations have run ahead of technological progress, the search for Quantum Gravity has become one of

finding a mathematically self-consistent theory. While the recent rise of gravitational wave astronomy and the studies of the cosmic microwave background give us hope for some experimental input, we are nonetheless data-starved. The lack of empirical data does not, thankfully, leave us grasping completely blindly, as we expect such a theory to satisfy several physical principles, such as general covariance, unitarity and renormalizability.

Naively, we have grounds to expect that combining the two theories would help us heal the problems in each of them at the same time. Consider for example that by Heisenberg uncertainty we need more energy to measure effects in small regions of space. However, when the Compton wavelength becomes smaller than the Schwarzschild radius for the given mass-energy, we would expect the formation of an event horizon by a gravitational collapse, thereby giving us a fundamental limit to observability, which in turn would define an effective “minimal length”. Such a minimal length would at the same time cure the divergences arising in Quantum Field Theories and remove the spacetime singularities of GR from the realm of observability.

Looking more closely however, we see that the framework of ordinary QFTs must break down when we add gravity to it, since a dynamical spacetime metric (which in general has no symmetries) does not provide the background necessary for the usual construction of the Fock space. One could still hope to work with QFTs on arbitrary spacetimes provided that the backreaction of matter on geometry was negligible. However, the central lesson of General Relativity is that backreaction of matter is non-negligible and is given by the Einstein equations

$$R_{\mu\nu} - \frac{1}{2}Rg_{\mu\nu} = 8\pi G_N T_{\mu\nu}. \quad (1.1)$$

Since the theory of matter is quantum mechanical, the stress-energy tensor would have to be considered as an operator in this equation. Trying to fix this by changing the right-hand side into the expectation value $\langle \hat{T}_{\mu\nu} \rangle$ however does not work, since quantum fluctuations would break the covariant conservation of the half-classical-half-quantum Einstein equations. We thus find ourselves in a need of a completely new framework for a theory of quantum matter interacting with quantum spacetime.

Historically, the two most active approaches to quantization of gravity have been String Theory [3, 4] and Loop Quantum Gravity [5, 6]. While String Theory has had truly impressive achievements in unifying gravity with other fundamental forces, they have come at the price of requiring supersymmetry and higher number of spacetime dimensions, compactification of which has resulted in the landscape problem. We thus do not know if String Theory can describe the Universe we live in. Additionally, the theory is so far only known in its perturbative expansion around fixed background spacetimes, and as such we cannot say that we handle on what the theory really is about. In this thesis, we will focus on the

covariant formulation of Loop Quantum Gravity, known as Spin Foams, which is based on a more minimalistic set of physical assumptions.

Spin foams are an attempt at a non-perturbative definition of a path integral for Quantum Gravity amplitudes [7, 8]. Similarly to the non-perturbative definition of gauge theories, Spin Foams are well defined thanks to a discrete regularization of spacetime. Unlike in lattice gauge theory however, in Quantum Gravity the discretization itself has to be dynamical, which leads to a completely new class of models. Formally, these models are usually constructed in analogy with a formulation of General Relativity, due to Plebanski [9], as a constrained topological BF theory. Each Spin Foam model is a proposal for a discretized version of these constraints, known as simplicity constraints. The most popular proposals are due to Engle-Pereira-Rovelli-Livine (EPRL) and Freidel-Krasnov (FK) [10, 11, 12, 13, 14, 15], though in this thesis we will work with the constraints written in spinorial language, which were introduced by Dupuis and Livine in [16, 85].

The dynamics of the discrete structure on which Spin Foams are defined is still not fully understood and is currently under intense investigation [17, 18, 19, 48]. Because of the symmetries of General Relativity, these dynamics are deeply connected with diffeomorphism invariance in the continuum theory, which can be studied through coarse-graining. Before we venture further, it will be instructive to discuss the problem of renormalizability in Quantum Gravity.

1.2 Problem of renormalizability

The difficulty in quantization of gravity comes from the fact that we cannot deal with it in the same way that has been successful in the construction of the Standard Model of particle physics. Let us sketch out the main reasons for this failure. In a covariant framework, we would like to define

$$\int \mathcal{D}g_{\mu\nu} e^{\frac{i}{16\pi G_N \hbar} \int d^4x \sqrt{-g} R(g)}, \quad (1.2)$$

but we are faced with the problems of both defining a measure over the space of metrics, and dealing with a non-linear action. The effective field theory approach suggests us to perform a perturbative expansion of the Einstein-Hilbert action. We can expand the metric as

$$g_{\mu\nu} = \eta_{\mu\nu} + \kappa h_{\mu\nu}, \quad (1.3)$$

where $\eta_{\mu\nu}$ is the Minkowski metric, $h_{\mu\nu}$ is a perturbation around this flat background and $\kappa = \sqrt{8\pi G_N}$. The first problem in this construction arises here, as perturbation theory

requires $h_{\mu\nu}$ to be infinitesimal, but for generic spacetimes in General Relativity it can be arbitrarily large¹. With this we get that the action becomes

$$S_{linearized} = \frac{1}{2} \int_{\mathcal{M}} d^4x \left(-h^{\mu\nu} \square h_{\mu\nu} + \frac{1}{2} h \square h + \mathcal{O}(h^3) \right). \quad (1.4)$$

This now has the form amenable to quantization, when we consider it as a theory of massless spin-2 fields (gravitons) gauged under linearized diffeomorphisms $h_{\mu\nu} \rightarrow h_{\mu\nu} + \partial_{(\mu} \epsilon_{\nu)}$. As in any interacting quantum field theory, the loop corrections lead to divergences, which we would like to renormalize. Where gravity differs from theories like QED is in the fact that it turns out to be perturbatively non-renormalizable at two-loop level. More precisely, while the divergences at one-loop can be hidden away in the coupling constants we already have, at two loops one produces a divergent term proportional to the cube of Weyl tensor [21, 22]. This divergence can be only removed by introduction of a counterterm with a new coupling constant. At higher loop orders we need more and more counterterms to cancel out the divergences, until we get an infinite number of coupling constants, which kills any predictivity the theory might have. This result can be seen also from naive power-counting arguments – G_N has a negative mass dimension, and so each next term in the perturbative series expansion is more relevant than the previous one, eventually making the original Einstein-Hilbert term irrelevant.

The splitting of the metric into a background and perturbation as in (1.3) fails also due to a much more fundamental reason. In the effective field theory described by the action (1.4), both the notion of what we consider spatial separation for commutation relations and the notion of causality are defined by the flat metric $\eta_{\mu\nu}$. The radiative graviton corrections in this theory do not modify these notions, which is just clearly wrong for a theory describing gravitational interactions.

One might now worry that this result spells doom for the whole program of quantizing gravity. Fortunately, there seem to be some holes in the argument. One way out is to introduce a UV-completion of the theory that changes the low-energy physics and determines the additional parameters. This is actually the path String Theory takes. There is also the possibility that there exists a non-trivial UV fixed point in the renormalization group flow of General Relativity, a scenario known as Asymptotic Safety [23]. In this light, the failure of perturbative approach above can be seen as an expansion around the wrong set of variables. The Asymptotic Safety program has had some very interesting results over the years [24, 25, 26, 27, 28], though a definitive proof of the existence of a fixed

¹Consider for example the very simple case of Schwarzschild black holes, which are noticeably quite different from the Minkowski metric

point with only few relevant couplings is still lacking. Alternatively, one might consider the perturbative split of the metric (1.3) a bad idea and develop non-perturbative methods for quantization leading to UV-finiteness, which is the path followed by Loop Quantum Gravity and Spin Foams.

One of the great achievements of the LQG program has been showing the existence of gaps in the spectra of the area and volume operators [29], which we discuss in Chapter 2. To see whether these indeed result in UV-finiteness, we would have to study the continuum limit of this discretized approach.

The natural path towards finding a continuum limit of a discrete theory involves studying coarse graining and applying renormalization methods. Note that already in flat space-time lattice QCD [30], this is non-trivial, as one needs to study the critical behavior of the model. In order to obtain a locally covariant continuum theory, it would seem that the usual global scale transformations might be not appropriate. Some early ideas [31, 32, 33] in Spin Foam models have instead focused on defining coarse graining via local scale transformations. A notion of refinement scale can be provided by embedding finer triangulations into coarser ones, while requiring so-called *cylindrical consistency* [17, 34, 35, 36, 37, 38]. Not much work has been done in this direction however, as the dynamics of Spin Foam models have not been understood beyond triangulations built out of more than few basic building blocks [18, 19]. Recently, a more global approach with the use of Tensor Network Renormalization scheme [39, 40, 41] has been used to numerically study dimensionally reduced analogue Spin Foam models - so-called spin nets [42, 43, 44, 45, 46, 47, 48, 49, 50]. Another approach under investigation is renormalization of Group Field Theories (GFT) [51, 52, 53, 54, 55, 56, 57, 58, 59, 60, 61, 62, 63, 64, 65, 66, 67], which generate Spin Foam amplitudes. However, the renormalizable GFTs studied so far have not been of relevance to 4d gravity. It thus still seems crucial to understand what are the dynamics of Spin Foams for configurations that can be iteratively coarse grained.

The most basic local coarse graining move on a simplicial decomposition of a manifold is a specific type of so-called Pachner moves [68]. Pachner moves are local changes of triangulation that allow to go from some triangulation of a manifold to any other triangulation in a finite number of steps. In 4 dimensions, there are three different Pachner moves: The 3-3 move, 4-2 move and 5-1 move (and their inverses). An $n-(2+d-n)$ Pachner move changes a triangulation composed out of n d-simplices to one with $(2+d-n)$ d-simplices. Only the $n-1$ Pachner moves are pure coarse graining moves. The action of classical 4d Regge Calculus [69] is known to be invariant under 5-1 and the 4-2 moves [70], but it has been a long standing open problem to make any statement about invariance under these moves for non-topological Spin Foam models. Only the naive degree of divergence of the 5-1 move has been estimated for the EPRL model [71]. This question is not even obvious

in linearized gravity, as the partition function of the quantum linearized Regge Calculus has recently been found to be not invariant, as it picks up a nonlocal measure factor [72].

1.3 Outline of the thesis

The main goal of the work in this thesis is to set up the groundwork necessary for the study of coarse graining in a 4-dimensional Spin Foam model with simplicity constraints and study the behavior of the amplitudes under the 5–1 Pachner move. While this might not sound as dramatic as what we claimed Quantum Gravity was really about in the opening sentences of this chapter, the answer to how the continuum limit behaves will distinguish whether Spin Foams probe the Truth², or are merely a mathematical game.

The thesis is then organized in the following way. We start with a review of the Spin Foam approach to quantum gravity in chapter 2. Before jumping into the covariant models, we begin with an overview of the canonical Loop Quantum Gravity. This discussion takes us from the classical General Relativity written in terms of tetrads to the Hamiltonian picture with Ashtekar variables. We show that the gauge-invariant kinematical Hilbert space is spanned by spin networks. After discussing the geometric observables and their discrete spectra, we sketch out the difficulties in solving the dynamics of the time evolution in the canonical approach. We then move onto the study of discretization of GR – the Regge Calculus, and present the first Spin Foam model in the form of Ponzano-Regge model [73]. Following this, we discuss the relation between gravity and the topological BF theory. This connection is relevant, because BF theory can be exactly quantized. 4-dimensional Spin Foam models are then shown to result from imposing so-called simplicity constraints onto BF amplitudes. After discussing the most popular Barrett-Crane [74] and EPRL-FK models, we move on to reviewing the holomorphic representation [75, 76], which simplifies the construction of SU(2) invariants [77, 78, 79, 80, 81, 82]. This allows us to write the partition function of BF theory in the holomorphic representation. We then review the holomorphic simplicity constraints [16, 83, 84].

In chapter 3 we show that these simplicity constraints can be imposed in two different ways. The usual way is to impose them on the boundary spin network function, resulting in the Dupuis-Livine model [16, 84], which is very similar to the EPRL-FK model. The alternative way is to impose the constraints onto a Spin(4) propagator. We then introduce

²Apologies to the readers deeply disturbed by the carefree use of this loaded term. Indeed, one would be hard-pressed to define the Truth in our reality, as any such assignment relies on using a system of axioms – truth is relative. Worse, by Gödel’s incompleteness theorems, some statements cannot be provably assigned a truth or false value. Moreover, is the Universe inherently mathematical?

an important mathematical trick in the form of the homogeneity map, which allows for simple calculation of amplitudes. Comparing the two approaches of imposing constraints, which we achieve by rewriting the Dupuis-Livine model also in terms of propagators, we find that at least superficially the two models look quite different. Surprisingly however, we find that the two models have the same semi-classical limit for one 4-simplex.

Next, in chapter 4 we review the calculation of Pachner moves in the Ponzano-Regge model for 3d Quantum Gravity. We start with defining the notion of Pachner moves. We then discuss the gauge fixing procedure for the internal rotational $SU(2)$ symmetry. Next, we derive a crucial identity (which we refer to as the *loop identity*, since it corresponds to integrating out a loop in a diagram) that allows for the calculation of Pachner moves. We finish the chapter with calculating the 3–2 and 4–1 Pachner moves and discussing the fate of diffeomorphism symmetry.

Chapter 5 finds us deriving the loop identities for the constrained models. We start with a toy case of a loop with a single constrained propagator, which exhibits behavior quite different from the topological case, with additional mixing of strands in graphs. We confirm this behavior for the case of a loop that appears in the evaluation of Pachner moves. Additionally, we evaluate the loop identity for the Dupuis-Livine model, showing that indeed the alternative imposition of simplicity constraints leads to greatly simplified calculations. We finish the chapter with making an observation that we can obtain interesting exact results in the case of 2-dimensional $SU(2)$ BF theory with arbitrary face weights and modifications of the propagators.

In chapter 6 we apply the results of the previous chapter to evaluation of the 4-dimensional Pachner moves for the constrained propagator model. We find that the model is not invariant under any of the moves, apart from some special symmetric cases of the 3–3 move. A discussion about the necessity for truncating renormalization flows ensues and we show that there is a natural truncation scheme of the loop identity, which makes the 4–2 and 5–1 moves invariant up to a possibly divergent factor depending on the boundary spins. We then go on to calculate and analyze the degrees of divergence of the 4–2 and 5–1 moves, and find that for a range of parameters, the latter can be divergent, while the former can be convergent. A suggestion for the renormalization of the propagators through the requirement of 5–1 invariance is presented at the end of the chapter.

Finally, in chapter 7 we discuss some earlier ideas about Spin Foam renormalization and then go on to show that the hope we expressed at the end of chapter 6 cannot be. This is because of the impossibility of rewriting the amplitude into the product of five local propagators. Rather than give up, we try rewriting the amplitude back into the spin basis. We find that here the result can be expressed neatly in terms of a renormalization of five

$15j$ symbols into a product of $15j$ symbol and a divergent nonlocal function of boundary spins. We study this nonlocal function numerically and find it has a transition point at which it is very slowly varying with the boundary spins, providing an approximated notion of translation invariance. We then propose a renormalized amplitude written as a product over propagators on edges and this nonlocal function at a vertex. We then argue that iteration of the 5–1 Pachner move provides a renormalization of this vertex amplitude and that only one coupling constant is necessary to absorb the divergences, thereby making the model renormalizable under the 5–1 move.

Chapter 2

Loopy review

Probably the last sound heard before the Universe folded up like a paper hat would be someone saying, 'What happens if I do this?'

Terry Pratchett
Interesting Times

In this chapter we will review the historical background and the concepts that led to the Spin Foam approach to quantizing gravity. We will start with canonical Loop Quantum Gravity entering the scene and teaching us some lessons about quantization. We then dive back in history to the early results in 3d quantum gravity. Next, we move onto a useful description of gravity in terms of constrained BF theory, which then segues into the brief overview of the Spin Foam approach. We finish the chapter with some recent developments in rewriting the Spin Foam amplitudes in terms of spinorial variables.

2.1 Loop Quantum Gravity

Loop Quantum Gravity is an attempt at canonical quantization of gravity that takes seriously the lessons of General Relativity about background independence. It can be thought of as a spiritual successor to the Wheeler-DeWitt equation [86] with a more rigorous mathematical structure that allows for a definition of a measure on the space of connections. The concepts we introduce in this section will be of use throughout the thesis.

Before we start the canonical analysis on gravity, let us rewrite the action of General Relativity by adding additional gauge freedom at each point on the manifold. Rather than working with the spacetime metric $g_{\mu\nu}$, we introduce the *tetrad* (or vierbein)

$$e^I(x) = e^I_\mu(x) dx^\mu, \quad (2.1)$$

which are formally spacetime one-forms on a $\text{SO}(3,1)$ (or $\text{SO}(4)$ in the Euclidean signature) principal bundle over the manifold \mathcal{M} . The $I \in \{0, \dots, 3\}$ internal index labels the local flat coordinates. The metric then can be obtained as

$$g_{\mu\nu}(x) = e^I_\mu(x) e^J_\nu(x) \eta_{IJ}, \quad (2.2)$$

where η_{IJ} is a flat internal metric. The redundancy we introduced can be seen in that the metric is left invariant under

$$e^I(x) \rightarrow \Lambda^I_J(x) e^J(x), \quad \Lambda^I_J(x) \in \text{SO}(3,1) \text{ (or } \text{SO}(4)\text{)}.$$

In these variables, the relevant connection is the *spin connection* ω , which is a $\mathfrak{so}(3,1)$ (or $\mathfrak{so}(4)$) valued spacetime one-form labeled by a pair of antisymmetric internal indices $\omega_\mu^{IJ} = -\omega_\mu^{JI}$. The curvature associated with the spin connection is defined by

$$F(\omega) \equiv d_\omega \omega = d\omega + \omega \wedge \omega, \quad (2.3)$$

where d_ω is the exterior covariant derivative. The Palatini action for General Relativity is then simply

$$S_{\text{Palatini}} = \frac{1}{8\pi G_N} \int_{\mathcal{M}} \text{Tr} [* (e \wedge e) \wedge F(\omega)]. \quad (2.4)$$

It is straightforward to show that this is equivalent to the usual Einstein-Hilbert action. The starting point for LQG lies in realizing that we can add an additional topological term to this action that does not change equations of motion. This so-called Holst term is proportional to $\epsilon_{\mu\nu\rho\sigma} R^{\mu\nu\rho\sigma}$, which vanishes on-shell due to the symmetries of the Riemann tensor. The Holst action in terms of tetrads is then

$$S_{\text{Holst}} = \frac{1}{16\pi G_N} \int_{\mathcal{M}} \text{Tr} \left[\left(*e \wedge e + \frac{1}{\gamma} e \wedge e \right) \wedge F(\omega) \right], \quad (2.5)$$

where we introduced the so-called *Barbero-Immirzi parameter* γ in front of the Holst term. The introduction of this additional term turns out to give a very nice set of canonical variables that bring GR closer to gauge theories.

The canonical decomposition of General Relativity rests on the ability to define Cauchy evolution, which requires the spacetime manifold to be globally hyperbolic¹, i.e. $\mathcal{M} = \Sigma \times \mathbb{R}$ for some fixed 3d compact manifold Σ . Introducing the lapse and shift vector (N, N^a) and defining the unit vector n^μ normal to Σ , we can perform the equivalent of the ADM decomposition for the tetrads with

$$e_0^I = Nn^I + N^a e_a^I, \quad g_{ab} = e_a^i e_b^j \delta_{ij}, \quad (2.6)$$

where $a, b = 1, 2, 3$ are spatial indices and i, j the corresponding internal indices, and g_{ab} is a 3-dimensional metric. The triad e_a^i now comes with local $\text{SO}(3)$ symmetry, which can be promoted to the double cover $\text{SU}(2)$ (since they have the same Lie algebra). Working in the time gauge $e_\mu^I n^\mu = \delta_0^I$, we can define the *densitized triad*

$$E_i^a = \det(e) e_i^a = \frac{1}{2} \epsilon_{ijk} \epsilon^{abc} e_b^j e_c^k. \quad (2.7)$$

We can also define the *Ashtekar-Barbero connection* as

$$A_a^i = \gamma \omega_a^{0i} + \frac{1}{2} \epsilon_{ijk} \omega_a^{jk}. \quad (2.8)$$

Together, these are known as the *Ashtekar variables*. They satisfy the rather simple Poisson brackets

$$\{E_i^a(x), A_b^j(y)\} = 8\pi G_N \gamma \delta_b^a \delta_i^j \delta(x, y). \quad (2.9)$$

In terms of these new variables, the action (2.5) becomes the totally constrained expression

$$S = \frac{1}{16\pi G_N \gamma} \int dt \int_\Sigma d^3x \left[\dot{A}_a^i E_i^a - A_0^i D_a E_i^a - N^a H_a - NH \right], \quad (2.10)$$

where the constraints are more explicitly given by

$$\begin{aligned} G_i &\equiv D_a E_i^a \\ H_a &= \frac{1}{\gamma} F_{ab}^j E_j^b \\ H &= \frac{\epsilon_k^{ij} E_i^a E_j^b}{\sqrt{\det E}} \left[F_{ab}^k - (1 \pm \gamma^2) \epsilon_{lm}^k K_a^l K_b^m \right] \end{aligned} \quad (2.11)$$

¹This means that we have to assume both causality and no topology change at the very beginning. This means that from the onset we preclude the existence of time travel and wormholes [87]. Interestingly, this is not a necessary assumption for path integral quantization, so we can see already here that covariant and canonical quantizations of GR are not necessarily equivalent.

where K_a^i is the extrinsic curvature, D_a is the covariant derivative with respect to A_a^i and the \pm sign depends on the signature: $+$ for Lorentzian and $-$ for Euclidean. We call G_i the Gauss constraint, H_a the spatial diffeomorphism constraint and H the scalar Hamiltonian constraint, which generates both the temporal diffeos and time evolution. Importantly, these constraints satisfy a closed algebra. The non-triviality in quantization of this theory can be seen in the difficulty of obtaining an anomaly-free closed constraint algebra.

Before we go on to discuss the quantization, it is necessary to consider the smearing of the canonical variables. The densitized triad is actually a 2-form, so it is naturally expressed smeared on a surface:

$$E_i(S) \equiv \int_S d^2\sigma n_a E_i^a, \quad (2.12)$$

where n_a is the normal to the surface S . The Ashtekar-Barbero connection A is still a 1-form, so it is naturally smeared over a path L . We will work with the holonomies defined as

$$h_L = \mathcal{P} \exp \left(\int_L A \right), \quad (2.13)$$

where \mathcal{P} is the path-ordering.

In a standard quantum theory, we would now promote both A and E to operators, use the background metric to define the measure on the space of connections A and impose the constraints according to the Dirac program of quantization of constrained systems, starting with $G_i\psi[A] = 0$. However, in General Relativity the metric is dynamical, so it is not so simple. One way would be to split the metric into a flat background and a dynamical part, which is the starting step in traditional perturbative approach. The other option, which LQG follows is to find a definition of measure on the space of connections. The key to this definition is the concept of *cylindrical functionals*, which depend on holonomies of A .

Consider a graph Γ , whose links $e \subset \Sigma$. A cylindrical functional of the Ashtekar-Barbero connection for a graph Γ with L links is the couple (Γ, f) , where f is a smooth function $f : \text{SU}(2)^L \rightarrow \mathbb{C}$, and is defined as

$$\psi_{(\Gamma, f)} = f(h_{e_1}[A], \dots, h_{e_L}) \in \text{Cyl}_\Gamma. \quad (2.14)$$

The reason for using these functionals to define the Hilbert space is that while a measure over the connection A is difficult to obtain, the holonomies are just $\text{SU}(2)$ group elements, and integration over $\text{SU}(2)$ is well-defined with the Haar measure. Cyl_Γ can be easily

turned into a Hilbert space \mathcal{H}_Γ with the inner product

$$\langle \psi_{(\Gamma, f)} | \psi_{(\Gamma, f')} \rangle = \int_{\text{SU}(2)^L} \prod_{e=1}^L dh_e \overline{f(h_{e_1}[A], \dots, h_{e_L})} f'(h_{e_1}[A], \dots, h_{e_L}). \quad (2.15)$$

The Hilbert space of all cylindrical functionals over all graphs is then defined simply as

$$\mathcal{H}_{kin} = \bigoplus_{\Gamma \subset \Sigma} \mathcal{H}_\Gamma. \quad (2.16)$$

One now could worry that we have found some Hilbert space, but that it has nothing to do with the one we were interested in the first place. However, a classic result of Ashtekar and Lewandowski [88] shows that the Hilbert space over connections is actually

$$L_2[A, d\mu_{AL}] = \mathcal{H}_{kin}, \quad (2.17)$$

where $d\mu_{AL}$ is the *Ashtekar-Lewandowski measure* defined by Eq. (2.15). Now that we have the Hilbert space, it is useful to find an orthogonal basis of states for it. Since we work with functions of SU(2) group elements, we will use the Peter-Weyl theorem, which expresses functions over group elements in terms of unitary irreducible representations:

$$f(g) = \sum_{j \in \mathbb{Z}/2} \sum_{m, n = -j}^j f_{mn}^j D_{mn}^{(j)}(g), \quad (2.18)$$

where $D_{mn}^{(j)}(g)$ are the representation matrices known as *Wigner-D functions*. The basis elements are then simply products of $D_{mn}^{(j)}(h_e)$ for each edge. The quantum states associated with this basis are spin states $|j; m, n\rangle$, which we can define by

$$D_{mn}^{(j)}(g) = \langle g | j; m, n \rangle, \quad (2.19)$$

where $|g\rangle$ is the group basis satisfying $\hat{f}(g)|g\rangle = f(g)|g\rangle$.

We can now proceed with seeing how the constraints (2.11) act to reduce this Hilbert space. Traditionally, the LQG program starts with imposition of the Gauss constraint $G_i \psi[A] = 0$. This restricts us to SU(2) gauge invariant states within \mathcal{H}_{kin} . To understand what kind of states these are, let us see what the action is on a typical link. Since gauge transformations take $h_e \rightarrow g_{s(e)} h_e g_{t(e)}^{-1}$, where $s(e)$ is the source node of edge e and $t(e)$ the target node, the same is true for the Wigner-D functions, due to linearity of group

representations. We can achieve this behavior by *group averaging* the elements of \mathcal{H}_{kin} at each of their N nodes in the following way:

$$f_{inv}(h_{e_1}, \dots, h_{e_L}) = \int_{\text{SU}(2)^N} \prod_{n=1}^N dg_n f\left(g_{s(e_1)} h_{e_1} g_{t(e_1)}^{-1}, \dots, g_{s(e_L)} h_{e_L} g_{t(e_L)}^{-1}\right). \quad (2.20)$$

Working in our orthogonal basis, we can implement this group averaging for arbitrary states by inserting a *Haar projector* P at each node, where

$$P = \int dg \prod_{e \in n} D^{(j_e)}(g). \quad (2.21)$$

Recall from the definition of representations that the product of $D^{(j)}$ lies in the following space

$$\prod_e D^{(j_e)}(h_e) \in \bigotimes_e V^{(j_e)}, \quad (2.22)$$

which in general is reducible, $\bigotimes_e V^{(j_e)} = \bigoplus_i V^{(j_i)}$. The Haar projector is then the map to the gauge invariant singlet space $P^{j_1, \dots, j_d} : D^{(j_1)} \otimes \dots \otimes D^{(j_d)} \rightarrow \text{Inv}_{\text{SU}(2)}[D^{(j_1)} \otimes \dots \otimes D^{(j_d)}]$. We can express this projector in terms of the orthogonal basis of the invariant subspace. The elements of this basis are the $\text{SU}(2)$ invariant tensors known as *intertwiners* ι_i :

$$P = \sum_{i=1}^{\dim \mathcal{H}_n} \iota_i \iota_i^*, \quad (2.23)$$

where \mathcal{H}_n is the Hilbert space of n -valent intertwiners:

$$\mathcal{H}_n = \bigoplus_{j_i} \mathcal{H}_{j_1, \dots, j_n} \equiv \bigoplus_{j_i} \text{Inv}_{\text{SU}(2)} [V^{j_1} \otimes \dots \otimes V^{j_n}]. \quad (2.24)$$

To get some feeling for these intertwiners, let us see the simplest case of 3-valent nodes. In this case the intertwiner space is 1-dimensional, and the unique 3-valent intertwiner is given by the so-called *Wigner 3j symbol* (which is related to the Clebsch-Gordan coefficients for addition of angular momentum):

$$\iota_{3\text{-valent}} = \begin{pmatrix} j_1 & j_2 & j_3 \\ m_1 & m_2 & m_3 \end{pmatrix} \equiv \frac{(-1)^{j_1 - j_2 - m_3}}{\sqrt{2j_3 + 1}} \langle j_1 m_1; j_2 m_2 | j_3 (-m_3) \rangle. \quad (2.25)$$

In general, the space of intertwiners is higher-dimensional, as we will see later in the thesis.

The gauge invariant states in \mathcal{H}_{kin} on a graph Γ can be obtained from contractions of Wigner-D functions with intertwiners. These states are known as *spin networks* and are given by

$$\psi_{(\Gamma, j_e, t_n)}[h_e] = \otimes_e D^{(j_e)}(h_e) \otimes_n t_n. \quad (2.26)$$

See Fig. 2.1 for an example of a spin network state.

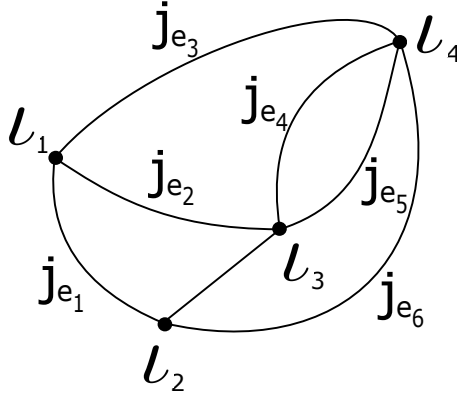


Figure 2.1: Example spin network state

Before we discuss the remaining two constraints, it is useful to note that at this point we can say something about the geometric observables of the theory. For example, classically we would define the area of a region by

$$A(S) = \int_S d^2\sigma \sqrt{E_i^a E^{bi} n_a n_b}, \quad (2.27)$$

so we can obtain the quantum operator just by putting using the quantum operators $\hat{E}(S)$. The action of $\hat{E}_i(S)\hat{E}^i(S)$ is proportional to the Casimir of $SU(2)$, so we have

$$\hat{A}(S)\psi_{(\Gamma, j_e, t_n)} = \sum_{p \in S \cup \Gamma} \gamma l_p^2 \sqrt{j_p(j_p + 1)} \psi_{(\Gamma, j_e, t_n)}, \quad (2.28)$$

where p are punctures of the graph Γ through the surface S and $l_p = \sqrt{\hbar G_N}$ is the Planck length. This expression gives us one of the big results of LGQ, namely that the spectrum of the area operator is discrete and has a gap. Similarly, the spatial volume operator can be found to also have a discrete spectrum with a finite volume gap, see [29].

The next step in the quantization lies in imposing the spatial diffeomorphism constraint. For details of this procedure, see [5]. Here, we just quote the result, which is that the states which remain after imposing $\hat{H}^a\psi[A]$ are spin networks on equivalence classes of graphs under diffeos, namely *knots*. Hence, the spatially diffeomorphism invariant states are knotted spin networks.

The difficulties in the canonical LQG program arise when dealing with the last scalar Hamiltonian constraint, i.e. with the dynamics of the theory. Technically, the two main difficulties lie in the terms $E_i^a E_j^b F_{ab}^k$ and $E_i^a E_j^b K_a^l K_b^m$, which have ordering ambiguities, and more importantly the $\frac{1}{\sqrt{\det E}}$ term. A solution to this was proposed by Thiemann [89], who showed that classically these terms can be rewritten as specific Poisson brackets, for example

$$\frac{\epsilon^{ijk} E_i^a E_j^b}{\sqrt{\det E}} = \frac{4}{\gamma} \epsilon^{abc} \{A_c^k, V\}, \quad (2.29)$$

where V is the volume of Σ . Using the expressions for the volume operator and expressing the connection in terms of holonomies allows to define the \hat{H} .

The problem with this Thiemann prescription is that we arrive at a Hamiltonian that acts in an ultra-local way only at the nodes of the spin networks and that the resulting constraint algebra vanishes too strongly, i.e. some commutators are explicitly zero, rather than proportional to the other constraints.

In [90] it has been shown that the Thiemann trick above might be anomalous under quantization, which might underlie some of these issues. The problems with the dynamics of the canonical theory have spurred increased interest in studying the covariant quantization of LQG – the Spin Foams, which we will now turn to. Before we go on however, it is noteworthy that work on the Hamiltonian constraint continues, with some interesting recent developments. For example, in [91] an alternative path was considered, in which the Hamiltonian constraint was imposed on a space of only partially diffeomorphism invariant states, which is preserved under the action of the constraint.

For a thorough review of LQG, see [5].

2.2 Discretized gravity and Ponzano-Regge model

Here we will briefly review the first Spin Foam model, but before then it is instructive to discuss the discretization of General Relativity, which is known as Regge Calculus [69]. In Regge Calculus the spacetime differential manifold is approximated by a piecewise flat

manifold. Besides having use in the topic of this thesis, quantum gravity, it is also often used in numerical relativity.

The building blocks of the piecewise flat manifolds are simplices: points, lines, triangles, tetrahedra, 4-simplices and so on. The collection of these blocks defines a simplicial complex. Let us start with the case of discretizing 3-dimensional General Relativity, which is more intuitive. Here, the main building blocks are tetrahedra and curvature can be expressed in terms of deficit angles associated with edges in the triangulation around which different tetrahedra meet. The Regge action in 3 dimensions is then given by

$$S_{\text{Regge}}^{(3d)} = \frac{1}{8\pi G_N} \sum_e l_e \theta_e, \quad (2.30)$$

where l_e is the length of the edge e in the triangulation and θ_e is the deficit angle associated with it. Varying this action with respect to edge lengths gives us the equation of motion

$$\frac{\delta}{\delta l_i} \sum_e l_e \theta_e \equiv \sum_e \delta_{ie} \theta_e = 0 \quad \Rightarrow \quad \theta_e = 0, \quad (2.31)$$

which implies that the only solutions are flat manifolds. Indeed, this is what 3-dimensional Einstein equations give as well.

The generalization to 4-dimensions is straightforward, with the curvature being given by the deficit angles associated with triangles around which 4-simplices are glued. The action is simply given by

$$S_{\text{Regge}}^{(4d)} = \frac{1}{8\pi G_N} \sum_i A_i \Theta_i, \quad (2.32)$$

where A_i is the area of the i -th triangle and Θ_i the associated deficit angle. In this action, the equations of motion with respect to edge lengths are no longer trivial.

We are now ready to discuss the first Spin Foam model, which arose when Ponzano and Regge [73] studied the asymptotics of the 6j symbol

$$\left\{ \begin{array}{ccc} j_1 & j_2 & j_3 \\ j_4 & j_5 & j_6 \end{array} \right\} = \sum_{m_1, \dots, m_6} (-1)^{\sum_i (j_i - m_i)} \begin{pmatrix} j_1 & j_2 & j_3 \\ m_1 & m_2 & -m_3 \end{pmatrix} \begin{pmatrix} j_1 & j_5 & j_6 \\ -m_1 & m_5 & -m_6 \end{pmatrix} \times \\ \times \begin{pmatrix} j_4 & j_5 & j_3 \\ m_4 & -m_5 & m_3 \end{pmatrix} \begin{pmatrix} j_4 & j_2 & j_6 \\ -m_4 & -m_2 & -m_6 \end{pmatrix}. \quad (2.33)$$

This object was originally defined for the description of recoupling three angular momenta in quantum mechanics. What Ponzano and Regge conjectured² was that if you consider

²Which was later proved in [92]

the limit where all the spins are scaled uniformly as Λj_e with $\Lambda \rightarrow \infty$, the $6j$ symbol asymptotes to

$$\{6j\} \sim \frac{\Lambda^{-3/2}}{\sqrt{12\pi V}} \cos \left(\Lambda \sum_e (j_e + 1) \frac{\theta_e}{2} + \frac{\pi}{4} \right). \quad (2.34)$$

Defining $l_e = j_e + \frac{1}{2}$ and interpreting l_e as edge lengths and θ_e as the dihedral angles between triangles sharing edge e , this gives us that the $6j$ symbol behaves as the cosine of the Regge action of 3d gravity. We can think of this way because the $3j$ symbols do define a closed triangle due to $SU(2)$ invariance. The $6j$ symbol hence corresponds to the quantum geometry of a tetrahedron.

This result allows to write down the partition function for the Ponzano-Regge model. With additional weights on the edges of the triangulated manifold, we get

$$Z_{\text{Ponzano-Regge}} = \sum_{j_e} \prod_{\text{edges } e} (-1)^{2j_e} (2j_e + 1) \prod_{\text{triangles } t} (-1)^{\sum_{e \cap t} j_e} \prod_{\text{tetrahedra } T} \{6j_e\}_T, \quad (2.35)$$

which actually gives us the full partition function for discrete 3d quantum gravity without a cosmological constant. Since 3d gravity is actually a topological theory, the correlation functions and observables in the continuum theory are the same as in the discretized case.

The generalization to the case with a cosmological constant is known as the Turaev-Viro model [93] and is achieved by using the quantum group $SU(2)_q$, rather than $SU(2)$.

2.3 Gravity and BF theory

Before we go onto the construction of more modern Spin Foam models, it is imperative that we review the deep connection between General Relativity and the topological BF theory.

Similarly as in the case of the Plebanski action, we will consider BF theory defined on a principal G -bundle over a d -dimensional manifold \mathcal{M} , with a \mathfrak{g} -valued connection ω . The F in BF theory stands for the curvature 2-form $F(\omega) = d\omega + \omega \wedge \omega$, which is the same as in the case of gravity. The B stands for an additional \mathfrak{g} -valued $d - 2$ form, which acts as a Lagrange multiplier imposing flatness. The action of BF theory is then simply

$$S_{BF} = \frac{1}{2\kappa^2} \int_{\mathcal{M}} \text{Tr} [B \wedge F(\omega)], \quad (2.36)$$

where $\kappa^2 = 8\pi G_N$. As implied above, the BF equations of motion are trivial³:

$$F(\omega) = 0, \quad d_\omega B = 0. \quad (2.37)$$

We say that BF theory is topological (i.e. has no local degrees of freedom), because the action is invariant under the gauge symmetry

$$B \rightarrow B + d\phi, \quad (2.38)$$

where ϕ is a \mathfrak{g} -valued $d-3$ form. This, together with the equation of motion, implies that all solutions of B are locally gauge equivalent.

It is important to note that in 3 dimensions, the BF theory is equivalent to 3-dimensional General Relativity, as the B field is a one-form – exactly the same as a triad. In the 4-dimensional case, we can see that restricting $B = *e \wedge e$ would reduce BF theory to gravity again. This restriction is known as *simplicity constraint* and can be achieved by adding an additional term to the action:

$$S = \frac{1}{2\kappa^2} \int_{\mathcal{M}} [B^{IJ} \wedge F_{IJ}(\omega) + \lambda_{IJKL} B^{IJ} \wedge B^{KL}], \quad (2.39)$$

where λ_{IJKL} is a Lagrange multiplier symmetric under the exchange of the (IJ) and (KL) pairs of indices that also satisfies $\epsilon^{IJKL} \lambda_{IJKL} = 0$. The additional equation of motion for this multiplier gives us that

$$B = \pm *e \wedge e, \quad \text{or} \quad B = \pm e \wedge e \quad (2.40)$$

Using both of these sectors with a proportionality constant γ , we recover the Holst action (2.5).

2.4 Quantized BF theory

The reason for discussing BF theory above is that the theory can be quantized exactly due to its topological nature. The partition function for quantum BF theory is formally

$$Z_{BF} = \int \mathcal{D}B \mathcal{D}\omega \, e^{iS_{BF}} = \int \mathcal{D}\omega \, \delta(F(\omega)). \quad (2.41)$$

³The equation for B field can be obtained by integrating by parts and using covariance, which implies that $\int \omega \wedge dB = \int \omega \wedge d_\omega B$.

To make this expression rigorous, we will introduce a discretization. However, since BF theory is topological, the discrete theory is equivalent to the continuum theory as far as any observables are concerned. Here we will restrict our attention to the case of BF theory for the group $SU(2)$, for reasons we will elaborate on later.

We start by discretizing the d -dimensional manifold \mathcal{M} into a simplicial complex Δ . Let Δ^* then be its dual 2-complex: each d -simplex in Δ corresponds to a vertex v , each $(d-1)$ -simplex to an edge e and each $(d-2)$ -simplex to a face f . With these established, we now need to discretize the curvature $F(\omega)$. Recall from Eq. (2.13) that an $SU(2)$ element can be considered a holonomy (or parallel transport) of the connection along a path (which can be made out of edges). Since to leading order a holonomy around a closed loop is equal to identity plus curvature, we have that the partition function of $SU(2)$ BF theory is defined in terms of the edges e and faces f of Δ^* by

$$Z_{BF}(\mathcal{M}) = \int \prod_{e \in \Delta^*} dg_e \prod_{f \in \Delta^*} \delta \left(\prod_{e \in f} \vec{g}_e \right). \quad (2.42)$$

The imposition of $\prod_{e \in f} \vec{g}_e = \mathbb{1}$ here is equivalent to the requirement that $F(\omega) = 0$. Note that some choices of the 2-complex can lead to redundant δ functions. This however turns out to be related to diffeomorphism invariance, as we will discuss in Chapter 4.

The δ functions for each face can be expanded in representations j_f using the Peter-Weyl theorem as

$$\delta(g) = \sum_{j_f} (2j_f + 1) \chi^{j_f}(g), \quad (2.43)$$

where $\chi^{j_f}(g) = \text{Tr}_{j_f}(g)$ is the character of the representation j_f . If we insert the resolution of identity on the representation space $V^{j_{f_1}} \otimes \dots \otimes V^{j_{f_d}}$ between each group element in the trace, we can write

$$Z_{BF}(\mathcal{M}) = \sum_{j_f} \prod_{f \in \Delta^*} (2j_f + 1) \prod_{e \in \Delta^*} P^{j_{f_1}, \dots, j_{f_d}}, \quad (2.44)$$

where $P^{j_{f_1}, \dots, j_{f_d}}$ is the Haar projector onto the $SU(2)$ invariant subspace of $V^{j_{f_1}} \otimes \dots \otimes V^{j_{f_d}}$ we have introduced in Eq. (2.21). For more details, see for example [8].

Now that we have written down the full partition function for BF theory, it is useful to introduce the cable diagram graphical notation, which is especially handy for the computations of Spin Foam partition functions (a good review of these techniques can be found in [32]). Here it is used to represent the structure of partition function on the dual

2-complex Δ^* . Cable diagrams are basically composed of strands passing through boxes: a strand denotes a group representation living on the edge e of Δ^* , and a box denotes the group averaging of a set of representations in the Haar projector.

$$D^{(j)} = \text{---} j \text{---} \quad \text{and} \quad P^{j_1, \dots, j_4} = \begin{array}{c} \begin{array}{|c|} \hline j_1 \\ \hline j_2 \\ \hline j_3 \\ \hline j_4 \\ \hline \end{array} \end{array} \quad (2.45)$$

Faces f in the dual 2-complex Δ^* correspond to closed loops of strands in this notation. A strand loop without any boxes in that case should correspond to a divergent factor of $\delta(\mathbb{1}) = \sum_{j_f} (2j_f + 1)^2$.

The fact that the Haar projector P^{j_1, \dots, j_4} can be expressed as a sum over intertwiners, as we have shown in Eq. (2.23), can be graphically represented as:

$$P^{j_1, \dots, j_4} = \sum_{\iota} \begin{array}{c} j_1 \\ j_2 \\ j_3 \\ j_4 \end{array} \rightarrow \iota \quad \iota \rightarrow \begin{array}{c} j_1 \\ j_2 \\ j_3 \\ j_4 \end{array} \quad (2.46)$$

where ι labels a basis of normalized intertwiners. We see that the Haar projector factorizes on the edges, while the intertwiners contract at the vertices of Δ^* . This allows expressing the partition function in terms of so called vertex amplitudes. For example, in the 3-dimensional BF theory, the partition function can be written as

$$Z_{BF}^{(3d)}(\mathcal{M}) = \sum_{j_f} \prod_{f \in \Delta^*} (2j_f + 1) \prod_{v \in \Delta^*} \begin{array}{c} j_{e_1} \\ j_{e_2} \\ j_{e_3} \\ j_{e_4} \\ j_{e_5} \\ j_{e_6} \end{array} \quad (2.47)$$

This way of writing the 3d BF theory immediately gives us the graphical representation Ponzano-Regge model, which we introduced in Eq. (2.35), where the tetrahedral vertex is just the 6j symbol. In the case of 4-dimensional BF theory, the vertex amplitudes are given by a suitable generalization of the 6j symbol – the 15j symbol labelled by 10 spins and 5 intertwiner labels, which can also be parametrized by spins. We will encounter these in the next section, where we will look at Spin Foam models for 4d gravity.

2.5 The Spin Foam program

We will now review the basics of the Spin Foam approach, including some early attempts and more recent work. The general idea behind Spin Foam models is to first quantize BF theory and only then impose simplicity constraints at the quantum level. The choice of the underlying group gives us the signature – $\mathrm{SL}(2, \mathbb{C})$ leads to the Lorentzian theory (since this is the double cover of $\mathrm{SO}(3,1)$), while $\mathrm{Spin}(4)=\mathrm{SU}(2)\times\mathrm{SU}(2)$ gives the Riemannian model. In most of this thesis we will work in the Riemannian case, but we will make several comments about the Lorentzian signature.

Because the $\mathrm{Spin}(4)$ group representations factorize into a product of two $\mathrm{SU}(2)$ representations, the $\mathrm{Spin}(4)$ BF partition function is a simple product of two $\mathrm{SU}(2)$ partition functions. We will label the two groups as $\mathrm{SU}(2)_L$ and $\mathrm{SU}(2)_R$ to distinguish them⁴.

Before we go on to discuss any specific model, it is worth noting that we can abstractly write an arbitrary Spin Foam model as a product over vertex, edge and face amplitudes:

$$Z_{\mathrm{Spin\ Foam}} = \sum_{j_f} \sum_{\iota} \prod_{f \in \Delta^*} \mathcal{A}_f(j_f) \prod_{e \in \Delta^*} \mathcal{A}_e(j_f, \iota_e) \prod_{v \in \Delta^*} \mathcal{A}_v(j_f, \iota_e). \quad (2.48)$$

The edge weight is usually taken to be trivial, the face weight is usually chosen to be proportional to $\dim_j = (2j + 1)$, and the vertex amplitude in 4d is usually some version of a $15j$ symbol.

One of the early popular attempts at Spin Foam quantization is known as the *Barrett-Crane model*. We will shortly review the construction and why it fails as a model of 4d quantum gravity. We start with noticing that the quadratic simplicity constraints in Eq. (2.39) imply that

$$\epsilon_{IJKL} B^{IJ} \wedge B^{KL} = 0. \quad (2.49)$$

Since the B field is an element of the Lie algebra of $\mathrm{Spin}(4)$, it can be split into $B = B_L + B_R$. The representation theory of the subspace of this Lie algebra that satisfies Eq. (2.49) is given by representations with vanishing Casimir. Since representations of $\mathrm{Spin}(4)$ are labeled by a pair of spins (j_L, j_R) , this translates into the equation

$$\epsilon_{IJKL} \hat{B}^{IJ} \hat{B}^{KL} = [j_L(j_L + 1) - j_R(j_R + 1)] \hat{1}. \quad (2.50)$$

The Barrett-Crane model is then given by a partition function over $\mathrm{Spin}(4)$ representations with $j_L = j_R$. However, the Eq. (2.49) does not necessarily imply that $B = *e \wedge e$. To

⁴In literature a common notation is also + and -.

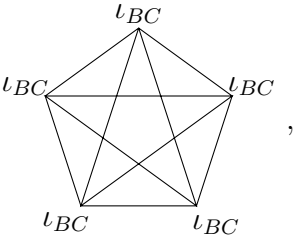
enforce this, an additional *cross-simplicity constraint* is necessary:

$$\epsilon_{IJKL} B_{\mu\nu}^{IJ} B_{\rho\sigma}^{KL} = \frac{1}{4!} \epsilon_{\mu\nu\rho\sigma} \epsilon^{\alpha\beta\gamma\delta} \epsilon_{MNPQ} B_{\alpha\beta}^{MN} B_{\gamma\delta}^{PQ}. \quad (2.51)$$

This additional set of constraints has the effect of reducing the space of 4-intertwiners to a single unique one, known as the *Barrett-Crane intertwiner*, given by

$$\iota_{BC}^{(kk')(ll')(mm')(nn')} = \sum_j (2j+1) \iota^{klf} \iota^{fmn} \iota^{k'l'f'} \iota^{f'm'n'}, \quad (2.52)$$

where ι^{ijk} is just the 3-valent SU(2) intertwiner from Eq. (2.25). This allows us to write the partition function of the BC model as

$$Z_{BC} = \sum_{j_f^L} \prod_{f \in \Delta^*} (2j_f^L + 1)^2 \prod_{v \in \Delta^*} \iota_{BC}, \quad (2.53)$$


where the vertex amplitude is a $10j$ symbol with the fixed BC intertwiners. Unfortunately, this model suffer from two crippling flaws – it is ultra-local and the semi-classical limit corresponds to the Area Regge Calculus. While the first is self-explanatory, the latter looks naively like a good thing, but the problem lies in the fact that in Area Regge Calculus, the deficit angles are also functions of area, which results in a model with too few degrees of freedom [94].

It would seem then that the imposition of simplicity constraints leads to the wrong model. The workaround to this issue was discovered the newer EPRL-FK models however, by imposing the constraints in a weaker sense, à la Gupta-Bleuler. The construction starts with the choice of an SU(2) subgroup of Spin(4), which will play the role of spatial slicing, like in the canonical theory. This is useful, because unitary representations of Spin(4) can be expressed in terms of those of SU(2) by

$$\mathcal{H}_{j_L, j_R} = \bigoplus_{j=|j_L-j_R|}^{j_L+j_R} \mathcal{H}_j. \quad (2.54)$$

Before we introduce the weaker constraints, it is necessary to discuss a bit of Spin(4) Lie algebra, which can be described in terms of six generators $J_{L,R}^i$ such that

$$[J_{L,R}^i, J_{L,R}^j] = \epsilon^{ij}_k J_{L,R}^k. \quad (2.55)$$

This can be split into the rotation subalgebra L^i and a “boost” generators K^i . For details of this algebra, see for example [8]. In terms of these generators, in [15] it was shown that the quadratic simplicity constraints are equivalent to the linear constraint on each face of a tetrahedron:

$$L_f^i - \frac{1}{\gamma} K_f^i \approx 0, \quad (2.56)$$

where the subgroup $SU(2) \subset Spin(4)$ is chosen independently at each tetrahedron (or $e \in \Delta^*$). Imposing these constraints in the basis $|j_L, j_R, j, m\rangle$ labeling $\mathcal{H}_j \subset \mathcal{H}_{j_L, j_R}$, we get a restriction on $Spin(4)$ representations:

$$j_{L,R} = |1 \pm \gamma| \frac{j}{2}. \quad (2.57)$$

We will call this restricted set of representations \mathcal{R}_γ . Notice that this constraint restricts also the value of the Barbero-Immirzi parameter to natural numbers. This strange restriction is only present in the Riemannian case, as in the Lorentzian model the $SL(2, \mathbb{C})$ representations have continuous labels.

Formally, the linearized simplicity constraints are then imposed weakly on states $|\psi\rangle$ in a $Spin(4)$ representation subspace satisfying Eq. (2.57) as

$$(K_f^i - \gamma L_f^i) |\psi\rangle = \mathcal{O}_j, \quad (2.58)$$

where \mathcal{O}_j vanishes in the large spin limit $j \rightarrow \infty$. This weaker requirement is exactly what allows the newer models to avoid the problems of the Barrett-Crane construction. Using these constraints, we could again write the partition function of EPRL model in terms of the $15j$ symbol, but it actually is more illustrative to discuss it in terms of the projectors P . Let us denote the projection onto simplicity constraints by

$$\mathcal{Y}_j : \mathcal{H}_{(1+\gamma)j/2, |1-\gamma|j/2} \rightarrow \mathcal{H}_j. \quad (2.59)$$

If we label the $Spin(4)$ projector as $P_{Spin(4)}^{(j_L^1, j_R^1), \dots, (j_L^4, j_R^4)}$, then the object that is replaced by it in the EPRL-FK model is given by

$$P_{EPRL-FK}(j_1, \dots, j_4) = P_{Spin(4)}^{(j_L^1, j_R^1), \dots, (j_L^4, j_R^4)} \left[\bigotimes_{i=1}^4 \mathcal{Y}_{j_i} \right] P_{Spin(4)}^{(j_L^1, j_R^1), \dots, (j_L^4, j_R^4)}. \quad (2.60)$$

It is important to note that $P_{EPRL-FK}$ is no longer strictly a projector, since we clearly have $(P_{EPRL-FK})^2 \neq P_{EPRL-FK}$. With this definition, the partition function of this model can be written as

$$Z_{EPRL-FK} = \sum_{j_L, j_R \in \mathcal{R}_\gamma} \prod_{f \in \Delta^*} \dim_{|1-\gamma|j/2} \dim_{(1+\gamma)j/2} \prod_{e \in \Delta^*} P_{EPRL-FK}^e(j_{e_1}, \dots, j_{e_4}). \quad (2.61)$$

This proposal for the 4d quantum gravity amplitudes does not suffer from the problems that plagued the Barrett-Crane model. In [95, 96] it was shown that the semi-classical limit of the EPRL-FK model is given by area-angle Regge Calculus [97], in which the angles are independent of the areas, and which is equivalent to the Regge Calculus in terms of edge lengths.

The EPRL-FK model can be rewritten in an interesting way using $SU(2)$ coherent states instead of the spin states. Consider the overcomplete basis $|j, g\rangle \in \mathcal{H}_j$ labeled by $SU(2)$ group elements defined by

$$|j, g\rangle = \sum_{m=-1}^j D_{mj}^{(j)}(g) |j, m\rangle. \quad (2.62)$$

These overcomplete states form a resolution of identity on \mathcal{H}_j :

$$\mathbb{1}_i = \dim_j \int_{SU(2)} dg |j, g\rangle \langle j, g|. \quad (2.63)$$

Since we have that the two-sphere $S^2 = SU(2)/U(1)$ and the phase cancels out in the resolution of identity, the resolution of identity can be written as an integral

$$\mathbb{1}_j = \dim_j \int_{S^2} d^2n |j, \vec{n}\rangle \langle j, \vec{n}|, \quad (2.64)$$

where \vec{n} is a 3-dimensional unit vector on the sphere. The $|j, \vec{n}\rangle$ form again an overcomplete basis for \mathcal{H}_j and are referred to as $SU(2)$ coherent states, since $\langle j, \vec{n} | \hat{J}^i | j, \vec{n} \rangle = j \vec{n}$ and $\Delta \hat{J}^2 = j$, which minimizes the fluctuations. Importantly, the coherent states also have the property that

$$|j, \vec{n}\rangle = \left| \frac{1}{2}, \vec{n} \right\rangle^{\otimes 2j} \equiv |\vec{n}\rangle^{\otimes 2j}. \quad (2.65)$$

Using these coherent states and rewriting the Spin(4) projectors in terms of integrals over group elements using Eq. (2.21), we can rewrite the EPRL-FK partition function in the case $\gamma < 1$ as

$$Z_{EPRL-FK} = \sum_{j_f} \prod_{f \in \Delta^*} \dim_{(1-\gamma)\frac{j_f}{2}} \dim_{(1+\gamma)\frac{j_f}{2}} \int \prod_{e \in \Delta^*} \dim_{j_{ef}} dn_{ef} dg_{ev}^L dg_{ev}^R e^{S_{j_L, R, \vec{n}}[g^L, R]}, \quad (2.66)$$

where the action is

$$S_{j_L, R, \vec{n}}[g^L, R] = \sum_{v \in \Delta^*} \left(S_{(1+\gamma)\frac{j_f}{2}, \vec{n}}^v [g^L] + S_{(1-\gamma)\frac{j_f}{2}, \vec{n}}^v [g^R] \right) \quad (2.67)$$

with the two terms given by

$$S_{j,\bar{n}}^v[g] = \sum_{a<b=1}^5 2j_{ab} \ln \langle n_{ab} | g_a^{-1} g_b | n_{ba} \rangle, \quad (2.68)$$

where the indices a, b label edges belonging to a vertex. For more details of this construction, see for example [8].

2.6 The Holomorphic Representation of SU(2)

In the rest of the thesis, rather than working in the spin or coherent state representations we introduced above, we will switch to a completely different basis that uses the recent developments in rewriting Spin Foams in terms of spinors.

We choose to use a spinor representation of SU(2) in the Bargmann-Fock space $L_{hol}^2(\mathbb{C}^2, d\mu)$ of holomorphic polynomials of a spinor [75, 76, 81]. One of the features of this representation that will facilitate our calculations is that the Hermitian inner product is Gaussian:

$$\langle f | g \rangle = \int_{\mathbb{C}^2} \overline{f(z)} g(z) d\mu(z), \quad (2.69)$$

where $d\mu(z) = \pi^{-2} e^{-\langle z | z \rangle} d^4 z$ and $d^4 z$ is the Lebesgue measure on \mathbb{C}^2 .

Given $z \in \mathbb{C}^2$ we denote its conjugate by \check{z} . We use a bra-ket notation for z and square brackets \check{z} as in

$$|z\rangle = \begin{pmatrix} z_0 \\ z_1 \end{pmatrix}, \quad [z] = \begin{pmatrix} -\bar{z}_1 \\ \bar{z}_0 \end{pmatrix}. \quad (2.70)$$

That is $|\check{z}\rangle = [z]$. Notice that while $\langle z |$ is anti-holomorphic, $[z]$ is holomorphic and orthogonal to $|z\rangle$, i.e. $[z | z\rangle = 0$. This non-standard notation for spinors will turn out to be useful, as we will always work with contractions of spinors, without the need for writing out the indices. Our notation is related to the usual one as follows: $z_A = |z\rangle$, $\bar{z}_{A'} = \langle z |$, and the spinor invariants are $[z | w\rangle = z_{A'} w_A \epsilon^{A'A}$ and $\langle z | w\rangle = \bar{z}_{A'} w_A \delta^{A'A}$. The bracket $[z | w\rangle$ associated with the ϵ tensor is skew-symmetric, holomorphic and SL(2, \mathbb{C}) invariant. The bracket $\langle z | w\rangle$ associated with the identity tensor is Hermitian, and only SU(2) invariant.

Let us now study the identity on the Bargmann-Fock space $L_{hol}^2(\mathbb{C}^2, d\mu)$. The delta distribution on this space is given by $\delta_w(z) = e^{\langle z | w \rangle}$, since for any holomorphic function $\int d\mu(z) f(z) e^{\langle z | w \rangle} = f(w)$. Let us use a line to represent the delta graphically by

$$e^{\langle z | w \rangle} = \langle z | \text{—————} | w \rangle \quad \text{and} \quad \frac{\langle z | w \rangle^{2j}}{(2j)!} = \langle z | \text{—————}^j | w \rangle. \quad (2.71)$$

Therefore the Gaussian integral $\int d\mu(w)e^{\langle z|w\rangle+\langle w|z'\rangle} = e^{\langle z|z'\rangle}$ implies the contraction

$$\int d\mu(w) \langle z| \overset{j}{\text{---}} |w\rangle\langle w| \overset{j'}{\text{---}} |z'\rangle = \delta_{j,j'} \langle z| \overset{j}{\text{---}} |z'\rangle . \quad (2.72)$$

For a function of four spinors (with obvious generalization to n spinors) we can thus define the *trivial projector*, which we will denote as

$$\mathbb{1}(z_i; w_i) = e^{\sum_{i=1}^4 \langle z_i|w_i\rangle} = \begin{array}{c} [z_1| \text{---} |w_1\rangle \\ [z_2| \text{---} |w_2\rangle \\ [z_3| \text{---} |w_3\rangle \\ [z_4| \text{---} |w_4\rangle \end{array} . \quad (2.73)$$

Next, we will study how $SU(2)$ acts on the elements of the Bargmann-Fock space. For a generic holomorphic function $f \in L_{hol}^2(\mathbb{C}^2, d\mu)$, the group action is given by

$$g \cdot f(z) = f(g^{-1}z). \quad (2.74)$$

The group $SU(2)$ acts irreducibly on the subspaces of holomorphic polynomials homogeneous of degree $2j$. Holomorphic polynomials with different degrees of homogeneity are orthogonal with each other. Indeed, $L_{hol}^2(\mathbb{C}^2, d\mu) = \bigoplus_{j \in \mathbb{N}/2} V^j$ and an orthonormal basis of V^j is given by

$$e_m^j(z) \equiv \frac{z_0^{j+m} z_1^{j-m}}{\sqrt{(j+m)!(j-m)!}} \quad (2.75)$$

and it is of dimension $2j + 1$. This orthonormal basis allows us to relate the spinor representation and the previously introduced spin basis. If we define

$$D_{z\tilde{z}}^{(j)}(g) = \langle z|g|\tilde{z}\rangle^{2j}, \quad (2.76)$$

then we have the simple change of basis relation

$$D_{z\tilde{z}}^{(j)}(g) = \sum_{m,n=-j}^j (2j)! e_m^j(z) e_n^j(\tilde{z}) D_{mn}^{(j)}(g). \quad (2.77)$$

In the study of gauge-invariant Spin Foam models, we will be interested in the $SU(2)$ invariant functions on n spinors

$$f(gz_1, gz_2, \dots, gz_n) = f(z_1, z_2, \dots, z_n), \quad \forall g \in SU(2). \quad (2.78)$$

We will denote the invariant elements of $L^2(\mathbb{C}^2, d\mu)^{\otimes n}$ to be in \mathcal{H}_n , which is the Hilbert space of n -valent intertwiners we defined in Eq. (2.24). We will follow the procedure we introduced earlier and construct elements of \mathcal{H}_n by averaging a function of n spinors over the group using the Haar measure. In this way the Haar projector $P : L^2(\mathbb{C}^2, d\mu)^{\otimes n} \rightarrow \mathcal{H}_n$ can be written as

$$P(f)(w_i) = \int \prod_i d\mu(z_i) P(\check{z}_i; w_i) f(z_1, z_2, \dots, z_n) = \int_{\text{SU}(2)} dg f(gw_1, gw_2, \dots, gw_n) \quad (2.79)$$

where the kernel is given by⁵

$$P(z_i; w_i) = \int_{\text{SU}(2)} dg e^{\sum_i [z_i | g | w_i]} = \left[\begin{array}{c} |z_1\rangle \\ |z_2\rangle \\ |z_3\rangle \\ |z_4\rangle \end{array} \right] \text{---} \boxed{} \text{---} \left[\begin{array}{c} |w_1\rangle \\ |w_2\rangle \\ |w_3\rangle \\ |w_4\rangle \end{array} \right], \quad (2.80)$$

where we use a box to represent group averaging with respect to the Haar measure over $\text{SU}(2)$. Hence the projector onto the invariant subspace is simply the group average of $\mathbb{1}(z_i; w_i)$. From the above, we see that a contraction of two spinors on the same strand but belonging to two different projectors is obtained by setting $z_i^1 = \check{w}_i^2$. This implies that the kernel of the projector satisfies the projection property

$$\int \prod_i d\mu(w_i) P(z_i; w_i) P(\check{w}_i; z'_i) = P(z_i; z'_i). \quad (2.81)$$

We will also refer from now on to the kernel $P(z_i; w_i)$ as a projector for convenience. As shown in [79, 98], we can perform the integration over g in Eq. (2.80) explicitly, which gives a power series in the holomorphic spinor invariants:

$$P(z_i; w_i) = \sum_{[k]} \frac{1}{(J+1)!} \prod_{i < j} \frac{([z_i | z_j][w_i | w_j])^{k_{ij}}}{k_{ij}!}, \quad (2.82)$$

where the sum is over a set of $n(n-1)/2$ non-negative integers $[k] \equiv (k_{ij})_{i \neq j=1, \dots, n}$ with $1 \leq i < j \leq n$ and $k_{ij} = k_{ji}$. A short proof of this statement is given in the Appendix A.3 for the reader's convenience. Thus a basis of n -valent intertwiners is given by

$$(z_i | k_{ij}) \equiv \prod_{i < j} \frac{[z_i | z_j]^{k_{ij}}}{k_{ij}!}. \quad (2.83)$$

⁵For a review of Gaussian integration techniques see Appendix A.1.

The non-negative integers $(k_{ij})_{i \neq j=1, \dots, n}$ are satisfying the n homogeneity conditions

$$\sum_{j \neq i} k_{ij} = 2j_i. \quad (2.84)$$

The sum of spins at the vertex is defined by $J = \sum_i j_i = \sum_{i < j} k_{ij}$ and is required to be a positive integer. We also see from Eq. (2.82) that the identity on \mathcal{H}_{j_i} is resolved as follows

$$\mathbb{1}_{\mathcal{H}_{j_i}} = \sum_{[k] \in K_j} \frac{|k_{ij}\rangle\langle k_{ij}|}{\|k_{ij}\|^2}, \quad \|k_{ij}\|^2 = \frac{(J+1)!}{\prod_{i < j} k_{ij}!}. \quad (2.85)$$

with the set K_j defined by integers k_{ij} satisfying Eq.(2.84). For more details on these intertwiners and the coherent states defined by them, see [99] where this basis was introduced for the first time.

Before we go on to the discussion of simplicity constraints, let us notice that using a multinomial expansion Eq.(2.82) can be written in terms of total spin:

$$P(z_i; w_i) = \sum_{J=0}^{\infty} \frac{\left(\sum_{i < j} [z_i | z_j] [w_i | w_j] \right)^J}{J!(J+1)!}, \quad (2.86)$$

which will turn out to be a quite useful expression for the projector for computation purposes. Note that this is an expansion in $U(N)$ coherent intertwiners of total area J .

2.7 Holomorphic Simplicity Constraints

Holomorphic simplicity constraints for spinorial Spin Foam models were first introduced in [16] for Riemannian gravity. Here we give a short summary, but refer the reader to the original paper for their full derivation.

For the Riemannian 4d Spin Foam models, we use the gauge group $\text{Spin}(4) = \text{SU}(2)_L \times \text{SU}(2)_R$, as before. The holomorphic simplicity constraints are isomorphisms between the two representation spaces of $\text{SU}(2)$: for any two edges i, j that are a part of the same vertex a , they are defined by

$$[z_{iL}^a | z_{jL}^a] = \rho^2 [z_{iR}^a | z_{jR}^a], \quad (2.87)$$

where ρ is a function of the Barbero-Immirzi parameter γ given by

$$\rho^2 = \begin{cases} (1-\gamma)/(1+\gamma), & |\gamma| < 1 \\ (\gamma-1)/(1+\gamma), & |\gamma| > 1 \end{cases} \quad (2.88)$$

The holomorphic simplicity constraints Eq.(2.87) essentially tell us that there exists a unique group element $g_a \in \text{SL}(2, \mathbb{C})$ for each vertex a , such that

$$\forall i, \quad g_a |z_{iL}^a\rangle = \rho |z_{iR}^a\rangle. \quad (2.89)$$

A general element of $\text{SL}(2, \mathbb{C})$ can be decomposed into the product of a Hermitian matrix times an element of $\text{SU}(2)$, so that $g_a = h_a u_a$ with $h_a^\dagger = h_a$. It is only when $h_a = \mathbb{1}$ that the holomorphic simplicity constraints imply the usual geometrical simplicity constraints. In the FK formulation of the spin foam model which is only partially holomorphic this is implied since the norm of the spinors is fixed. The fully holomorphic formulation of DL therefore relaxes at the quantum level the simplicity constraints. Fortunately, one can check following [99] that in the semi-classical limit of Holomorphic amplitudes the Gauss constraints due to the gauge invariance of the amplitude can be realized in the form

$$\sum_i |z_{iL}^a\rangle \langle z_{iL}^a| = A_L \mathbb{1}, \quad \sum_i |z_{iR}^a\rangle \langle z_{iR}^a| = A_R \mathbb{1}. \quad (2.90)$$

This imposes that in the classical limit $h_a = \mathbb{1}$ and the geometrical simplicity constraints $u_a |z_{iL}^a\rangle = \rho |z_{iR}^a\rangle$ with $u_a \in \text{SU}(2)$ are satisfied.

Geometrically, each spinor defines a three vector $\vec{V}(z) \in \mathbf{R}^3$ through the equation,

$$|z\rangle \langle z| = \frac{1}{2} \left(\mathbb{1} \langle z|z\rangle + \vec{V}(z) \cdot \vec{\sigma} \right), \quad |z][z| = \frac{1}{2} \left(\mathbb{1} [z|z] - \vec{V}(z) \cdot \vec{\sigma} \right). \quad (2.91)$$

where $\vec{\sigma}$ is the vector made by Pauli matrices. Thus, around a node in a spin-network, each link dual to a triangle in the simplicial manifold is associated with two 3-vectors $\vec{V}_L(z)$ and $\vec{V}_R(z)$ given by the left and right spinors. Classically, these vectors correspond to the selfdual b_+ and anti-selfdual b_- components of the B field respectively:

$$V_L^i(z) = b_+^i := B^{0i} + \frac{1}{2} \epsilon_{kl}^i B^{kl}, \quad V_R^i(z) = b_-^i := -B^{0i} + \frac{1}{2} \epsilon_{kl}^i B^{kl}. \quad (2.92)$$

Note here that the time norm is chosen to be $N_I = (1, 0, 0, 0)^T$. For the Hodge dual of the B field, we find $(*b)_+ = b_+ = \vec{V}_L(z)$, and $(*b)_- = -b_- = -\vec{V}_R(z)$.

For the vectors $\vec{V}_L(z)$ and $\vec{V}_R(z)$ defined by the spinors of the two copies of $\text{SU}(2)$ this means that the holomorphic simplicity constraints imply

$$g_a \triangleright \vec{V}_L(z_i^a) = \rho^2 \vec{V}_R(z_i^a), \quad \forall i \in a \quad (2.93)$$

which leads to the constraint that the norm of the selfdual and anti-selfdual components of the bivector $(g_a, \mathbb{1}) \triangleright (B + \gamma * B)$ have to be equal to each other:

$$|(1 + \gamma)g_a \triangleright b_+| = |(1 - \gamma) \triangleright b_-|. \quad (2.94)$$

Thus B and $*B$ are simple bivectors, and for the spin network vertex a , there exists a common time norm to all the bivectors:

$$\mathcal{N}_a = (g_a, \mathbb{1})^{-1} \triangleright (1, 0, 0, 0). \quad (2.95)$$

The existence of this shared time norm implies the linear simplicity constraints introduced by the EPRL and FK models [12, 13, 14, 15].

It is interesting to note that g_a can be expressed purely in terms of spinors as

$$g_a = \frac{|z_{iR}^a\rangle\langle z_{iL}^a| + |z_{iR}^a][z_{iL}^a|}{\sqrt{\langle z_{iL}^a|z_{iL}^a\rangle\langle z_{iR}^a|z_{iR}^a\rangle}}, \quad \forall i \in a. \quad (2.96)$$

It is easy to check that this satisfies Eq. (2.89). Note here that g_a is a unique group element for all strands belonging to the same vertex.

Chapter 3

Two spinorial models

There is a theory which states that if ever anyone discovers exactly what the Universe is for and why it is here, it will instantly disappear and be replaced by something even more bizarre and inexplicable. There is another theory which states that this has already happened.

Douglas Adams
The Restaurant at the End of the Universe

In this chapter, we will start from reviewing the holomorphic Spin Foam model, which was proposed by Dupuis and Livine in [16, 84], after which we will introduce an alternative model through imposing the holomorphic simplicity constraints on the Haar projectors. We then introduce the *homogeneity map*, which is a key mathematical tool that will facilitate the exact calculations in this thesis. We then close the chapter by comparing the two models – first by rewriting the DL model in terms of propagators, and then by evaluating the semi-classical limit of both of the models, which in both cases turns out to be the same as that of the EPRL-FK model.

3.1 Imposing constraints

We will now impose the holomorphic simplicity constraints on the Spin(4) BF theory in order to obtain a model of 4d Riemannian Quantum Gravity. There are two natural ways

of imposing these constraints - either on the boundary spin network defined by contraction of coherent states [16], or on the whole projector (2.80). We will first summarize the usual approach, which we will refer to as the DL prescription. We then introduce an alternative model in which the constraint is imposed on the whole projector. Surprisingly, we will see later that the alternative model actually has the same asymptotic behavior as the DL prescription and EPRL-FK model (with $|\gamma| < 1$) [95, 96, 100], i.e. the amplitude is weighted by a cosine of the Regge [69] action. It however leads to greatly simpler evaluations of amplitudes, as compared to the DL model.

3.1.1 DL prescription

In [16, 84] Dupuis and Livine introduced a Spin Foam model similar to the EPRL/FK models, but written in terms of spinorial coherent states with the holomorphic simplicity constraints. Since BF amplitudes can be seen as evaluations of spin network functions, the simplicity constraints in this model are imposed in the usual way – on the evaluation of the boundary spin network of a 4-simplex given by the amplitude. The amplitude for a single 4-simplex σ is given by a product of contraction of coherent states for left and right sectors, with the simplicity constraints imposed on the boundary spinors as follows

$$\mathcal{A}_\sigma(\{z_\Delta^\tau\}) = \int [dg_\tau^L]^5 [dg_\tau^R]^5 e^{\sum_{a,b \in \tau} \rho^2 [z_b^a | g_a^{L\dagger} g_b^L | z_a^b] + [z_b^a | g_a^{R\dagger} g_b^R | z_a^b]} \quad (3.1)$$

where τ is the set of tetrahedra labeled by a, b . Graphically this is presented in Fig. 3.1. This amplitude corresponds to two copies of 20j symbols from BF theory constrained by

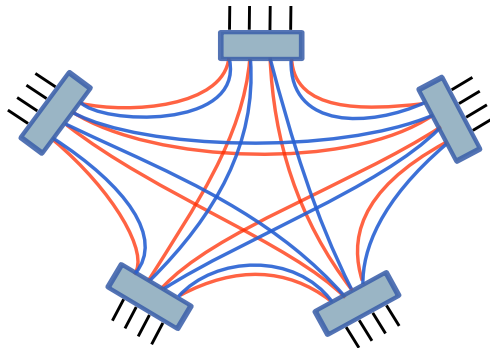


Figure 3.1: Graph for the 4-simplex amplitude in the DL model. The contractions inside correspond to two copies of BF 20j symbols, constrained on the boundary.

$$[z_L^{s(\Delta)} | z_L^{t(\Delta)} \rangle = \rho^2 [z_R^{s(\Delta)} | z_R^{t(\Delta)} \rangle \text{ on the boundary.}$$

3.1.2 Constrained projector

Since spin foam amplitudes for BF theory are constructed by gluing together projectors (2.86) into graphs corresponding to 4d quantum geometries, we find it natural to instead impose the constraints on the arguments of the projectors themselves. Let us consider the Spin(4) projector obtained by taking a product of two SU(2) projectors

$$P(z_i; w_i)P(z'_i; w'_i) = \sum_J \frac{\left(\sum_{i<j} [z_i|z_j][w_i|w_j]\right)^J}{J!(J+1)!} \sum_{J'} \frac{\left(\sum_{i<j} [z'_i|z'_j][w'_i|w'_j]\right)^{J'}}{J'!(J'+1)!}, \quad (3.2)$$

where we use a prime to distinguish the left and right SU(2) sectors. We will now impose the holomorphic simplicity constraints on both incoming and outgoing strands in the Spin(4) projector

$$[z'_i|z'_j] = \rho^2 [z_i|z_j] \quad [w'_i|w'_j] = \rho^2 [w_i|w_j].$$

This will make the two products of spinors in the two projectors proportional to each other, with the proportionality constant being ρ^4 . Note that the imposition of simplicity constraints on all of the spinors also forces the measure of integration on \mathbb{C}^2 to change to

$$d\mu_\rho(z) := \frac{(1+\rho^2)^2}{\pi^2} e^{-(1+\rho^2)\langle z|z\rangle} d^2z. \quad (3.3)$$

The factor of $(1+\rho^2)^2$ is added for normalization. It insures that

$$\int d\mu_\rho(z) = 1. \quad (3.4)$$

Moreover this choice of normalization is confirmed by the study of asymptotics of both this and the DL model later in this chapter. It is exactly this choice that insures that both models have the same semi-classical limit. We are now ready to define a new *constrained propagator* P_ρ by applying the simplicity constraints on the Spin(4) projector

$$P_\rho(z_i; w_i) \equiv P(z_i; w_i)P(\rho z_i; \rho w_i) = \sum_J \sum_{J'} \frac{\rho^{4J'}}{J!(J+1)!J'!(J'+1)!} \left(\sum_{i<j} [z_i|z_j][w_i|w_j]\right)^{J+J'}. \quad (3.5)$$

The two sums over integers J and J' are independent, so we can simplify this expression for the constrained propagator into a single sum by letting $J+J' \rightarrow J$. This allows us to arrive at a more compact form of the constrained propagator, given by

$$P_\rho(z_i; w_i) = \sum_J F_\rho(J) \frac{\left(\sum_{i<j} [z_i|z_j][w_i|w_j]\right)^J}{J!(J+1)!}, \quad (3.6)$$

where we have recognized that the numerical factor in front of the spinors is actually the power series expansion of the hypergeometric function

$$F_\rho(J) := {}_2F_1(-J-1, -J; 2; \rho^4) = \sum_{J'=0}^J \frac{J!(J+1)!\rho^{4J'}}{(J-J')!(J-J'+1)!J!(J'+1)!}. \quad (3.7)$$

Notice that the constrained Spin(4) propagator is just an SU(2) projector with non-trivial weights (greater than 1) for each term that depend on the Barbero-Immirzi parameter. In general, this hypergeometric function is a complicated function of ρ and J , as can be seen in Fig.3.2

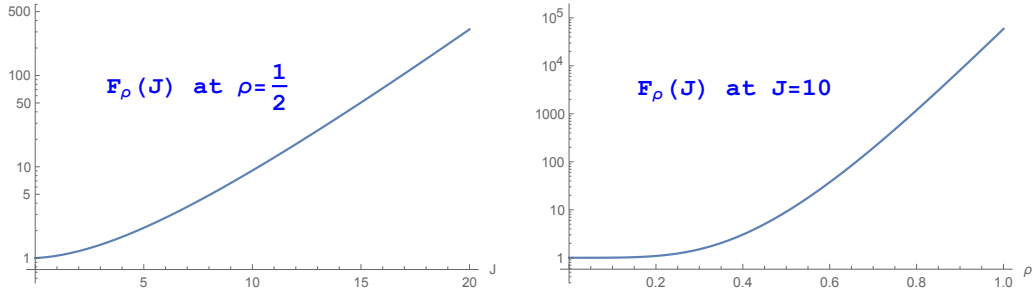


Figure 3.2: Left: behavior of $F_\rho(J)$ at fixed ρ as a function of spin J . Right: at fixed spin, $F_\rho(J)$ is rapidly increasing as $\rho \rightarrow 1$.

There are however two interesting limiting cases. For $\rho = 0$, which corresponds to $\gamma \rightarrow 1$, we have

$${}_2F_1(-J-1, -J; 2; 0) = 1, \quad (3.8)$$

so we end up with pure SU(2) BF theory. This is obvious, as $\rho = 0$ forces all the left spinors to be 0. Another limit often considered is $\rho = 1$, which in this construction surprisingly corresponds to both of the limits $\gamma \rightarrow 0$ and $\gamma \rightarrow \infty$. In this limit we get also a relatively simple expression

$${}_2F_1(-J-1, -J; 2; 1) = \frac{(2J+2)!}{(J+2)!(J+1)!}. \quad (3.9)$$

This limit does not have an obvious interpretation apart from its simplicity. For all other values of ρ we can either calculate $F_\rho(J)$ explicitly, or we can try to approximate it by its power series expansion for large spins, which was shown by Chen in [101] to be given to

the leading order by

$$F_\rho(J) = \frac{e^{(\frac{3}{2}+J)\zeta_\rho}(1-\rho^4)^{\frac{3}{2}+J}}{16\sqrt{2\pi}(3+2J)^{\frac{7}{2}}\rho^5} \left[4(3+2J) [8\rho^2(3+2J) - 3(1+\rho^4)] - 3\frac{1+\rho^4}{\zeta_\rho} + 6\frac{\rho^2}{\zeta_\rho^2} + \mathcal{O}(J^{-2}) \right], \quad (3.10)$$

where $\zeta_\rho = \cosh^{-1} \left[\frac{1+\rho^4}{1-\rho^4} \right]$. Note that this expression is only valid for $0 < \rho < 1$, and the limits are quite discontinuous. In Fig. 3.3 we see that truncating at this order is an excellent approximation even at small spins.

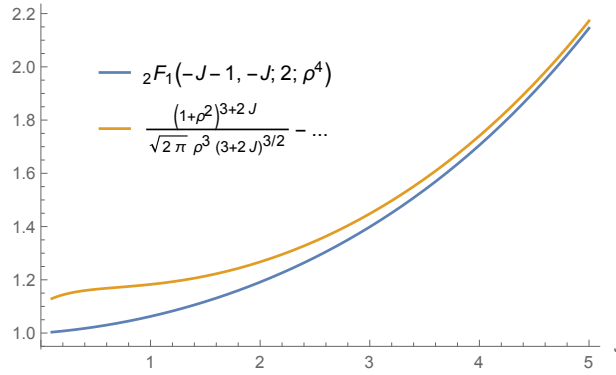


Figure 3.3: The expression (3.10) is an excellent approximation to $F_\rho(J)$ even at small spins. Plotted at $\rho = \frac{1}{2}$.

It is also interesting to note that we have

$$\frac{e^{J\zeta_\rho}(1-\rho^4)^J}{(1+\rho^2)^{2J}} = 1, \quad (3.11)$$

which due to the change in measure (3.3) will pop up all over the place. This factor might look a bit arbitrary, but becomes a lot more understandable, when we rewrite it in terms of the Barbero-Immirzi parameter: $(1-\rho^4)^J(1+\rho^2)^{-2J} = \gamma^J$. This implies that $\gamma = e^{-\zeta_\rho}$. Using Eq. (3.11) we then have that to the leading order in the large spin limit $J \rightarrow \infty$, the hypergeometric function is given by

$$F_\rho(J) \sim \frac{(1+\rho^2)^{3+2J}}{2\sqrt{\pi}\rho^3 J^{\frac{3}{2}}}. \quad (3.12)$$

We do not expect his compact form to be such a great approximation as (3.10) at small spins, but for large J it does capture the behavior. We show this in Fig. 3.4.

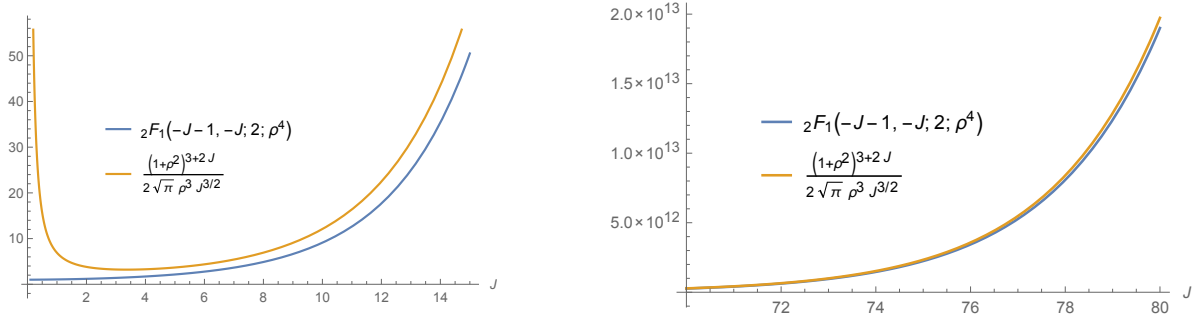


Figure 3.4: Left: for small spins (3.12) is a rather poor approximation. Right: as we increase spin however, we rapidly converge. Plotted at $\rho = \frac{1}{2}$.

We can now define the partition function for the Spin Foam model made up from these constrained propagators. Since the propagators are just BF projectors with non-trivial weight, we can write the partition function on a 2-complex Δ^* as

$$Z_G^{\Delta^*} = \sum_{j_f} \prod_{f \in \Delta^*} \mathcal{A}_f(j_f) \int \left\{ \prod_{\text{all}} d\mu_\rho(z) d\mu_\rho(w) \right\} \sum_{k_{f,f'}^e \in K_j} \prod_e P_\rho^{k_{ij}^e}(z_i^e; w_i^e), \quad (3.13)$$

where $\mathcal{A}_f(j_f)$ is a face weight, the set K_j was defined previously in Eq. (2.84) to be the set of integers k_{ij} satisfying $\sum_{i \neq j} k_{ij} = 2j_i$ and contraction of spinors according to the 2-complex Δ^* on different edges is implied. The constrained propagator at fixed spins is given by

$$P_\rho^{k_{ij}^e}(z_i^e; w_i^e) := \frac{F_\rho(J_e)}{(J_e + 1)!} \prod_{i < j} \frac{([z_i^e | z_j^e][w_i^e | w_j^e])^{k_{ij}^e}}{k_{ij}^e!}. \quad (3.14)$$

Each constrained propagator comes with an orientation, with spinors z incoming into the box and spinors w outgoing in the convention of this thesis. A change of this edge orientation results in overall minus sign for the amplitude. Additionally, we also put an orientation on each strand, which dictates how spinors on different propagators are contracted. An example is shown in Fig. 3.5. When we glue 4-simplices, we have two propagators contracted on the dual edge along which they are glued.

It is interesting to note here that, unlike in the usual Spin Foam models, this definition in terms of propagators does not necessarily constrain the partition function to be a product of vertex amplitudes, thus allowing for more general non-geometrical structures.

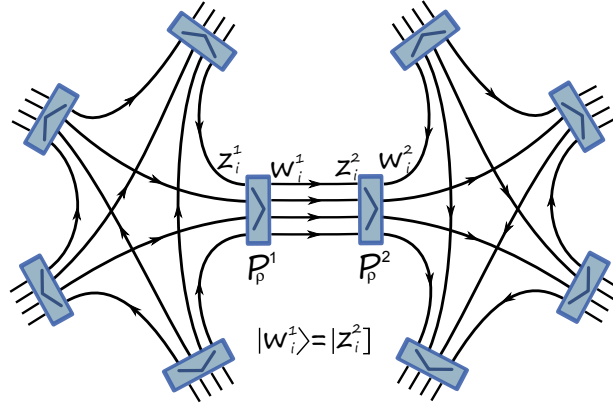


Figure 3.5: Graph for the amplitude of contraction of two 4-simplices. Propagators P_ρ^1 and P_ρ^2 belong to the same edge but two different 4-simplices. The spinors belonging on the same strand but belonging to different propagators are contracted according to the strand orientation. For example, spinors $w_i^1 = z_i^2$.

3.2 The Homogeneity Map

In this section we will introduce a very useful tool that will allow us to make calculations of Pachner moves more tractable. Notice that the propagator P_ρ is a polynomial obtained from products of monomials $[z_i|z_j][w_i|w_j]^{k_{ij}}$ which possess a degree of homogeneity of $4k_{ij}$. These products of monomials of different homogeneity degrees are orthogonal in the Bargmann-Fock space. The homogeneity property allows us to always separate out and track terms of given homogeneity in a power series expansion. This means that we can perform transformations term by term in the series expansion of the propagator and independently integrate each term.

Let us hence define a more general propagator G_τ that can be exponentiated

$$G_\tau(z_i; w_i) = \sum_J \tau^J \frac{\left(\sum_{i<j} [z_i|z_j][w_i|w_j]\right)^J}{J!} = e^{\tau \sum_{i<j} [z_i|z_j][w_i|w_j]} \quad (3.15)$$

and denote it graphically by

$$G_\tau(z_i; w_i) = \begin{array}{c} \left[\begin{array}{l} z_1 \\ z_2 \\ z_3 \\ z_4 \end{array} \right] \end{array} \begin{array}{c} \text{---} \\ \text{---} \\ \text{---} \\ \text{---} \end{array} \begin{array}{c} \boxed{\tau} \\ \boxed{\tau} \\ \boxed{\tau} \\ \boxed{\tau} \end{array} \begin{array}{c} \text{---} \\ \text{---} \\ \text{---} \\ \text{---} \end{array} \begin{array}{l} |w_1\rangle \\ |w_2\rangle \\ |w_3\rangle \\ |w_4\rangle \end{array} . \quad (3.16)$$

We can see that τ^J tracks homogeneity of the polynomial in spinors. If we transform each of these τ^J into a function of J , the integrals of the polynomials stay the same. In this way we can perform complicated calculations with G_τ and in the end we can use the following map, defined by a functional H_f mapping G_τ to the desired function f :

$$H_\rho : G_\tau \rightarrow P_\rho \quad \text{with} \quad H_\rho : \tau^J \rightarrow \frac{F_\rho(J)}{(J+1)!} \quad (\text{Simplicity Constraints}) \quad (3.17)$$

$$H_P : G_\tau \rightarrow P \quad \text{with} \quad H_P : \tau^J \rightarrow \frac{1}{(J+1)!} \quad (\text{BF Theory}) \quad (3.18)$$

in order to recover the propagators of the BF theory or the one of the gravity model with simplicity constraints imposed. Note that $P_0 = P$ so the BF model is included in our more general description. We are of course not limited to only these choices and could in principle study a much wider class of spin foam models built by non-trivial propagators.

By considering how BF projectors compose in Eq. (2.81), it is quite easy to find the homogeneity map for composing the propagator P_ρ n times: $P_\rho \circ \dots \circ P_\rho$. To do this, we just realize that if one reintroduces back the factor of $1/(J+1)!$ into the definition of G_τ , it then defines just the BF projector P with the spinors z rescaled to $\sqrt{\tau}z$. The homogeneity map for the composition is therefore given by¹

$$\tau^J \rightarrow \frac{F_\rho(J)^n}{(J+1)!(1+\rho^2)^{2(n-1)J}} \quad \text{for} \quad G_\tau \rightarrow P_\rho^n \quad (n \text{ Propagators}). \quad (3.19)$$

For the purpose of calculating Pachner moves, we will need to consider contracted loops of spinors. In BF theory, such a loop should correspond to an $SU(2)$ delta function. Using the spinorial language however, we get

$$\begin{array}{c} \circlearrowleft \\ \text{---} \end{array} = \int d\mu(z) e^{\langle z|z \rangle} = \sum_j \int d\mu(z) \frac{\langle z|z \rangle^{2j}}{(2j)!} = \sum_j \chi^j(\mathbb{1}) = \sum_j (2j+1), \quad (3.20)$$

whereas a delta function is $\delta_{SU(2)}(\mathbb{1}) = \sum_j (2j+1)^2$. One way of going around this is to change measure of integration for this loop to $d\tilde{\mu}(z) = (\langle z|z \rangle - 1)d\mu(z)$, as was suggested in [84]. This provides the additional factor of $(2j+1)$. An alternative way is to follow in

¹Note that the factor of $(1+\rho^2)^{2J}$ in (3.17) comes from the fact that the measure has changed under the simplicity constraints to $d\mu_\rho(z) = (1+\rho^2)^{2J} \pi^{-2} e^{-(1+\rho^2)\langle z|z \rangle}$. Hence every contraction produces a factor $(1+\rho^2)^{-2j}$ where j is the representation of the line. There is one such contraction for each j where $J = \sum j$ for each τ .

the spirit of the homogeneity map and introduce a τ' that tracks the homogeneity in this loop. For clarity, we add a symbol for this face weight into the graph:

$$\begin{array}{c} \circlearrowleft \\ \textcircled{f} \end{array} = \int d\mu(z) e^{\tau' \langle z|z \rangle} = \sum_j \tau'^{2j} (2j+1). \quad (3.21)$$

The replacement of $\tau'^{2j} \rightarrow (2j+1)$ now defines a homogeneity map for a BF loop. Of course, we now do not have to restrict ourselves to this simple face weight and can choose an arbitrary function of spin. A popular choice is the face weight regulated by a heat kernel $(2j+1)e^{-\alpha j(j+1)}$ for $\alpha > 0$, but in this work we will actually mostly work with $(2j+1)^\eta$ for $\eta \in \mathbb{R}$.

The homogeneity map we have developed in this section will be very useful in computing the 4-dimensional Pachner moves. In later sections, we will define additional homogeneity maps as we go on, to simplify the calculations.

3.3 Comparing the two models

Let us now try to compare our two ways of imposing the simplicity constraints. To do so, we will rewrite the DL vertex amplitude (3.1) in a form more similar to the constrained projector model. To do this, notice that the DL model can be written as a contraction of a product of propagators $P_L(\rho z_{\Delta_i}, w_{\Delta_i}^L) P_R(\rho z_{\Delta_i}, w_{\Delta_i}^R)$. We can now integrate out the group elements, same as in the BF theory. This means that inside a 4-simplex graph we have left and right copies of spinors, but on the boundary just one copy. We find that a propagator constrained in such a way is given by

$$P_{constr}(z_i; w_i^{L,R}) = \sum_{J_L, J_R} \frac{\left(\sum_{i < j} [z_i | z_j] [w_i^L | w_j^L] \right)^{J_L}}{J_L! (J_L + 1)!} \frac{\left(\sum_{i < j} [z_i | z_j] [w_i^R | w_j^R] \right)^{J_R}}{J_R! (J_R + 1)!} \rho^{2J_R}. \quad (3.22)$$

This obviously is not a projector, as number of incoming strands is half that of outgoing ones. To construct a propagator that allows gluing of two 4-simplices, we have to contract two such objects (as can be seen in Fig. 3.6)

$$P_{DL}(w_i^{L,R}; v_i^{L,R}) = \int \left\{ \prod_{i=1}^4 d\mu_\rho(z_i) \right\} P_{constr}(z_i; w_i^{L,R}) P_{constr}(\tilde{z}_i; v_i^{L,R}) \quad (3.23)$$

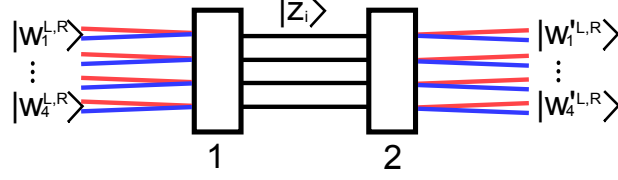


Figure 3.6: DL projector. Red strands correspond to $SU(2)_L$, blue strands to $SU(2)_R$. Simplicity constraints are imposed on spinors $|z_i\rangle$, which are integrated over.

To perform this integral, let us track homogeneity of the left and right spinors, and rewrite it as

$$\int \left\{ \prod_{i=1}^4 d\mu_\rho(z_i) \right\} e^{\tau_w^L \sum_{i<j} [z_i|z_j][w_i^L|w_j^L] + \rho^2 \tau_w^R \sum_{i<j} [z_i|z_j][w_i^R|w_j^R] - \tau_v^L \sum_{i<j} \langle z_i|z_j \rangle [v_i^L|v_j^L] - \rho^2 \tau_v^R \sum_{i<j} \langle z_i|z_j \rangle [v_i^R|v_j^R]} \quad (3.24)$$

where each τ^J keeps track of a factor $1/(J+1)!$. We can simplify this by defining the following quantities:

$$w_{ij} \equiv \frac{\tau_w^L [w_i^L|w_j^L] + \rho^2 \tau_w^R [w_i^R|w_j^R]}{1 + \rho^2}, \quad v_{ij} \equiv \frac{\tau_v^L [v_i^L|v_j^L] + \rho^2 \tau_v^R [v_i^R|v_j^R]}{1 + \rho^2}. \quad (3.25)$$

Notice that these are antisymmetric, $w_{ij} = -w_{ji}$. These definitions allow us now to perform the relatively simple Gaussian integrals over spinors $|z_i\rangle$ in Eq. (3.24), the result of which simplifies to

$$P_{DL}^\tau = \frac{1}{(1 - \sum_{i<j} w_{ij} v_{ij} + \frac{1}{16} \sum \epsilon^{abcd} \epsilon^{ijkl} w_{ab} w_{cd} v_{ij} v_{kl})^2} \quad (3.26)$$

Note that the last term is really just a sum of 9 terms, due to antisymmetries of w_{ij} and v_{ij} . Let us expand this in power series:

$$P_{DL}^\tau = \sum_{A,B} \frac{(A+B+1)!}{A!B!} (-1)^B \left(\sum_{i<j} w_{ij} v_{ij} \right)^A \left(\frac{1}{16} \sum_{a,b,c,d} \sum_{i,j,k,l} \epsilon^{abcd} \epsilon^{ijkl} w_{ab} w_{cd} v_{ij} v_{kl} \right)^B \quad (3.27)$$

We can now reexponentiate this by using two more τ 's to track the homogeneity of the A and B terms, to get

$$P_{DL}^\tau = e^{\tau_A \sum_{i<j} w_{ij} v_{ij} - \frac{\tau_B}{16} \sum \epsilon^{abcd} \epsilon^{ijkl} w_{ab} w_{cd} v_{ij} v_{kl}}, \quad (3.28)$$

where $\tau_A^J \tau_B^{J'}$ keeps track of a factor $(J+J'+1)!$ and the other τ 's inside w_{ij} 's and v_{ij} 's keep track of factors of $1/(J+1)!$. To get the P_{DL} propagator from P_{DL}^τ we just have to expand

the latter in powers series expansion and reintroduce all the factorials by homogeneity. This calculation is not however very illuminating, so we will not discuss it here. Additionally, for the sake of calculating amplitudes, it is easier to keep these factors in and only apply the homogeneity maps at the end of the calculation. As is now obvious, this way of imposing constraints makes calculations possible, but at the price of greater complexity.

3.4 Asymptotics

In this section we will calculate the asymptotics of the two models with different imposition of simplicity constraints. First we show that the Dupuis-Livine model indeed has the same asymptotic behavior as the EPRL-FK models. We then show that there are nontrivial cancellations in the asymptotic expansion of the constrained propagator model that lead to the same semiclassical limit as the DL model.

3.4.1 The dihedral angle

Before we calculate the asymptotic expansion of the spin foam amplitudes, we have to understand how to reconstruct from our data the angle appearing in the classical area-angle Regge action [97]:

$$S_{Regge} = \sum_{a < b} A_{ab} \xi_{ab}, \quad (3.29)$$

where A_{ab} is the area of face shared by tetrahedra a and b , which share a common face with each other, and ξ_{ab} is the 4D dihedral angle, which is the angle between the two 4-vectors $\mathcal{N}_a, \mathcal{N}_b$ normal to the two tetrahedra a, b .

We can find the expression for the 4D dihedral angle using Eq. (2.95) from the section on simplicity constraints:

$$\begin{aligned} \cos(\xi_{ab}) &= \mathcal{N}_a \cdot \mathcal{N}_b \\ &= \frac{1}{2} \text{tr} [g_a^{-1} \cdot g_b] = \frac{1}{2} \text{tr} [g_b^{-1} \cdot g_a] \end{aligned} \quad (3.30)$$

Using the expression of Eq. (2.96), we can write the cosine of dihedral angle in terms of spinors,

$$\cos(\xi_{ab}) = \frac{[z_{iR}^a | z_{jR}^b] \langle z_{jL}^b | z_{iL}^a \rangle + \langle z_{iL}^a | z_{jL}^b \rangle \langle z_{jR}^b | z_{iR}^a \rangle + c.c.}{2 |z_{iL}^a| |z_{iR}^a| |z_{jL}^b| |z_{jR}^b|} \quad (3.31)$$

From the above two expressions, we can see that to decide the cosine of the dihedral angle ξ_{ab} , we need the data of two group elements associated with two nodes (tetrahedra), or the data of both left and right spinors of any one strand from each of the two tetrahedra. In summary,

$$\{g_a, g_b\} \rightarrow \cos(\xi_{ab}), \text{ or } \{z_{iR}^a, z_{iL}^a, z_{jR}^b, z_{jL}^b\} \rightarrow \cos(\xi_{ab}) \quad \forall i \in a, \forall j \in b$$

Let us recall additionally, that the models we consider have Spin(4) symmetry, so we can rotate these results by a Spin(4) transformation $G = (g_L, g_R)$.

3.4.2 The asymptotics of DL model

An apparent difference between the holomorphic simplicity constraints and the ones in Euclidean EPRL/FK models is that they are constraints on spinors. However, they lead to the same constraint between spins,

$$\langle z_L | z_L \rangle = j_L = \rho^2 j_R = \rho^2 \langle z_R | z_R \rangle \quad (3.32)$$

for the coherent intertwiners in the large $|z|$ limit [16]. In this section, we briefly show that for the amplitude of a 4-simplex, the DL model has the same action at critical points as EPRL/FK models for Barbero-Immirzi parameter $\gamma < 1$.

We can rewrite the amplitude (3.1) of a 4-simplex σ by expanding it in power series as

$$\begin{aligned} \mathcal{A}_\sigma &= \int \prod_{a < b} dg_{a,b}^{L,R} e^{\rho^2 [z_b^a | g_a^{L-1} g_b^L | z_a^b] + [z_b^a | g_a^{R-1} g_b^R | z_a^b]} \\ &= \int \prod_{a < b} dg_{a,b}^{L,R} \sum_{j_{ab}^{L,R}} \frac{(\rho^2 [z_b^a | g_a^{L-1} g_b^L | z_a^b])^{2j_{ab}^L} ([z_b^a | g_a^{R-1} g_b^R | z_a^b])^{2j_{ab}^R}}{(2j_{ab}^L)! (2j_{ab}^R)!}. \end{aligned} \quad (3.33)$$

Now that we have made the summation over spins explicit, we can reexponentiate this expression to get the effective action of a 4-simplex amplitude $\mathcal{A}_\sigma = \sum_{j_{ab}^{L,R}} \int \prod_a dg_a^{L,R} e^{S_{eff}(j_{ab}^{L,R})}$ with

$$S_{eff}(j_{ab}^{L,R}) = \sum_{a,b \in \sigma} 2j_{ab}^L \ln [z_b^a | g_a^{L-1} g_b^L | z_a^b] + 2j_{ab}^R \ln [z_b^a | g_a^{R-1} g_b^R | z_a^b] + N. \quad (3.34)$$

where the numerical factor N is given by

$$N = \sum_{a,b \in \sigma} 4j_{ab}^L \ln \rho - \ln(2j_{ab}^L)! - \ln(2j_{ab}^R)! \quad (3.35)$$

It is important to note that this action is complex valued. To study the asymptotic behavior of the amplitude, we have to separate the real and imaginary parts. The real part of the action is

$$\begin{aligned} \mathbf{Re}S_{eff}(j_{ab}^{L,R}) &= \sum_{a,b \in \sigma} j_{ab}^L \ln \frac{1}{2} (|z_b^a|^2 |z_a^b|^2 - (g_a^L \triangleright \vec{V}_b^a) \cdot (g_b^L \triangleright \vec{V}_a^b)) + \\ &+ j_{ab}^R \ln \frac{1}{2} (|z_b^a|^2 |z_a^b|^2 - (g_a^R \triangleright \vec{V}_b^a) \cdot (g_b^R \triangleright \vec{V}_a^b)) + N. \end{aligned} \quad (3.36)$$

In the asymptotic analysis of complex functions the main contribution to the integral comes from critical points, which are stationary points of the action for which the real part is maximized. The critical point equations we get from variation of spinors $|z\rangle$ are the closure constraints

$$\sum_{b \neq a} |z_b^a\rangle \langle z_b^a| = \sum_{b \neq a} j_{ab}^R \mathbb{1} \quad (3.37)$$

and the orientation condition requiring certain vectors to be antiparallel, which we get from the maximization of the real part of the action:

$$g_a^L \triangleright \hat{v}_b^a = -g_b^L \triangleright \hat{v}_a^b, \quad g_a^R \triangleright \hat{v}_b^a = -g_b^R \triangleright \hat{v}_a^b, \quad \text{where } \hat{v} = \vec{V}/|\vec{V}|. \quad (3.38)$$

Using the relation (2.91) between vectors and spinors, we find that these conditions imply that the action of group elements on a spinor z_a^b rotates it up to a phase into \hat{z}_b^a :

$$g_a^{L-1} g_b^L |z_a^b\rangle = e^{i\phi_L^{ab}} |z_b^a\rangle, \quad g_a^{R-1} g_b^R |z_a^b\rangle = e^{i\phi_R^{ab}} |z_b^a\rangle. \quad (3.39)$$

This implies that the following identity holds:

$$g_b^{R-1} g_a^R g_a^{L-1} g_b^L |z_a^b\rangle = e^{i\phi_L^{ab} - \phi_R^{ab}} |z_b^a\rangle. \quad (3.40)$$

The reconstruction theorem from [96] tells us now that given nondegenerate boundary data satisfying the closure constraint (3.37) and a set of group elements $g_a^{L,R} \in \text{SU}(2)$, $a = 1, \dots, 5$ solving the orientation condition (3.38), we can reconstruct a geometric 4-simplex with the B field given by

$$B_{ab} = \pm(j_{ab}^R + j_{ab}^L)(g_a^L, g_a^R) \triangleright (v_b^a, v_b^a), \quad (3.41)$$

with the outward-pointing normal \mathcal{N}_a obtained by acting with the Spin(4) element (g_a^L, g_a^R) on the vector $N_a = (1, 0, 0, 0)$.

At this point, it is clear that the critical action of DL model is exactly the same as the one calculated in the asymptotic analysis of the EPRL model in [96], and the imaginary part of the action reads

$$\mathbf{Im}S_{eff}(j_{ab}^{L,R}) = \sum_{a,b \in \sigma} 2j_{ab}^L \phi_L^{ab} + 2j_{ab}^R \phi_R^{ab} = \sum_{a,b \in \sigma} k_{ab}(\phi_L^{ab} + \phi_R^{ab}) + \gamma k_{ab}(\phi_R^{ab} - \phi_L^{ab}), \quad (3.42)$$

where $k_{ab} = j_{ab}^L + j_{ab}^R$. To relate this to the area-angle Regge action, we have to relate the ϕ 's to the dihedral angle. We cannot directly use our expression in Eq. (3.31) for the dihedral angle, since we no longer have the information about both the left and right spinors. We can however use the result of the reconstruction theorem from the Eq.(3.41) to construct the dihedral angle by the data $\{g_a^R g_a^{L-1}, g_b^R g_b^{L-1}\}$ as follows

$$\begin{aligned} \cos(\xi_{ab}) &= \mathcal{N}_a \cdot \mathcal{N}_b \\ &= \frac{1}{2} \text{Tr} [g_a^R g_a^{L-1} \cdot g_b^L g_b^{R-1}] \end{aligned} \quad (3.43)$$

Notice however that we can obtain the same trace from the Eq. (3.40), which tells us that we can identify the cosine between the phase $(\phi_L^{ab} - \phi_R^{ab})$ and the dihedral angle ξ_{ab}

$$\cos(\phi_L^{ab} - \phi_R^{ab}) = \cos(\xi_{ab}). \quad (3.44)$$

In [96] it has been shown explicitly that the phase difference $(\phi_R^{ab} - \phi_L^{ab})$ and the dihedral angle ξ_{ab} can be identified up to a \pm sign, which is due to the relative orientation of the bivector and 4-simplex. The angle $(\phi_L^{ab} + \phi_R^{ab})$ can be shown to be proportional to 2π [96].

Hence the semiclassical limit of the Dupuis-Livine model is the same as the EPRL-FK models and is given by the action

$$S = \sum_{a,b \in \sigma} \gamma k_{ab} \xi_{ab}. \quad (3.45)$$

Since in loop quantum gravity the spectrum of the area operator is given by $A_j = \gamma \sqrt{j(j+1)}$, in the large spin limit we have obtained exactly the area-angle Regge action [69, 97].

3.4.3 The asymptotics of constrained propagator model

Let us now finally show that the constrained propagator model also leads to the same semi-classical limit as the EPRL-FK models. We first have to rewrite the amplitude in

terms of group variables. Recall that we can write an $SU(2)$ propagator as

$$P(z_i; w_i) = \int_{SU(2)} dg e^{\sum_i [z_i | g | w_i]} \quad (3.46)$$

Thus taking two copies of such projectors and constraining them both in the $|w\rangle$ and in the $|z\rangle$ spinors, we get that the constrained propagator (3.6) can be written as

$$P_\rho(z_i; w_i) = \int_{SU(2)_L \times SU(2)_R} dg^L dg^R e^{\sum_i [z_i | g^R + \rho^2 g^L | w_i]}. \quad (3.47)$$

The 4-simplex amplitude is now just a simple contraction of 5 such propagators. To compare it however to the amplitude in the DL model, we have to integrate out the $|w_i\rangle$ spinors in order to have the same number of variables. After the $|w_i\rangle$ integration, the amplitude becomes

$$\tilde{A}_\sigma = \int \prod_a dg_a^{L,R} e^{(1+\rho^2)^{-1} [z_b^a | (g_a^{R-1} + \rho^2 g_a^{L-1}) (g_b^R + \rho^2 g_b^L) | z_a^b]}. \quad (3.48)$$

We can see that there is a mixing between left and right sectors – while in the DL model the left and right group elements g^L , g^R are multiplied separately, as in Eq. (3.33), here the relevant group elements become a combination $(g^R + \rho^2 g^L)$. Expanding this in a power series would seem to give us four independent terms. However, since in the large z limit the holomorphic simplicity constraints imply that we have $j^L = \rho^2 j^R$, one can show that only three summations are independent, so the amplitude can be written as

$$\begin{aligned} \tilde{A}_\sigma = & \int \prod_a dg_a^{L,R} \sum_{j_{ab}^{L,R}, J_{ab}} \frac{([z_b^a | g_a^{R-1} g_b^R | z_a^b])^{2j_{ab}^R - 2J_{ab}} (\rho^4 [z_b^a | g_a^{L-1} g_b^L | z_a^b])^{2j_{ab}^L - 2J_{ab}}}{(2j_{ab}^R - 2J_{ab})! (2j_{ab}^L - 2J_{ab})!} \times \\ & \times \frac{(\rho^2 [z_b^a | g_a^{R-1} g_b^L | z_a^b])^{2J_{ab}} (\rho^2 [z_b^a | g_a^{L-1} g_b^R | z_a^b])^{2J_{ab}}}{(2J_{ab})! (2J_{ab})!} (1 + \rho^2)^{-2(j_{ab}^L + j_{ab}^R)}, \end{aligned} \quad (3.49)$$

with the spins satisfying

$$j_{ab}^R \geq J_{ab}, \quad j_{ab}^L \geq J_{ab}. \quad (3.50)$$

This means that the mixed left-right terms never overtake the pure left and right sectors. For the details of this calculation, see the Appendix.

We thus get that the effective action of the constrained propagator model for a single 4-simplex is simply

$$\begin{aligned} \tilde{S}_{eff}(j_{ab}^{L,R}, J_{ab}) = & \sum_{a,b \in \sigma} 2(j_{ab}^R - J_{ab}) \ln [z_b^a | g_a^{R-1} g_b^R | z_a^b] + 2(j_{ab}^L - J_{ab}) \ln [z_b^a | g_a^{L-1} g_b^L | z_a^b] \\ & + \underbrace{2J_{ab} \ln [z_b^a | g_a^{R-1} g_b^L | z_a^b] + 2J_{ab} \ln [z_b^a | g_a^{L-1} g_b^R | z_a^b]}_{\text{mixed}} + \tilde{N}, \end{aligned} \quad (3.51)$$

where the numerical factor \tilde{N} carries all the normalization factors and is a function of the different spins and ρ given by

$$\tilde{N} = \sum_{a,b \in \sigma} 8j_{ab}^L \ln \rho - 2(j_{ab}^L + j_{ab}^R) \ln(1 + \rho^2) - \ln(2j_{ab}^L - 2J_{ab})! - \ln(2j_{ab}^R - 2J_{ab})! - 2 \ln(2J_{ab})! \quad (3.52)$$

We can see that compared with the DL model, the effective action of the constrained propagator model has two additional terms which are underbraced and an additional spin J_{ab} . Nonetheless, we again obtain the closure equation from the variation of spinor $|z\rangle$,

$$\sum_{b \neq a} |z_b^a\rangle \langle z_b^a| = \sum_{b \neq a} j_{ab}^R \mathbb{1}. \quad (3.53)$$

To see how these additional terms change the asymptotics, let us examine the terms in the real part of this action

$$\begin{aligned} & (j_{ab}^L - J_{ab}) \ln \frac{1}{2} \left(|z_b^a|^2 |z_a^b|^2 - (g_a^L \triangleright \vec{V}_b^a) \cdot (g_b^L \triangleright \vec{V}_a^b) \right) + (j_{ab}^R - J_{ab}) \ln \frac{1}{2} \left(|z_b^a|^2 |z_a^b|^2 - (g_a^R \triangleright \vec{V}_b^a) \cdot (g_b^R \triangleright \vec{V}_a^b) \right) \\ & + J_{ab} \ln \frac{1}{2} \left(|z_b^a|^2 |z_a^b|^2 - (g_a^R \triangleright \vec{V}_b^a) \cdot (g_b^L \triangleright \vec{V}_a^b) \right) + J_{ab} \ln \frac{1}{2} \left(|z_b^a|^2 |z_a^b|^2 - (g_a^L \triangleright \vec{V}_b^a) \cdot (g_b^R \triangleright \vec{V}_a^b) \right) + \tilde{N}. \end{aligned} \quad (3.54)$$

At the critical points, we also require the real part of the effective action to be maximized. Since the real part of the action can be written as $\mathbf{Re} \tilde{S}_{eff} = S_{LL} + S_{RR} + S_{RL} + S_{LR}$ and all the coefficients in front of the logarithms are positive, the maximization condition implies that all the four terms have to be maximized independently. Thus, the following critical equations substitute the Eq. (3.38) in DL model:

$$g_a^L \triangleright \hat{v}_b^a = -g_b^L \triangleright \hat{v}_a^b = g_a^R \triangleright \hat{v}_b^a = -g_b^R \triangleright \hat{v}_a^b, \quad \text{where } \hat{v} = \vec{V}/|\vec{V}|. \quad (3.55)$$

When written in terms of spinors $|z\rangle$ and $|z]$, this means that apart from the spinorial orientation condition in Eq.(3.39),

$$g_a^{L-1} g_b^L |z_a^b\rangle = e^{i\phi_L^{ab}} |z_b^a], \quad g_a^{R-1} g_b^R |z_a^b\rangle = e^{i\phi_R^{ab}} |z_b^a],$$

relating $|z_a^b\rangle$ to $|z_b^a]$ up to a phase, we also have two additional phases ψ and θ appearing between the mixed left-right terms

$$g_a^{L-1} g_b^R |z_a^b\rangle = e^{i\psi^{ab}} |z_b^a], \quad g_a^{R-1} g_b^L |z_a^b\rangle = e^{i\theta^{ab}} |z_b^a]. \quad (3.56)$$

Let us now plug in the critical point equations (3.39) and (3.56) into the the effective action to find the semiclassical behavior of the amplitude. The imaginary part of the effective action becomes a function of three spins and four angles, given by

$$\mathbf{Im}\tilde{S}_{eff}(j_{ab}^{L,R}, J_{ab}) = \sum_{a,b \in \sigma} 2(j_{ab}^L - J_{ab})\phi_L^{ab} + 2(j_{ab}^R - J_{ab})\phi_R^{ab} + 2J_{ab}(\psi^{ab} + \theta^{ab}) \quad (3.57)$$

At first sight this is quite different from the effective action of the DL model, with two extra angles and an additional spin label to sum over. Let us notice however, that using the critical point equations (3.39) and (3.56), we can get the relation

$$g_b^{L-1} g_b^R |z_a^b\rangle = e^{i(\psi^{ab} - \phi_L^{ab})} |z_b^a\rangle = e^{i(\phi_R^{ab} - \theta^{ab})} |z_b^a\rangle. \quad (3.58)$$

This condition implies that the additional angles ψ and θ we had to introduce are actually related to the angles ϕ_L and ϕ_R by

$$\psi^{ab} + \theta^{ab} = \phi_L^{ab} + \phi_R^{ab} \pmod{2\pi}. \quad (3.59)$$

This is exactly the combination of angles that allows us to drop the terms proportional to J_{ab} in the action. Hence, we have that the imaginary part of the effective action is exactly the same as the one in DL model,

$$\mathbf{Im}\tilde{S}_{eff}(j_{ab}^{L,R}, J_{ab}) = \sum_{a,b \in \sigma} 2j_{ab}^L \phi_L^{ab} + 2j_{ab}^R \phi_R^{ab} = \mathbf{Im}S_{eff}(j_{ab}^{L,R}) \quad (3.60)$$

The rest of the asymptotic analysis of this action carries over in exactly the same way, as in the EPRL-FK models. Thus, we have proved that the constrained propagator model has in the asymptotic expansion the same effective action as the DL model, which in turn has the same semiclassical limit as the EPRL-FK models.

It is important to note here that in the case of both of the models we have not performed the full asymptotic analysis, which would require the calculation of the Hessian, as it is not necessary for establishing that the models are described by Regge Calculus in the semiclassical limit. We expect that where the two models show differences is exactly in the Hessian and the overall normalization as well as possibly in the higher order terms in the asymptotic expansion.

Chapter 4

Lessons from 3d quantum gravity

Wisdom comes from experience. Experience is often a result of lack of wisdom.

Terry Pratchett

In this chapter we review the notion of Pachner moves and their calculation in 3d $SU(2)$ BF theory, to set up the stage for comparison to the 4-dimensional models. A crucial tool that allows the calculation is a so called *loop identity*, which we derive both in the spin as well as the holomorphic representations.

4.1 Definition of Pachner Moves

To show that a theory defined on a triangulated manifold is topologically invariant, we need a way to relate different triangulations. This is provided by the Pachner moves, which are local replacements of a set of connected simplices by another set of connected simplices.

Theorem 4.1.1. *Any simplicial piecewise linear manifold \mathcal{M} can be transformed into any other simplicial piecewise linear manifold \mathcal{M}' homeomorphic to \mathcal{M} by a finite sequence of Pachner moves.*

For proof, see [68].

Pachner moves are constructed by adding (or removing) vertices, edges, triangles etc. to (from) the existing triangulation. They can be also obtained in d dimensions by gluing

a $(d+1)$ -simplex onto the d -dimensional triangulation. There are several Pachner moves in each dimension and they correspond to changing a configuration of n basic building blocks (d -simplices) into a configuration of m building blocks - we call them n - m Pachner moves. In two dimensions we hence have the moves 2-2, 1-3 moves and their reverse. The

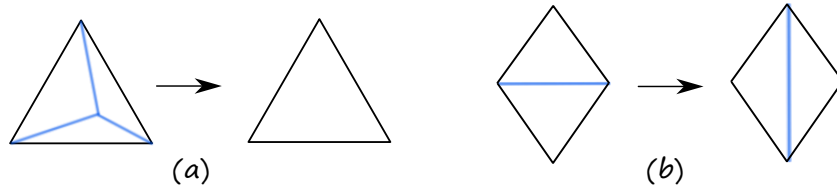


Figure 4.1: Two dimensional Pachner moves: a) 3-1 move, in which three triangles are merged into one by removing a vertex inside; b) 2-2 move, in which two triangles exchange the edge, along which they are glued.

2-2 move corresponds to changing the edge along which two triangles are glued, while the 1-3 move corresponds to adding a vertex inside a triangle and connecting it to the other vertices by three edges, arriving in a configuration with three triangles. Fig. 4.1 shows the inverse. In three dimensions we have 3-2, 4-1 moves and their reverse, see Fig. 4.2. The 3-2 move corresponds to removing an edge, along which three tetrahedra were glued

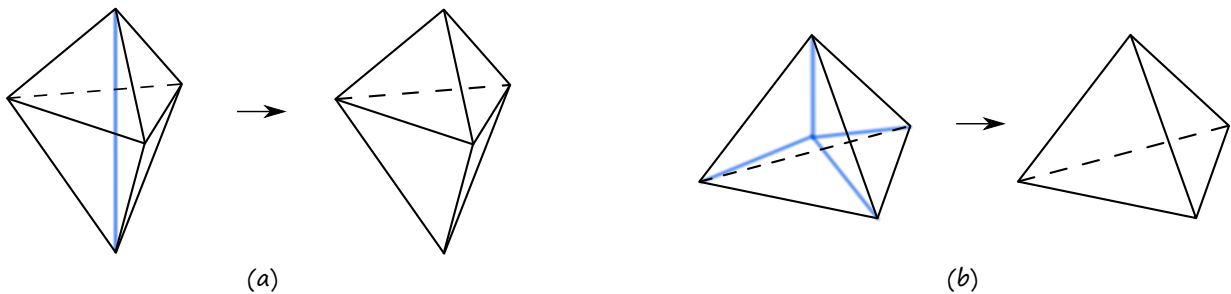


Figure 4.2: Three dimensional Pachner moves: a) 3-2 move, in which three tetrahedra are changed into two tetrahedra by removing a common edge; b) 4-1 move, in which four tetrahedra are combined into one by removing a common vertex.

and changing it into a configuration of two tetrahedra. The 4-1 move is combining four tetrahedra into one tetrahedron through removing a common vertex.

4.2 Fixing the gauge

Recall that 3d Quantum Gravity described by BF theory has two important gauge symmetries – internal rotational “Lorentz” $SU(2)$ gauge symmetry and the *translational* symmetry following from the Bianchi identity $d_\omega F = 0$. In [102] it was shown that on-shell the translational symmetry together with the $SU(2)$ invariance give rise to diffeomorphism invariance of 3d gravity.

Let us now understand how to fix the “Lorentz” gauge on a spin network. Since the volume of the group $SU(2)$ is finite, the gauge fixing amounts to only a change of variables along a maximal tree. We follow [103] in defining the gauge fixing procedure. Consider a graph Γ with E edges and V vertices. Each edge is oriented so that it starts at a source vertex $s(e)$ and ends at target $t(e)$. Consider now a spin network function such that

$$\psi^\Gamma(g_{e_1}, \dots, g_{e_E}) = \psi^\Gamma(h_{s(e_1)}^{-1} g_{e_1} h_{t(e_1)}, \dots, h_{s(e_E)}^{-1} g_{e_E} h_{t(e_E)}). \quad (4.1)$$

Now choose a maximal tree T in Γ , i.e. a collection of $V - 1$ edges which passes through every vertex, without forming loops. Choose a vertex A to be the root¹ of the tree T and label g_{vA}^T the product of group elements g_{e_i} along T that connect vertex v and A . Next we will use Eq. (4.1) with $h_v = g_{vA}^T$, so that $\psi^\Gamma = \psi^\Gamma(G_1^T, \dots, G_E^T)$ with $G_e^T = g_{As(e)}^T g_e g_{t(e)A}^T$.

Now, for any edge $e \in T$, there is a unique path along the tree connecting A and $s(e)$ or $t(e)$. Let us choose this to be $t(e)$, since the other case works in the same way. It follows that $g_{s(e)A}^T = g_e g_{t(e)A}^T$ and so $G_e^T = \mathbb{1}$ for $e \in T$. Hence the procedure for gauge fixing is to set all the group elements on the maximum tree to $\mathbb{1}$ and change all the other to $g_{e_i} = G_{e_i}^T$. Since $\int_{SU(2)} dg = 1$, ending up with empty integrations does not lead to any divergences. In the language of amplitudes written in terms of projectors, this corresponds to replacing the projectors $P(z_i; w_i) = \int_{SU(2)} dg e^{\sum_i [z_i | g | w_i]}$ on the maximal tree by the trivial propagators $\mathbb{1}(z_i; w_i) \equiv e^{\sum_i [z_i | w_i]}$. This procedure carries over to the 4-dimensional case trivially, since $\text{Spin}(4)$ is just a product $SU(2) \times SU(2)$.

We will postpone the discussion of the translational symmetry to until after we have calculated the 4-1 Pachner move, as we will see that it is directly related to the divergence coming from that calculation. It can thus be fixed simply by dividing by this divergent factor. One should now ask how this generalizes to the higher dimensional case we are interested in. It turns out that while the “Lorentz” symmetry is present in 4-dimensional Spin Foam models and can be dealt with in the same fashion, the relation between divergences and translational symmetry is unknown – we will discuss this in later in the thesis.

¹One can show that the gauge fixing procedure is independent of this choice.

4.3 The Loop Identity

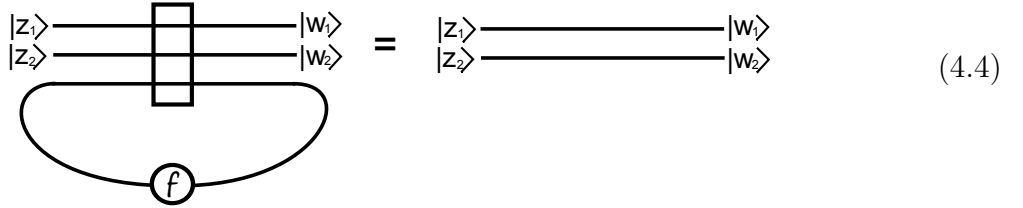
The BF theory partition function is independent of the triangulation Δ . This can be shown by demonstrating its invariance (up to an overall factor) with respect to a finite set of coarse graining moves, constructed out of Pachner moves. The Pachner moves can all be derived from one identity which we will call the loop identity. This identity follows from the coherent state representation of the $SU(2)$ delta function

$$\delta(g) = \int d\tilde{\mu}(z) e^{\langle z|g|z \rangle}, \quad (4.2)$$

where $d\tilde{\mu}(z) = d\mu(z)(\langle z|z \rangle - 1)$. Therefore

$$\begin{aligned} \int d\tilde{\mu}(z_n) P(z_1, \dots, z_n; w_1, \dots, \check{z}_n) &= \int dg e^{\sum_{i=1}^{n-1} \langle z_i|g|w_i \rangle} \int d\tilde{\mu}(z_n) e^{\langle z_n|g|z_n \rangle} \\ &= \int dg e^{\sum_{i=1}^{n-1} \langle z_i|g|w_i \rangle} \delta(g) \\ &= e^{\sum_{i=1}^{n-1} \langle z_i|w_i \rangle} \\ &= \mathbb{1}(z_1, \dots, z_{n-1}; w_1, \dots, w_{n-1}), \end{aligned} \quad (4.3)$$

which is represented graphically by



$$(4.4)$$

Since each closed loop of the BF partition function (2.47) has a factor of $2j_f + 1$ we will use the convention that two lines are contracted with $d\mu(z)$ as in (2.72), however, the contraction of a line with itself, i.e. a loop, is contracted with the measure $d\tilde{\mu}(z)$ as in (4.4). An alternative way would be to use the homogeneity map to keep track of this face weight.

4.4 Alternative method

The expression for the loop identity we have just derived, while compact, does not generalize straightforwardly to the case of 4-dimensional QG models with simplicity constraints

(due to the presence of the group integrals). We will thus redo the above calculation with the projector written in terms of only spinors without group integration.

We expect that the loop identity (4.3) applied to the projector (2.86) implies that

$$\sum_{j_n} (2j_n + 1) \int d\mu(z_n) \frac{\left(\sum_{i < j} [z_i | z_j] [w_i | w_j] \right)^J}{J!(J+1)!} = \prod_{i=1}^{n-1} \frac{[z_i | w_i]^{2j_i}}{(2j_i)!}, \quad (4.5)$$

where the integration is performed with $w_n = \check{z}_n$. Below we will directly show this. Let us perform the integration on the LHS explicitly by using the homogeneity map to keep track of the $1/(J+1)!$ and the face weight $(2j_n + 1)$ and then summing over j_i . Namely, let us use the homogeneity maps $\tau^J \rightarrow 1/(J+1)!$ and $\tau'^{2j_n} \rightarrow (2j_n + 1)$. The result is then

$$\int d\mu(z_n) \exp \left(\tau \sum_{i < j < n} [z_i | z_j] [w_i | w_j] - \tau \tau' \sum_{i < n} \langle z_n | z_i \rangle [w_i | z_n] \right) = \frac{e^{\tau \sum_{i < j < n} [z_i | z_j] [w_i | w_j]}}{\det \left(\mathbb{1} - \tau \tau' \sum_{i < n} |w_i\rangle [z_i| \right)}. \quad (4.6)$$

To continue, we have to be able to evaluate the determinant in the denominator. This is thankfully not too difficult, as the matrix in question is just a 2×2 matrix made up by spinors. Indeed, the following lemma comes in handy

Lemma 4.4.1. *Let $M = \mathbb{1} - \sum_i C_i |A_i\rangle [B_i|$ then*

$$\det M = 1 - \sum_i C_i [B_i | A_i] + \sum_{i < j} C_i C_j [A_i | A_j] [B_i | B_j].$$

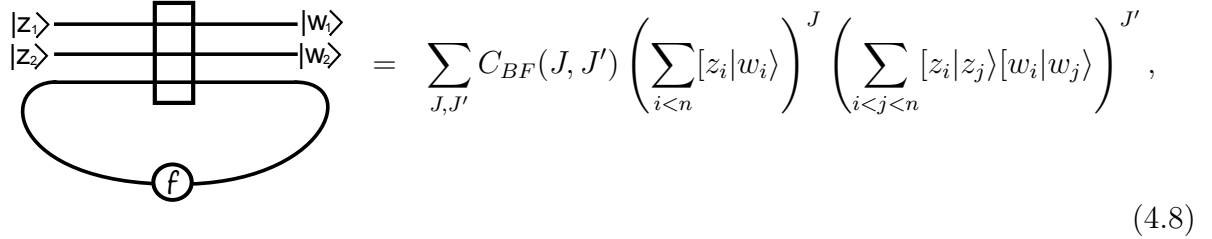
The proof is given in Appendix A.4.

Using this result, we can immediately find the determinant in (4.6). In our case, all $C_i = \tau \tau'$, hence we get that the loop identity for the homogenized projector P_τ becomes

$$\frac{e^{\sum_{1 \leq i < j < n} \tau \tau' [z_i | z_j] [w_i | w_j]}}{1 - \sum_{i \neq n} \tau \tau' [z_i | w_i] + \sum_{1 \leq i < j < n} \tau^2 \tau'^2 [z_i | z_j] [w_i | w_j]}. \quad (4.7)$$

Now we can expand both the numerator and the denominator in a power series and then use the homogeneity map to restore the $1/(J+1)!$ terms and the face weight. This allows

us to get the loop identity for the projector (2.86)



$$= \sum_{J, J'} C_{BF}(J, J') \left(\sum_{i < n} [z_i | w_i] \right)^J \left(\sum_{i < j < n} [z_i | z_j] [w_i | w_j] \right)^{J'} , \quad (4.8)$$

where we have defined the coefficient $C_{BF}(J, J')$ to be given by

$$C_{BF}(J, J') = \sum_K (-1)^{J'-K} \frac{(J + J' - K)!(J + 2J' - 2K + 1)}{J!(J' - K)!K!(J + 2J' - K + 1)!} . \quad (4.9)$$

At first glance, this is a worrisome result, as we do not only get the trivial projection (raised to power J), but also an unwanted *mixing* term (raised to power J'). Notice though, that we have an additional free sum over the variable K in the definition of the coefficient. We can actually explicitly evaluate this sum over K to find the expected result

$$C_{BF}(J, J') = \frac{\delta_{J', 0}}{J!} . \quad (4.10)$$

Hence only the $J' = 0$ term is non-vanishing, so the mixing terms always drop out in BF theory. We thus recover the result (4.5) that we set out to prove. This calculation readily is generalized in the following section to the case with simplicity constraints. The major difference in this case is the lack of the cancellation of the mixing terms.

4.5 Invariance under Pachner moves and symmetry

We will now proceed to show the invariance of the 3-dimensional $SU(2)$ BF theory under 3–2 and 4–1 Pachner moves using the language of spinors. In the case of 4–1 move we find a divergence directly related to the translational symmetry.

3–2 move

As can be seen in the Fig. 4.2 a), the configuration of three tetrahedra in the 3–2 move is glued along one edge. This corresponds to a loop of a single strand in the cable diagram, see Fig.4.3.

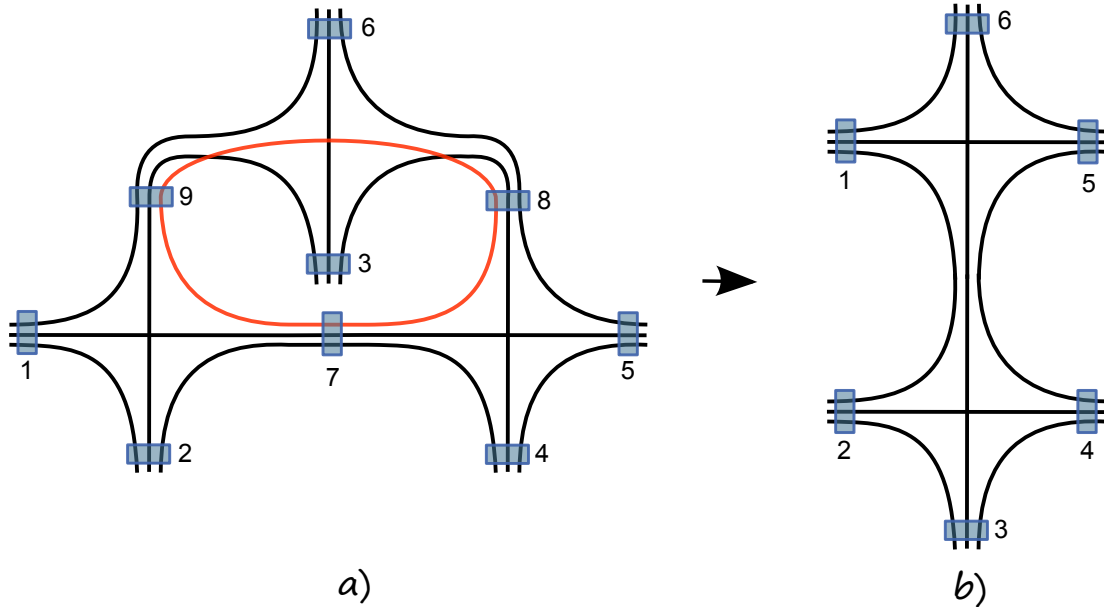


Figure 4.3: a) Cable diagram for the 3-2 move. The internal loop is colored. b) After gauge-fixing projectors 7 and 9 and performing loop identity on projector 8, the diagram reduces to gluing of two tetrahedral graphs.

By choosing a maximum tree (with a root at the projector 1) in the diagram, we can gauge fix the projectors number 7 and 9. This allows us to apply the loop identity (4.3) to integrate out the strand number 10 by performing the group integral in projector number 8. We can identify now that the resulting cable diagram is exactly that of the two tetrahedra glued together, see Fig. 4.2 b). Hence it is immediate that the $SU(2)$ BF theory is invariant under the 3–2 Pachner move, as the two configurations are gauge equivalent.

4–1 move

The configuration of four tetrahedra in the 4–1 move shares in total four edges, which corresponds to four loops in a cable diagram, see Fig. 4.4 a).

We choose a maximum tree with a root at vertex 1, which allows us to gauge fix the projectors number 5, 6 and 9. We can now apply the loop identity (4.3) to the projector 10 to remove the blue loop. Similarly we can apply the loop identities to projectors 7 and 8 to remove the yellow and green loops respectively. This leaves us with the last loop and no projectors left inside the graph, as in Fig. 4.4 b). This final loop corresponds to the

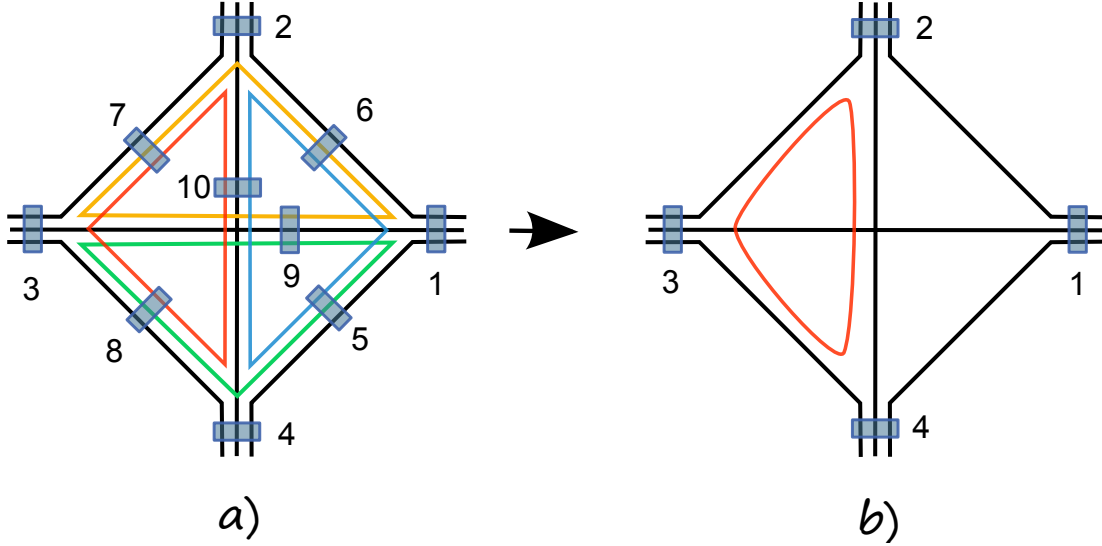


Figure 4.4: a) Cable diagram for the 4–1 move. The 4 different loops are colored. b) After applying three loop identities we are left with a tetrahedral cable graph with an insertion of one loop.

following integral

$$\begin{aligned}
 \int d\tilde{\mu}(z)e^{\langle z|z\rangle} &= \sum_j \int d\tilde{\mu}(z) \frac{\langle z|z\rangle^{2j}}{(2j)!} = \sum_j (2j+1) \int d\mu(z) \frac{\langle z|z\rangle^{2j}}{(2j)!} \\
 &= \sum_j (2j+1)\chi^j(\mathbb{1}) = \delta_{SU(2)}(\mathbb{1}).
 \end{aligned} \tag{4.11}$$

Hence, we have shown that the BF partition function is invariant under the 4–1 move up to an overall divergent factor. The divergence we obtain in $SU(2)$ BF theory is exactly a $SU(2)$ delta function $\delta_{SU(2)}(\mathbb{1}) = \sum_j (2j+1)^2$. In [102] it was shown that this is the same as the volume of the $\mathfrak{su}(2)$ Lie algebra. If we put on a cut-off Λ on spins, then the divergence scales as $\sum_j (2j+1)^2 \sim \Lambda^3$. Since in 3d spin is proportional to length, we get a divergence that corresponds to the translation symmetry of placing the extra vertex anywhere in the 3-dimensional space. In [104] it was shown that the dominant contribution to this divergence comes from “spikes”, where the vertex is placed far out of the tetrahedron. A correct Fadeev-Popov procedure introduced in [102] divides the amplitude by exactly this divergence, so the Ponzano-Regge model is invariant after gauge fixing under both the 3–2 and 4–1 Pachner moves. This gauge fixing procedure was subsequently refined in [105, 106, 107, 108] to lead to a complete definition of 3 dimensional manifold invariant.

Chapter 5

Loop identity with constraints

It is a mistake to think you can solve any major problem just with potatoes.

Douglas Adams
Life, the Universe and Everything

In this chapter, we evaluate the simplicity constrained version of the loop identity for both of the holomorphic models we introduced previously. In the case of the constrained propagator model, the difference from the topological result is the presence of mixing of strands that exchanges the trivial propagators and delta functions with more complicated operators. In the case of the DL model we obtain a rather complicated expression, which motivates us to focus on the other model. We finish with discussing some interesting results in a 2 dimensions.

5.1 Toy Loop

To capture the essence of the computation without too much complexity, let us start with repeating the calculation of the BF loop identity, but with the constrained propagator $P_\rho(z_i; w_i)$ (3.6) rather than the SU(2) projector. We will follow the treatment of the loop identity from Section 4.4. We will thus find the loop identity for the generating functional

$$G_\tau(z_i; w_i) = e^{\tau \sum_{i < j} [z_i | z_j] [w_i | w_j]}$$

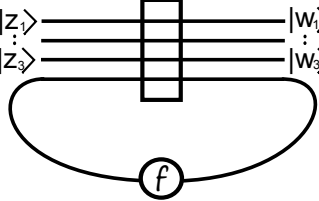
and at the end of the calculation use the homogeneity map to get the loop identity for $P_\rho(z_i; w_i)$ by changing $\tau^J \rightarrow F_\rho(J)/(J+1)!$. We also want to be able to insert a face weight, which is a function of the spin we will sum over. This face weight could be *a priori* arbitrary, but for the sake of definiteness, let us choose it to be $(2j+1)^\eta$ with $\eta \in \mathbb{R}$ being a free parameter, which keeps track of divergence properties of the Spin Foam model. The method we use allows us of course to modify the face weight to an arbitrary function of spin. To insert the face weight, we follow the calculation in BF theory and rescale the spinor in the loop by an additional factor of τ' , which will keep track of homogeneity of that specific spinor. At the end of the calculation we can restore the face weight by replacing $\tau'^{2j} \rightarrow (2j+1)^\eta$ in the series expansion. Let us now calculate the constrained loop identity:

$$\int d\mu_\rho(z_4) e^{\tau \sum_{i<j<4} [z_i|z_j][w_i|w_j] - \tau\tau' \sum_{i<4} \langle z_4|z_i \rangle [w_i|z_4]} = \frac{e^{\tau \sum_{i<j<4} [z_i|z_j][w_i|w_j]}}{\det \left(\mathbb{1} - \frac{\tau\tau'}{1+\rho^2} \sum_{i<4} |w_i\rangle [z_i| \right)}. \quad (5.1)$$

Unsurprisingly, we get nearly the same result as in Section 4.4, the difference being the additional factor of $1/(1+\rho^2)$, which arises from the modified integration measure $d\mu_\rho(z)$. Of course, the τ also carries a hypergeometric function of ρ . We can again use the lemma 4.4.1 to evaluate the determinant. We arrive thus at the result

$$\begin{aligned} \int d\mu_\rho(z_4) G_\tau(z_1, \dots, \tau' z_4; w_1, \dots, \check{z}_4) &= \frac{e^{\tau \sum_{i<j<4} [z_i|z_j][w_i|w_j]}}{1 - \frac{\tau\tau'}{1+\rho^2} \sum_{i<4} [z_i|w_i] + \sum_{i<j<4} \frac{\tau^2\tau'^2}{(1+\rho^2)^2} [z_i|z_j][w_i|w_j]} \\ &= e^{\tau \sum_{i<j<4} [z_i|z_j][w_i|w_j]} \sum_{N,M} \frac{(N+M)!}{N!M!} \left(\frac{\tau\tau'}{1+\rho^2} \right)^{N+2M} \left(\sum_{i<4} [z_i|w_i] \right)^N \left(- \sum_{i<j<4} [z_i|z_j][w_i|w_j] \right)^M \end{aligned} \quad (5.2)$$

We can now expand the exponential, combine the mixing terms and use the homogeneity map to reintroduce the face weight and the hypergeometric function of ρ . We hence find that the constrained loop identity for $P_\rho(z_i; w_i)$ is given by



$$\begin{aligned} \begin{array}{c} |z_i\rangle \\ |z_j\rangle \\ |z_k\rangle \end{array} \begin{array}{c} \text{---} \\ \text{---} \\ \text{---} \end{array} \begin{array}{c} |w_i\rangle \\ |w_j\rangle \\ |w_k\rangle \end{array} = \sum_{J,J'} C_\rho(J, J') \left(\sum_{i<n} [z_i|w_i] \right)^J \left(\sum_{i<j<n} [z_i|z_j][w_i|w_j] \right)^{J'} \end{aligned} \quad (5.3)$$

with the coefficient $C_\rho(J, J')$ given by

$$C_\rho(J, J') = \sum_K (-1)^{J'-K} \frac{(J+J'-K)!(J+2J'-2K+1)^\eta F_\rho(J+2J'-2K)}{J!(J'-K)!K!(J+2J'-K+1)! (1+\rho^2)^{J+2J'-2K}}, \quad (5.4)$$

where $F_\rho(J) = {}_2F_1(-J-1, -J; 2; \rho^4)$. We have hence arrived at an expression very similar to the one in BF theory – we again got the trivial propagation terms $\sum_{i < 4} [z_i | w_i \rangle$ together with additional mixing terms like $\sum_{i < j < 4} [z_i | z_j \rangle [w_i | w_j \rangle$. Unlike in the BF loop identity however, there is no miraculous cancellation of the $J' \neq 0$ terms, unless we choose $\rho = 0$ and $\eta = 1$, i.e. we reduce this to SU(2) BF theory. Hence the way in which simplicity constraints break the topological symmetry is by introducing additional mixing terms in the loop identity. We can represent this graphically as

$$(5.5)$$

5.2 The Constrained Loop Identity

We are now going to see that the loop identity we need for Pachner moves is somewhat different with the one we considered in the previous section. When we glue together 4-simplices, we need to glue them along their boundaries, necessitating the gluing of two propagators, i.e. we should work with $P_\rho \circ P_\rho$, rather than a single P_ρ . The reason for this being that in our model the propagator P_ρ is inserted around each vertex and we get the composition of them along an edge. Since P_ρ is not a projector unless $\rho = 0$ we have $P_\rho \circ P_\rho \neq P_\rho$. Additionally, the loops arising in all the Pachner moves always are composed of three groups of propagators $P_\rho \circ P_\rho$, rather than the single one we have considered. Fortunately, two of these can be always gauge fixed by a proper choice of a maximal tree, so that we have to consider the loop identity shown in Fig.5.1. In BF theory the gauge-fixing reduces the projectors to trivial propagators $\mathbb{1}(z_i; w_i)$, so we did not have to worry about this issue.

We thus have to first find the equivalent of the trivial propagator in the constrained case, i.e. the analog of setting $g = \mathbb{1}$ in (2.80) to get (2.73) but for the propagator (3.6). We thus have to restore the group integration. Fortunately, by tracking homogeneity for each term, we know that

$$\frac{\left(\sum_{i < j} [z_i | z_j \rangle [w_i | w_j \rangle\right)^J}{J!(J+1)!} = \sum_{\sum j_i = J} \int dg \prod_{i=1}^4 \frac{[z_i | g | w_i \rangle^{2j_i}}{(2j_i)!}. \quad (5.6)$$

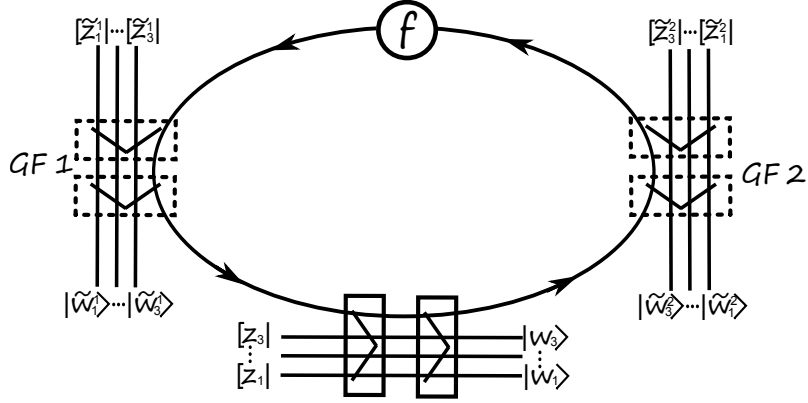


Figure 5.1: Loop identity with for the constrained projector with two extra gauge fixed projectors

Setting this $SU(2)$ group element to identity and summing over all J allows us to get the partially gauge fixed propagator, which we denote $\mathbb{1}_\rho$

$$\mathbb{1}_\rho(\tilde{z}_i; \tilde{w}_i) = \sum_J {}_2F_1\left(-\frac{J}{2} - 1, -\frac{J}{2}; 2; \rho^4\right) \frac{(\sum_i [\tilde{z}_i | \tilde{w}_i])^J}{J!}. \quad (5.7)$$

Note that for the convenience of notation later, we will always add a tilde on the spinors which belong to the partially gauge fixed propagator. As in the case of the propagator, we find that setting $\rho = 0$ we recover the BF trivial propagator $\mathbb{1}(z_i; w_i)$, as we would expect. We can now use the homogeneity map to define a homogenized trivial propagator $\mathbb{1}_{\tilde{\tau}}$ as

$$\mathbb{1}_{\tilde{\tau}} = e^{\tilde{\tau} \sum_i [\tilde{z}_i | \tilde{w}_i]} \quad \text{with} \quad \tilde{\tau}^J \rightarrow F_\rho(J/2) \quad \text{for} \quad \mathbb{1}_{\tilde{\tau}} \rightarrow \mathbb{1}_\rho. \quad (5.8)$$

We thus have arrived at the expression for the gauge fixed propagators that are necessary for the loop identity. We will have to consider however $P_\rho \circ P_\rho$ and $\mathbb{1}_\rho \circ \mathbb{1}_\rho$, rather than single propagators, as we have mentioned above. We will thus use the following homogeneity maps: for the pair of gauge-fixed propagators we will have

$$\mathbb{1}_{\tilde{\tau}} \circ \mathbb{1}_{\tilde{\tau}} = e^{\tilde{\tau} \sum_i [\tilde{z}_i | \tilde{w}_i]} \quad \text{with} \quad \tilde{\tau}^J \rightarrow \frac{F_\rho(J/2)^2}{(1 + \rho^2)^J} \quad \text{for} \quad \mathbb{1}_{\tilde{\tau}} \circ \mathbb{1}_{\tilde{\tau}} \rightarrow \mathbb{1}_\rho \circ \mathbb{1}_\rho, \quad (5.9)$$

while for the pair of propagators P_ρ we get

$$G_\tau \circ G_\tau = e^{\tau \sum_{i < j} [z_i | z_j] [w_i | w_j]} \quad \text{with} \quad \tau^J \rightarrow \frac{F_\rho(J)^2}{(1 + \rho^2)^{2J} (J + 1)!} \quad \text{for} \quad G_\tau \circ G_\tau \rightarrow P_\rho \circ P_\rho. \quad (5.10)$$

With this, we are ready to perform the calculation of this loop identity. The addition of the extra two pairs of gauge-fixed propagators leads to very simple contractions, using our results of spinor Gaussian integrals in the Appendix. Integrating over the three strands inside the loop leads to nearly the same calculation as in the previous section, with the difference being the addition of the trivial propagation in the extra strands connected to the gauge-fixed propagators. Using the homogeneity map, we finally find that the constrained loop identity is given by

$$\begin{aligned}
& \text{Diagrammatic Loop Identity} = \sum_{A, B, J, J'=0}^{\infty} \frac{N(A, B, J, J', \rho)}{A!B!J!J'} \times \\
& \times \underbrace{\left(\sum_{i=1}^3 [\tilde{z}_i^1 | \tilde{w}_i^1 \rangle] \right)^A}_{GF1} \underbrace{\left(\sum_{i=1}^3 [\tilde{z}_i^2 | \tilde{w}_i^2 \rangle] \right)^B}_{GF2} \underbrace{\left(\sum_{i=1}^3 [z_i | w_i \rangle] \right)^J}_{\text{Trivial projection}} \underbrace{\left(\sum_{i < j < 4} [z_i | z_j \rangle [w_i | w_j \rangle] \right)^{J'}}_{\text{Mixing terms}}, \tag{5.11}
\end{aligned}$$

with the coefficient $N(A, B, J, J', \rho)$ given by

$$\begin{aligned}
N(A, B, J, J', \rho) \equiv & \sum_{K=0}^{J'} \frac{J!(J+K)!(J+2K+1)^\eta}{K!(J'-K)!(J+J'+K+1)!} \frac{(-1)^K}{(1+\rho^2)^{(A+B+12K+7J+2J')}} \times \\
& \times F_\rho^2(J+J'+K) F_\rho^2((A+J)/2+K) F_\rho^2((B+J)/2+K),
\end{aligned}$$

where we have defined $F_\rho(J) \equiv {}_2F_1(-J-1, -J; 2; \rho^4)$. The variables $|\tilde{z}_i^1\rangle, |\tilde{w}_i^1\rangle$ appear in the strands attached to the first gauge fixing term, similarly $|\tilde{z}_i^2\rangle, |\tilde{w}_i^2\rangle$ appear in the second gauge fixing, while $|z_i\rangle, |w_i\rangle$ are labelled for the strands we haven't gauge fixed. The face weight coupling constant η should be fixed by requirements of divergence, which we will discuss in a later section. A more detailed calculation of this loop identity can be found in the Appendix.

Even though the expression in Eq.(5.11) has a few layers of summations like a Russian nesting doll and the coefficients look complicated, the physical meaning behind the expression is quite clean – up to a weight, we get the trivial propagation, like in BF theory, but we also get additional mixing terms for $J' \neq 0$. We will study the properties of this identity in section 6.3.

For the purpose of calculating the 4-dimensional Pachner moves, it will be convenient to again define an exponentiated expression for this loop identity, which can then be transformed into the proper expression by the homogeneity map. Before using the homogeneity

map in Eq. (5.11), we would have an expression purely in terms of τ 's that can be exponentiated. We hence define the exponentiated loop identity to have the following very simple form:

$$L_\tau(z_i, w_i; \tilde{z}_i^1, \tilde{w}_i^1; \tilde{z}_i^2, \tilde{w}_i^2) = \exp\left(\sum_{i=1}^3 \tilde{\tau}_1[\tilde{z}_i^1|\tilde{w}_i^1] + \tilde{\tau}_2[\tilde{z}_i^2|\tilde{w}_i^2] + \tau_N[z_i|w_i] + \tau_M \sum_{i < j < 4} [z_i|z_j][w_i|w_j]\right). \quad (5.12)$$

The full loop identity can then be recovered through the following homogeneity map:

$$\tau_N^J \tau_M^{J'} \rightarrow \sum_{K=0}^{J'} \frac{(-1)^K (J+K)! J!}{K! (J'-K)!} (J+2K+1)^\eta \tau^{J'-K} \left(\frac{\tilde{\tau}_1 \tilde{\tau}_2 \tau}{(1+\rho^2)^3} \right)^{J+2K} \quad (5.13)$$

and the $\tilde{\tau}$'s and τ keep track of the F_ρ factors according to the rules given in Eq. (5.9) and Eq. (5.10).

5.3 The Loop Identity for the DL model

For comparison, let us now calculate the loop identity for the exponentiated DL propagator (3.28). We will perform the calculation first without any face weight for clarity and then modify it to accommodate arbitrary face weights. As in the previous section, we need to begin by obtaining the gauge-fixed propagators.

To study the gauge-fixed propagator, we need to reintroduce the group elements to the propagator P_{DL} as

$$\int \left\{ \prod_{i=1}^4 d\mu_\rho(z_i) \right\} \int dg_{L,R}^{1,2} e^{\sum_i [w_i^L | g_L^1 | z_i] + \rho [w_i^R | g_R^1 | z_i] + \langle z_i | g_L^2 | v_i^L \rangle + \rho \langle z_i | g_R^2 | v_i^R \rangle}. \quad (5.14)$$

Gauge fixing by choosing a maximum tree in the cable graph allows for setting all $g_L^1, g_R^1, g_L^2, g_R^2$ to identity. We find thus that the gauge-fixed constrained projector in the DL model is given by

$$P_{DL}^0 = e^{\frac{1}{1+\rho^2} \sum_i ([w_i^L | v_i^L] + \rho [w_i^L | v_i^R] + \rho [w_i^R | v_i^L] + \rho^2 [w_i^R | v_i^R])} \quad (5.15)$$

It is worthwhile to notice that, both in the full DL propagator and its gauge-fixed variant, there is a mixing between left and right strands. This mixing doesn't just occur for the spinors, but for spins as well. We show this in the Appendix.

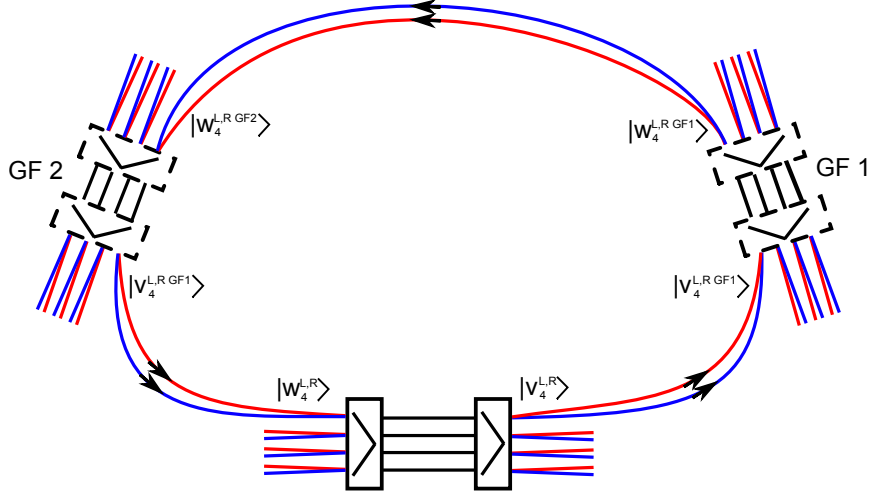


Figure 5.2: Loop identity for the DL propagator with two extra gauge fixed ones.

Since the gauge-fixed DL propagators (5.15) are nontrivial, let us calculate the loop identity with two of them, as in Fig. 5.2.

Recall from Eq. (3.28) that the exponentiated DL projector can be written as

$$P_{DL}^\tau = e^{\tau A \sum_{i<j} w_{ij} v_{ij} - \frac{\tau B}{16} \sum \epsilon^{abcd} \epsilon^{ijkl} w_{ab} w_{cd} v_{ij} v_{kl}},$$

where the w_{ij}, v_{ij} are antisymmetric and are combinations of left and right spinors also carrying additional homogeneity factors. The only spinors that we need to integrate over in the loop identity are w_4 and v_4 plus the ones coming from gauge-fixed propagators. Let us track what happens when we contract the strand between the full DL propagator and the gauge-fixed propagator number 1. The gluing constraints are going to be $v_4 = \check{v}_4^{GF1}$, so the integral of that strand will result in

$$\begin{aligned} |v_4^L\rangle &\mapsto -\frac{1}{1+\rho^2} (|w_4^{L\ GF1}\rangle + \rho |w_4^{R\ GF1}\rangle) \\ |v_4^R\rangle &\mapsto -\frac{1}{1+\rho^2} (\rho |w_4^{L\ GF1}\rangle + \rho^2 |w_4^{R\ GF1}\rangle) \end{aligned} \tag{5.16}$$

The minus sign is due to the antisymmetry $[w_i|v_i] = -[v_i|w_i]$. Let us now contract the strand between the first and second gauge-fixed propagators. For this integral, we have a

contraction $w_4^{GF1} = \check{w}_4^{GF2}$. This integral results in

$$\begin{aligned} |w_4^{L\ GF1}\rangle &\mapsto \frac{1}{1+\rho^2} (|v_4^{L\ GF2}\rangle + \rho|v_4^{R\ GF2}\rangle) \\ |w_4^{R\ GF1}\rangle &\mapsto \frac{1}{1+\rho^2} (\rho|v_4^{L\ GF2}\rangle + \rho^2|v_4^{R\ GF2}\rangle). \end{aligned} \quad (5.17)$$

Now recall that v_{ij} in the DL propagator are given by $v_{ij} \equiv \frac{\tau_v^L}{1+\rho^2}[v_i^L|v_j^L\rangle + \frac{\rho^2\tau_v^R}{1+\rho^2}[v_i^R|v_j^R\rangle]$. The above contractions lead to the following change for v_{i4} :

$$v_{i4} \mapsto -\frac{\tau_v^L}{(1+\rho^2)^2} (|v_i^L|v_4^{L\ GF2}\rangle + \rho|v_i^L|v_4^{R\ GF2}\rangle) + \frac{\rho^2\tau_v^R}{(1+\rho^2)^2} (\rho|v_i^R|v_4^{L\ GF2}\rangle + \rho^2|v_i^R|v_4^{R\ GF2}\rangle). \quad (5.18)$$

The last gluing constraint is $v_4^{GF2} = \check{w}_4$, which will bring us one last factor of $(1+\rho^2)^{-1}$. Let us check what happens to P_{DL} under the above substitution and this gluing constraint. The term proportional to τ_A in the propagator (3.28) that we ultimately have to integrate can be now written as

$$[w_4^L|A_L|w_4^L] + [w_4^R|A_R|w_4^R] + [w_4^L|\rho A_L|w_4^R] + [w_4^R|\frac{A_R}{\rho}|w_4^L], \quad (5.19)$$

where we have introduced the matrices mixing left and right sectors given by

$$\begin{aligned} A_L &= \frac{\tau_w^L}{(1+\rho^2)^3} \sum_{i=1}^3 |w_i^L\rangle ([v_i^L|\tau_v^L + [v_i^R|\rho^2\tau_v^R\rho]) \\ A_R &= \frac{\rho^2\tau_w^R}{(1+\rho^2)^3} \sum_{i=1}^3 |w_i^R\rangle ([v_i^L|\rho\tau_v^L + [v_i^R|\rho^2\tau_v^R\rho^2]). \end{aligned} \quad (5.20)$$

While the term proportional to τ_B looks a lot more fearsome, it still has only one instance of v_{i4} in each of its terms. The main difference lies in the slightly worrisome fact that unlike in the case of terms proportional to τ_A , here every single term has an instance of v_{i4} , so all of them will enter the loop identity! A little bit of perseverance makes us realize that the main difference actually lies in changing $\sum_i \rightarrow \sum_i \epsilon_{ijk}\epsilon_{lmn}w_{jk}v_{lm}$ and proper normalization. It is then not too difficult to see that the term proportional to τ_B is also going to be

$$[w_4^L|B_L|w_4^L] + [w_4^R|B_R|w_4^R] + [w_4^L|\rho B_L|w_4^R] + [w_4^R|\frac{B_R}{\rho}|w_4^L], \quad (5.21)$$

where the matrices mixing the left and right sectors for this term are given by the slightly more complicated expressions:

$$\begin{aligned}
B_L &= \frac{\tau_w^L}{(1 + \rho^2)^3} \sum_{i,j,k=1}^3 \sum_{l,m,n=1}^3 \frac{\epsilon_{ijk}\epsilon_{lmn}}{4} w_{jk} v_{mn} |w_i^L\rangle ([v_l^L | \tau_v^L + [v_l^R | \rho^2 \tau_v^R \rho) \\
B_R &= \frac{\rho^2 \tau_w^R}{(1 + \rho^2)^3} \sum_{i,j,k=1}^3 \sum_{l,m,n=1}^3 \frac{\epsilon_{ijk}\epsilon_{lmn}}{4} w_{jk} v_{mn} |w_i^R\rangle ([v_l^L | \rho \tau_v^L + [v_l^R | \rho^2 \tau_v^R \rho^2).
\end{aligned} \tag{5.22}$$

Hence with the combinations $M_L = \tau_A A_L - \tau_B B_L$ and $M_R = \tau_A A_R - \tau_B B_R$ that naturally present themselves, we can finally write down the loop identity for the DL model without any face weight as

$$\begin{aligned}
\text{Diagram} &= \int d\mu(w_4^{L,R}) e^{[w_4^L | M_L | w_4^L] + [w_4^R | M_R | w_4^R] + [w_4^L | \rho M_L | w_4^R] + [w_4^R | \frac{M_R}{\rho} | w_4^L] + \tau_A \sum_{i < j < 4} w_{ij} v_{ij}} \\
&= \frac{e^{\tau_A \sum_{i < j < 4} w_{ij} v_{ij}}}{1 - \text{Tr}(M_L + M_R) + \det(M_L + M_R)}.
\end{aligned} \tag{5.23}$$

The final loop identity can be obtained by expanding this expression in a power series and using the homogeneity maps to restore all the factorials, which might seem a bit daunting, but is clearly doable. To calculate the loop identity with an arbitrary face weight, we would have to track the homogeneity of the left and right sectors separately. We show in the Appendix that this is possible, but results in a rather monstrous expression. However, if we satisfy ourselves with face weights that depend only on the sum $j^L + j^R$, we can get away with a simple expression – we only need to rescale both M_L and M_R in Eq. (5.23) by a single factor of τ , which allows us to track a face weight of $\mathcal{A}_f(j^L + j^R)$ by $\tau^{j^L + j^R}$.

As we can see, the technique of the homogeneity map applies also to the DL model. While we could in principle continue to use it, the calculations with our model using the fully constrained propagator are greatly simplified. As such, we will only follow with the simpler model, but leave these results here in case some brave individuals decide to use the model that is more similar to the standard EPRL framework.

5.4 Exact results in 2d

It is interesting to notice that in the case of the constrained propagator, the loop identity would be so much simpler if there was no mixing of strands. As we have seen, this happens

naturally when we restrict the face weights and work in $\rho = 0$ limit, i.e. for BF theory. There is also another case where things simplify, though one that is of less physical interest – consider only two strands per propagator. In this 2-dimensional case, the loop identity simply cannot have any mixed strands. While this case is in some ways trivial, as the group integration of $[z_1|g|w_1]^{2j_1}[z_2|g|w_2]^{2j_2}$ sets $j_1 = j_2$, we can nonetheless consider arbitrary modifications of the propagator, face weight and the measure (at least Gaussian ones) in this 2d SU(2) propagator model.

Let us consider the propagator with an arbitrary function of spin

$$P_{2d} = \sum_J f(J) \frac{([z_1|z_2][w_1|w_2])^J}{J!(J+1)!}, \quad (5.24)$$

together with an arbitrary face weight $\mathcal{A}_f(J)$ and the measure of integration modified to $d\mu_\alpha(z) = \frac{\alpha^2}{\pi^2} e^{-\alpha|z|} d^2z$. If this is still too conservative for one's tastes, one can at the end of the calculation substitute α^J into another arbitrary function of spin, using the homogeneity map technique. We will use the generalized propagators G_τ we have introduced in Eq. (3.15) and then restore our arbitrary functions with a homogeneity map. We will restore the face weights in the same way as in the previous sections.

For the equivalent of the toy loop identity, integrating $|w_2\rangle = |z_2\rangle$, we trivially get

$$\begin{array}{c} |z\rangle \text{---} \square \text{---} |w\rangle \\ \text{---} \circ \text{---} \end{array} = \frac{1}{\det(\mathbb{1} - \frac{\tau\tau'}{\alpha} |w_1\rangle\langle z_1|)} = \sum_J \left(\frac{\tau\tau'}{\alpha} |z_1\rangle\langle w_1| \right)^J \xrightarrow{H} \sum_J \frac{f(J)\mathcal{A}_f(J)}{\alpha^J(J+1)!} |z_1\rangle\langle w_1|^J. \quad (5.25)$$

Interestingly enough, we can perform this loop identity for an arbitrary number of propagators around the loop, without any need for gauge fixing. Even more, each of these propagators can carry a different function of spin. To see this, let us look at the example of three propagators around the loop, with the identifications $|w_2^A\rangle = |z_2^C\rangle$, $|w_2^C\rangle = |z_2^B\rangle$ and $|w_2^B\rangle = |z_2^A\rangle$. Note that these identifications each introduce a minus sign, so we get

$$\begin{aligned} \int \left(\prod_{a \in \{A,B,C\}} d\mu_\alpha(w_2^a) G_{2d}^a \right) &= \frac{1}{\det \left(\mathbb{1} - \frac{\tau_A \tau_B \tau_C \tau'}{\alpha^3} [w_1^A|z_1^C][w_1^C|z_1^B]\langle z_1^A| \langle w_1^B| \right)} \\ &= \sum_J \left(\frac{\tau_A \tau_B \tau_C \tau'}{\alpha^3} \right)^J \left([w_1^A|z_1^C][w_1^C|z_1^B][w_1^B|z_1^A] \right)^J \\ &\xrightarrow{H} \sum_J \frac{f_A(J)f_B(J)f_C(J)\mathcal{A}_f(J)}{\alpha^{3J}(J+1)!} \left([w_1^A|z_1^C][w_1^C|z_1^B][w_1^B|z_1^A] \right)^J \end{aligned} \quad (5.26)$$

Defining the matrix $M_a = -\alpha^{-1}|z_1^a\rangle[w_1^a]$, we thus get that a loop identity in this theory for N propagators is given by

$$\int \left(\prod_{n=1}^N d\mu_\alpha(w_2^n) P_{2d}^n \right) = \sum_J \frac{\mathcal{A}_f(J) \prod_n f_n(J)}{(J+1)!} \left[\text{Tr} \left(\prod_n M_n \right) \right]^J. \quad (5.27)$$

These results now allow the exact evaluation of arbitrary amplitudes in the theory defined with these near-trivial propagators. While probably not very useful in physical models, these results are at least cleaner than what follows, as we move onto the evaluation of Pachner moves in 4 dimensions.

Chapter 6

Evaluating 4d Pachner moves

The only way of discovering the limits of the possible is to venture a little way past them into the impossible.

Arthur C. Clarke

In this chapter, we will finally collect all that we have learned and attempt the evaluation of the 4-dimensional Pachner moves. We will see that while the 3–3 move can be invariant in a symmetric case, the other two moves are not invariant due to the mixing of strands introduced by the loop identities. In the case of the 5–1 move we will compare this to a Renormalization Group step, where additional couplings are introduced. This will motivate a truncation scheme for the loop identity that removes the mixing and restricts the flow to the space of 4-simplices. With this, we get invariance up to a factor depending on boundary spins. We finish the chapter with the study of divergences and propose a renormalization of the propagators.

6.1 Computing Pachner Moves with Simplicity Constraints

In this section we compute all the Pachner moves in the 4-d holomorphic Spin Foam model based on the techniques we have developed in the previous chapters. All these moves are based on the configurations of 6 vertices ($ABCDEF$). In the following we adopt the

following notation: a simplex A indicates the 4-simplex opposite to the vertex A , i.e. it is composed by $[BCDEF]$. AE indicates the tetrahedron $A \cap E$ composed of the vertices $[BCDF]$, with vertex A and E removed from the triangulation. Triangle ABD indicates the one composed by $[CEF]$. Also in order to keep track of which vertex is “active”, i.e. dual to a 4-simplex and which vertex is “inactive”, i.e. not dual to a 4-simplex, we introduce a distinction in our notation: an upper case letter $A, B \dots$ denotes an active vertex, while a lower case letter $c, d \dots$ denotes an inactive vertex.

6.1.1 3–3 move

According to these conventions the move 3–3 corresponds to

$$ABCdef \rightarrow abcDEF.$$

The 3–3 move is shown as Fig.6.1. In the first figure the 4-simplices A, B, C are sharing the blue triangle. After the move the configuration is changed into three 4-simplices D, E, F which share the green triangle.

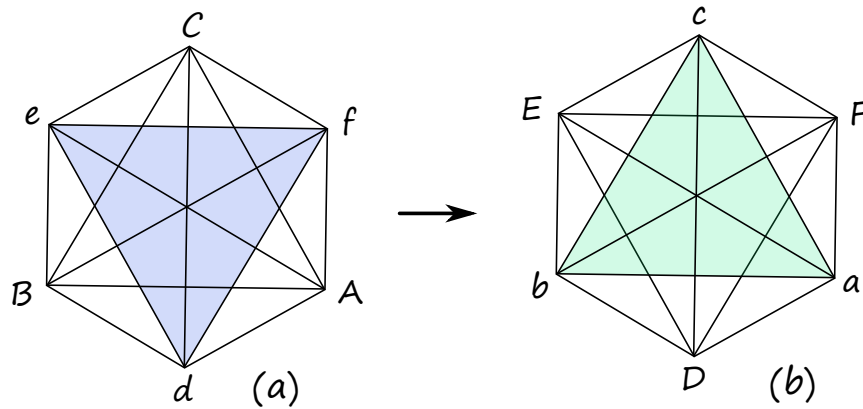


Figure 6.1: Triangulations for the 3–3 move.

The corresponding cable diagram is shown in Fig.6.2. The various colors of strands in the graph are used to indicate the different positions of triangles. The blue loop to be integrated out corresponds to the triangle ABC . The purple strands in (a) for example are dual to the triangles $Adf \subset A$, $Bde \subset B$, $Cef \subset C$ and they run from the tetrahedra $Af \rightarrow Ad$, $Bd \rightarrow Be$, $Ce \rightarrow Cf$. After performing the 3–3 Pachner move, the same triangles (still indicated by the purple strands) are no longer shared by two tetrahedra within a given 4-simplex. They become commonly shared by tetrahedra belonging to the

three different 4-simplices: $aDF \subset (D \cap F)$, $bDE \subset (D \cap E)$, $cEF \subset (E \cap F)$. The same happens to the black strands, whereas the opposite happens for the red and light blue strands. In summary, on one hand, due to the 3–3 move from (a) to (b), the red and light blue strands, shared between different simplices in (a) become unshared strands which belong to one simplex in (b). On the other hand, the unshared strands (the black and purple strands) in (a) become the commonly shared ones in (b). The dark blue loop and the green loop correspond to faces which are dual to the internal triangles ABC and DEF respectively.

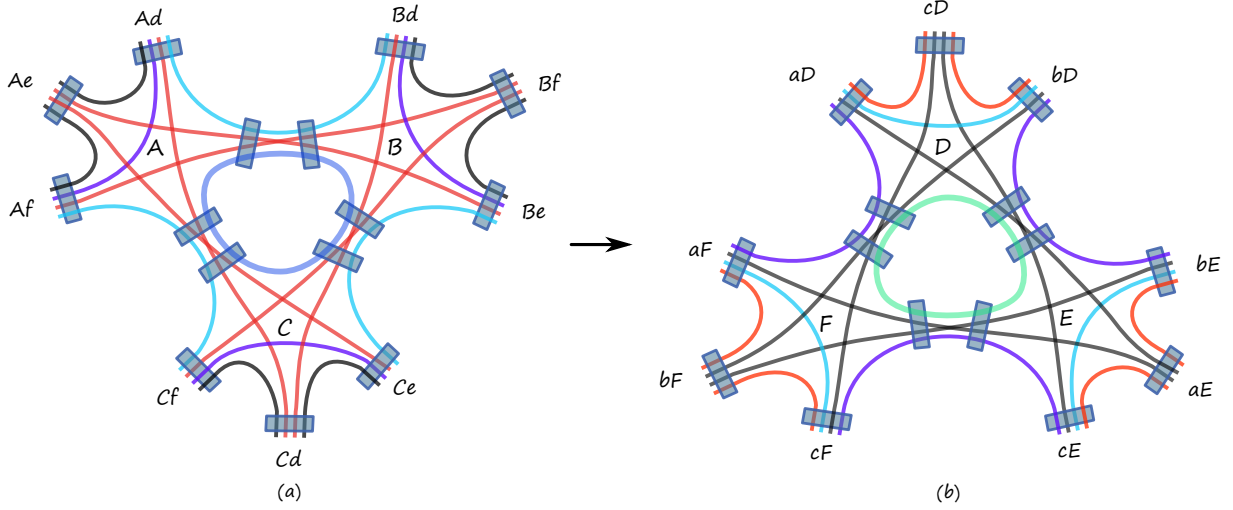


Figure 6.2: Cable diagram for the 3–3 move $ABCdef \rightarrow abcDEF$.

To compare the partition function/amplitudes between the configurations (a) and (b), we need to integrate out the shared loop on both sides. Based on the discussion in section 4.2, we can gauge fix two out of three pairs of the constrained propagators around the loop by a choice of a maximal tree in a way that leaves the amplitude invariant. We then need to apply only once the constrained loop identity which we obtained in the previous section to complete the 3–3 Pachner move. In order to do so, it is important to introduce some notation for the spinors. Let us describe the parametrization of (a) = $(ABCdef)$. For each 4-simplex $\alpha \in \{A, B, C\}$ we need to introduce a collection of spinors associated with each strand within that 4-simplex. Each strand carries a label which corresponds to a pair of tetrahedra $\alpha\beta$ sharing a face. Within A we have two types of tetrahedra: three external ones Ad, Ae, Af and two internal ones AB, AC . The strands run either between two internal tetrahedra or from one internal to one external tetrahedron. Accordingly, we label the external strands by boundary spinors $z_\gamma^{\alpha\beta}$ where $\alpha \in \{A, B, C\}$,

$\beta \in \{d, e, f\}$, $\gamma \in \{A, B, C, d, e, f\}$ for (a) in Fig.6.2 , and $\alpha \in \{D, E, F\}$, $\beta \in \{a, b, c\}$, $\gamma \in \{a, b, c, D, E, F\}$ for (b). $\alpha\beta$ are the indices labeling boundary tetrahedra, and $z_\gamma^{\alpha\beta}$ indicate boundary spinors. The boundary propagators are then labeled as $P_\rho(z_\gamma^{\alpha\beta}; w_\gamma^{\alpha\beta})$.

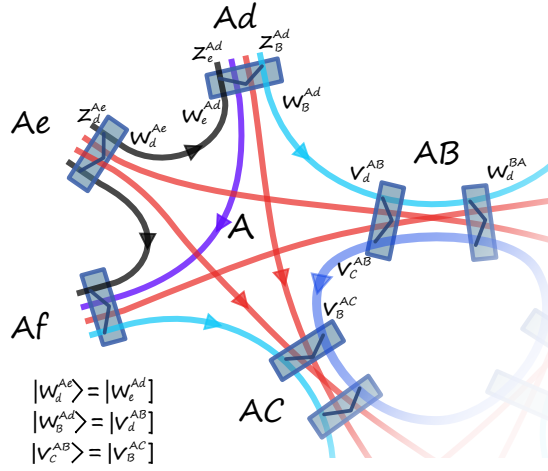


Figure 6.3: Zoomed in part of the cable diagram for the 3–3 move with some of the labels and contractions of spinors explicitly written down.

Let us label the internal pairs of propagators by $P_\rho \circ P_\rho(v_\gamma^{\alpha\alpha'}, w_\gamma^{\alpha'\alpha})$, where $\alpha, \alpha' \in \{A, B, C\}$ for (a) and $\alpha, \alpha' \in \{D, E, F\}$ for (b). We need to contract these spinors with the spinors $w_\gamma^{\alpha\beta}$ of the external propagators. An example of this is shown in Fig. 6.3 with all the labels and orientations written explicitly of a part of (a). The contractions are done according to the orientations of strands, and for example we have $|w_B^{Ad}\rangle = |v_d^{AB}\rangle$. In summary, the amplitude is constructed from $z_\gamma^{\alpha\beta}$ and $w_\gamma^{\alpha\beta}$ for the external propagators and on $w_\gamma^{\alpha\alpha'}, v_\gamma^{\alpha\alpha'}$ for the internal ones. The amplitude is obtained then after integration over the internal spinors after imposing the contractions, thus becomes a function of $z_\gamma^{\alpha\beta}$ only.

We thus find that the amplitude for three 4-simplices combined as in Fig.6.2 can be written as

$$\mathcal{A}_3(z_\gamma^{\alpha\beta}) = \int \prod_{all} d\mu_\rho(v) d\mu_\rho(w) \prod_{\alpha\beta} P_\rho(z_\gamma^{\alpha\beta}; w_\gamma^{\alpha\beta}) . \quad (6.1)$$

The spinors of the three internal propagators which share a loop are labeled by v and w and each of them is contracted with different boundary constrained propagators, with the gluing depending on the orientation of the graph.

The crucial difference between amplitude (a) and (b) is that the non-trivial coefficient $N(J, J', A, B, \rho)$ of Eq.(5.11) encodes the spin information of different strands. In (a), the coefficient N encodes the spin information of the blue and red strands in one configuration, while in (b) it encodes the spin of the black and purple strands. Unless the corresponding boundary spins are chosen to be the same, the 3–3 move cannot be invariant.

It is thus very easy to see where the topological invariance of BF theory is broken. Let us come back to BF theory and look at the 3–3 move. The BF loop identity (4.4) does not have any factor depending on spins and hence gives a trivial equality, as the diagrams in Fig. 6.4 are combinatorially equivalent. Thus for BF theory, the partition function/amplitudes are invariant under 3–3 move.

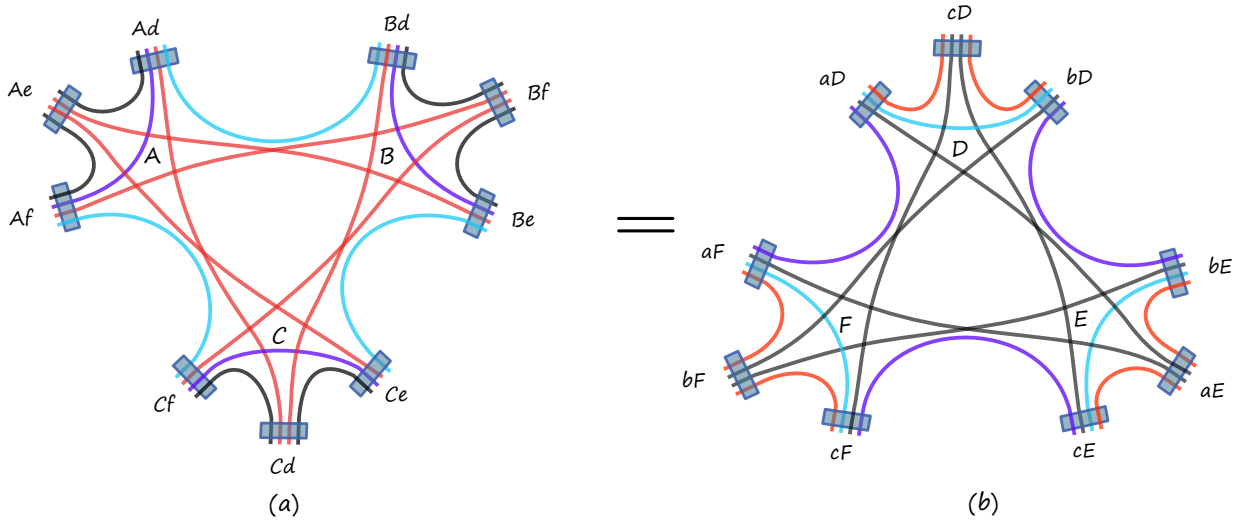


Figure 6.4: For 4-d BF theory, after integrating out the middle loops in the 3–3 move, the rest of the strands are combinatorially equivalent.

6.1.2 4–2 move

The 4–2 move $ABCDef \mapsto abcdEF$ is shown in Fig.6.5. In (a), four 4-simplices A, B, C, D are sharing 6 tetrahedra. After removing four triangles (or four loops in the dual cable graph) and changing the combinatorial structure, the four 4-simplices are rearranged in two 4-simplices E, F glued by one tetrahedron. The corresponding cable diagram of the four 4-simplices is shown in Fig.6.6.

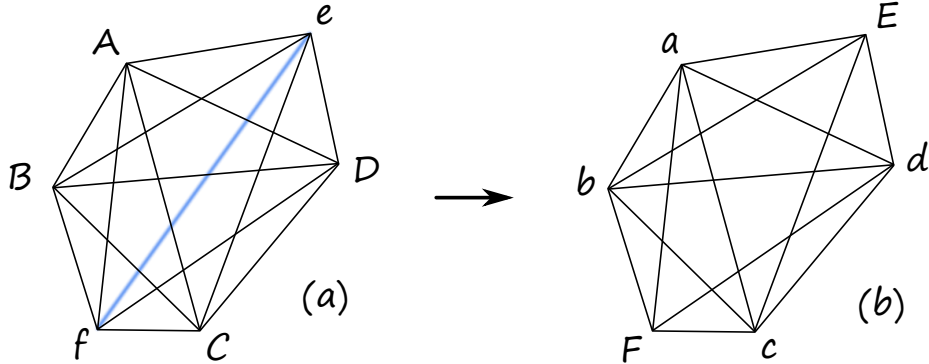


Figure 6.5: Triangulations for the 4–2 move.

We can perform gauge fixing of this graph by choosing vertex C as the root of the maximal tree in such a way that we can gauge fix 3 couples of propagators BC, AC, CD . This allows us to apply the constrained loop identities Eq.(5.11) to three of the four loops. More specifically, we can apply the constrained loop identity to the propagators (AB, BC, CA) to drop the blue loop, then apply it to the propagators (AC, CD, DA) to integrate the green loop and propagators (BC, CD, DB) to remove the big yellow loop. This results in integrating out all couples of constrained propagators, and hence we are left with one last (red) loop, which is mixed with the external strands, as can be seen in Fig.6.7.

Note, that we have applied the three loop identities, but the last loop is left without any extra group averaging. Similar to the case of the loop identity, we have to add in a face weight for this last loop. We will do so again by inserting a factor of τ' on one of the strands of the left-over loop (say the red strand for edge AD), so that we can use homogeneity map $\tau'^{2j} \rightarrow (2j + 1)^\eta$.

Similar as in the previous section, we will denote the spinors on the boundary as z , and spinors in the bulk as w and v with indices labeling the propagator and the strand they belong to. Each spinor carries three indices: $z_\gamma^{\alpha\beta}$ with indices α labeling the 4-simplex, $\alpha\beta$ labelling the tetrahedron they belong to, γ labelling which strands they represent. With assuming a specific orientation of the graph as $C \rightarrow A, C \rightarrow B, C \rightarrow D, A \rightarrow B, D \rightarrow A, D \rightarrow B$ ¹, the amplitude in terms of the exponentiated loop identity Eq.(5.12) is given

¹When one reverses the orientation of one propagator, the corresponding $[v|w] \rightarrow [w|v] = -[v|w]$

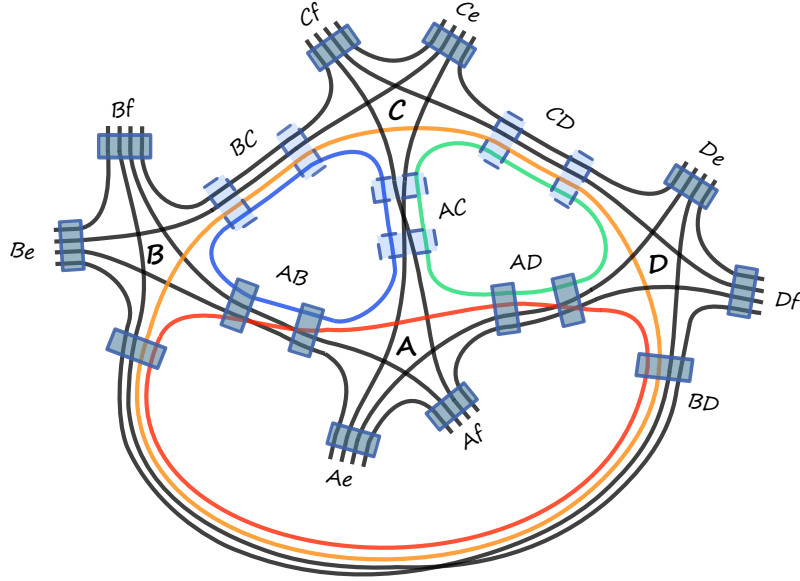


Figure 6.6: Cable diagram for the 4–2 move with gauge fixing along BC, AC, CD .

then by

$$\begin{aligned} \mathcal{A}_{4-2}^\tau(z_\gamma^{\alpha\beta}) &= \int \left\{ \prod_{\text{all}} d\mu_\rho(v) d\mu_\rho(w) \right\} \prod_{\alpha\beta} P_\rho(z_\gamma^{\alpha\beta}; w_\gamma^{\alpha\beta}) \cdot \exp \left[\sum_{\sigma i} \tilde{\tau}_{\sigma C} [\tilde{v}_i^{C\sigma} | \tilde{w}_i^{\sigma C}] \right] \\ &\times \exp \left[\sum_{\mu\nu} (\tau_N^{\mu\nu} \sum_j \alpha_j^{\mu\nu} [v_j^{\mu\nu} | w_j^{\nu\mu}] + \tau_M^{\mu\nu} \sum_{j<k} \alpha_j^{\mu\nu} [w_j^{\nu\mu} | w_k^{\nu\mu}] [v_j^{\mu\nu} | v_k^{\mu\nu}]) \right]. \end{aligned} \quad (6.2)$$

For the external propagators $\alpha \in \{A, B, C, D\}$ and $\beta \in \{e, f\}$ label the tetrahedron, while $\gamma \in \{A, B, C, D, e, f\}$ labels the strands in each tetrahedron. For internal gauge fixed propagators, $\sigma \in \{A, B, D\}$, $i \in \{e, f\}$, and for the non-gauge fixed propagators, $\mu\nu \in \{AB, AD, BD\}$, $j, k \in \{e, f, r\}$, where r indicates the red strand of the left-over loop. We define $\alpha_j^{\mu\nu}$ as

$$\alpha_j^{\mu\nu} = 1 + \delta_{AD}^{\mu\nu} \delta_j^r (\tau' - 1) \quad (6.3)$$

for keeping track of the homogeneity factor for the face weight of the last loop.

The equation (6.2) gives a compact and explicit expression for the amplitude associated with the 4–2. It is obtained by using the exponentiated loop identity Eq.(5.12), which then can be transformed using the homogeneity map to obtain the full expression after performing all of the contractions of spinors and all the Gaussian integrals. The homogeneity maps we need to apply to this expression to get the full result were defined in Eq. (5.9) for the

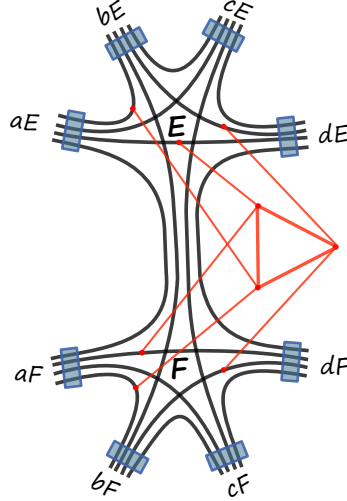


Figure 6.7: Performing the calculation we get a configuration of two 4-simplices with a nonlocal gluing.

$\tilde{\tau}$, in Eq.(5.13) for τ_N and τ_M and the homogeneity map for τ' is $\tau'^{2j} \rightarrow (2j + 1)^\eta$. The calculation can be straightforwardly done, but the resulting expression itself is a complicated, one with lots of mixed strands that is difficult to manipulate. The integrals also contain potential divergences that have to be taken care of. We will delay the discussion of the resulting expression and the significance of the mixing terms until the next section, as we first encounter a similar behavior for the 5–1 Pachner move as well. Here in the expression Eq.(6.2), we intentionally leave the last red loop unintegrated to pave the way for truncation in section 6.3.

6.1.3 5–1 move

We now calculate the 5–1 Pachner move. The 5–1 move corresponds to a change of a configuration of five 4-simplices sharing an internal vertex into a single 4-simplex by removing the common vertex, see Fig. 6.8.

The cable diagram for this move can be seen in Fig. 6.9. We have a total of 10 loops and 10 pairs of constrained propagators inside the bulk of the graph. Even though there is an increase in complexity, compared to the 4–2 move, the calculation will go over in nearly the same way. We start by choosing a maximal tree in the diagram, which allows us to gauge fix 4 of the pairs of propagators. A careful choice of this tree corresponds to a root

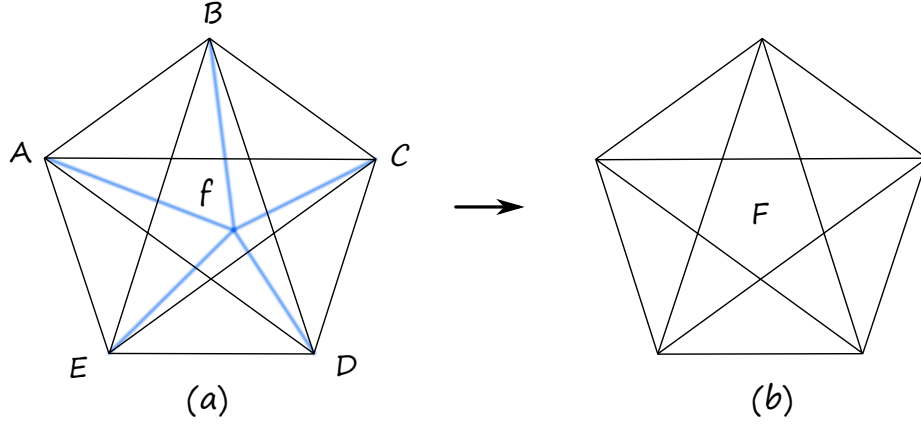


Figure 6.8: Triangulations for the 5–1 Pachner move.

at one of the 4-simplices and allows us to apply loop identities to 6 of the loops, leaving us with 4, as can be seen in Fig. 6.10.

We can write the amplitude for the 5–1 move using the exponentiated loop identity Eq.(5.12) as in the case of the 4–2 move. We will again have to add the face weights for the last four loops by adding factors of τ' . The expression for the full Pachner move then would be obtained by applying the homogeneity map to the resulting power series. We keep to the notation of inside spinors being w and v labeled by the strands and propagators they belonged to. With assuming the orientation of the graph as $E \rightarrow A, E \rightarrow B, E \rightarrow C, E \rightarrow D$, the amplitude in terms of boundary spinors z is formally given then as

$$\begin{aligned} \mathcal{A}_{5-1}^\tau(z_\gamma^{\alpha f}) &= \int \left\{ \prod_{\text{all}} d\mu_\rho(v) d\mu_\rho(w) \right\} \prod_\alpha P_\rho(z_\gamma^{\alpha f}; w_\gamma^{\alpha f}) \cdot \exp \left[\sum_\beta \tilde{\tau}_{E\sigma} [\tilde{v}^{E\sigma} | \tilde{w}^{\sigma E}] \right] \\ &\times \exp \left[\sum_{\mu\nu} (\tau_N^{\mu\nu} \sum_i \beta_i^{\mu\nu} [v_i^{\mu\nu} | w_i^{\nu\mu}] + \tau_M^{\mu\nu} \sum_{i<j} \beta_i^{\mu\nu} [w_i^{\nu\mu} | w_j^{\nu\mu}] [v_i^{\mu\nu} | v_j^{\mu\nu}]) \right], \end{aligned} \quad (6.4)$$

where the indices run over the following ranges: $\sigma \in \{A, B, C, D\}$, $\mu\nu \in \{AB, AC, AD, BD, BC, CD\}$, $i, j \in \{f, b, r, y, g\}$, where b, r, y, g indicates the blue (ABD), red (BCD), yellow (ACD), green (ABC) strands of the left-over loops respectively, and f indicates the black strands which compose the simplex F after the move. The external propagators $P_\rho(z_\gamma^{\alpha f}; w_\gamma^{\alpha f})$ are defined the same way as in previous sections, namely $\alpha \in \{A, B, C, D, E\}$ labels the simplices in which the boundary tetrahedra belong to, and γ labels the strands in each tetrahedra. The coefficients $\beta_i^{\mu\nu}$ that keep track of homogeneity of the face weights are defined this time as

$$\beta_i^{\mu\nu} = 1 + \delta_{AD}^{\mu\nu} \delta_i^y (\tau'_y - 1) + \delta_{AC}^{\mu\nu} \delta_i^g (\tau'_g - 1) + \delta_{AB}^{\mu\nu} \delta_i^b (\tau'_b - 1) + \delta_{BC}^{\mu\nu} \delta_i^r (\tau'_r - 1). \quad (6.5)$$

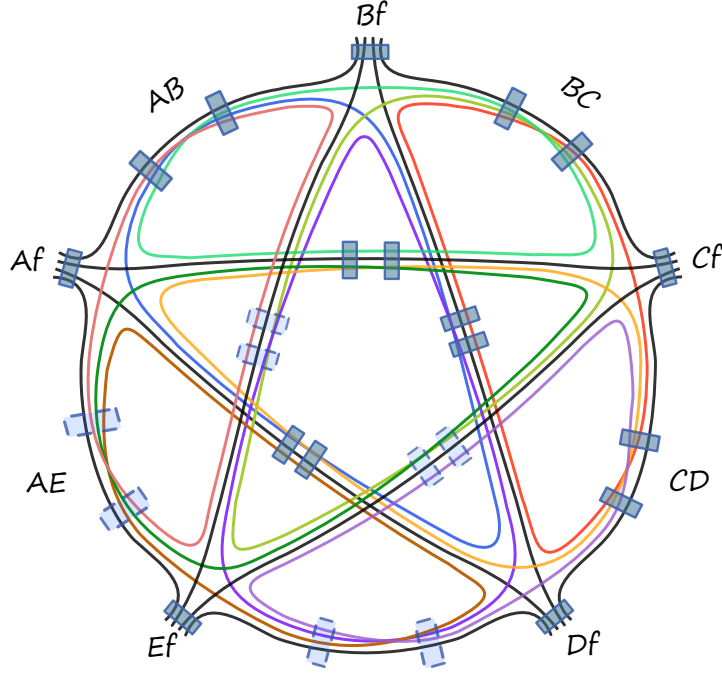


Figure 6.9: Cable diagram for the 5-1 move. The loops inside are colored.

The formal expression of 5-1 is of similar structure as the 4-2 move, with the difference being the range of the indices due to bigger number of loops and propagators. The expression (6.4) is relatively compact for such a complicated calculation and it contains all the information necessary to evaluate the amplitude after the Gaussian integrations are performed. In order to do so we just need to specify is the homogeneity map

$$H_{5-1}[\mathcal{A}_{5-1}^r] = \mathcal{A}_{5-1}. \quad (6.6)$$

The 5-1 homogeneity map H_{5-1} is given by the composition of :

$$\begin{aligned} \tau_N^{\mu\nu J} \tau_M^{\mu\nu J'} &\rightarrow \sum_K \frac{(-1)^{J'-K} (J+J'-K)! J!}{K! (J'-K)!} (J+2J'-2K+1)^\eta \tau_{\mu\nu}^K \left(\frac{\tilde{\tau}_{E\mu} \tilde{\tau}_{E\nu} \tau_{\mu\nu}}{(1+\rho^2)^3} \right)^{J+2J'-2K} \\ \tau_{\mu\nu}^J &\rightarrow \frac{F_\rho(J)^2}{(1+\rho^2)^{2J} (J+1)!}, \quad \tilde{\tau}_{E\sigma}^J \rightarrow \frac{F_\rho(J/2)^2}{(1+\rho^2)^J}, \quad \tau_i^{2j} \rightarrow (2j+1)^\eta, \end{aligned} \quad (6.7)$$

with $F_\rho(J)$ previously defined as the hypergeometric function $F_\rho(J) = {}_2F_1(-J-1, -J; 2; \rho^4)$. The same map can be used to find the full expression for the 4-2 Pachner move as well. The Gaussian integrals for the last four loops can be performed explicitly. Using the results

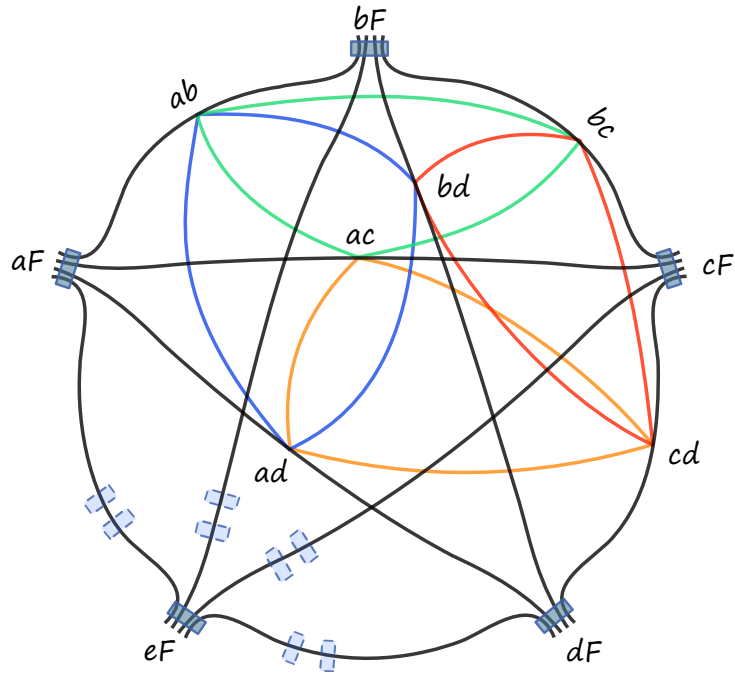


Figure 6.10: Gauge-fixing 4 strands allows to apply loop identities 6 times, leaving the 4 colored loops.

from [98], we can write this as an inverse of a determinant of a large matrix. We leave these integrals undone however to make the truncation procedure in the next section more clear.

Let us now try to understand our result. In $SU(2)$ BF theory the 5–1 Pachner move would lead to 4 decoupled loops, each giving a factor of a $SU(2)$ delta function evaluated at identity. This would correspond to setting all the τ_{MS} to 0 and all the other τ s to 1 in our expression. For the constrained propagator, as in the previous case of the 4–2 move, the loops inside are coupled to each other and to the strands of the boundary spinors. This means that as expected the spin foam model we consider is not invariant under both the 4–2 and 5–1 Pachner moves. It is natural to conjecture here, that this would be the case for the other spin foam models as well.

The new feature of the model is the mixing between internal loops and external edges that creates a coupling between all the different strands not present in the original form of the vertex amplitude.

Let us try to study this mixing in some more detail. By splitting the 6-valent vertices

in the loops, as in Fig. 6.11, it is obvious that we can try to interpret these coupled loops as an insertion of an operator. The connections between loops and the boundary spinors

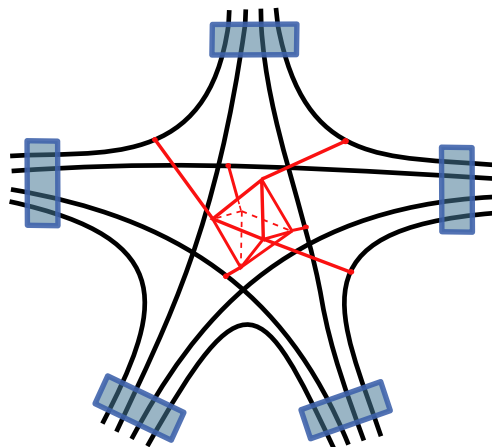


Figure 6.11: Performing the calculation we get a 4-simplex with an insertion of a nonlocal operator.

corresponds to gauge invariant operators inserted inside the 4-simplex amplitude. It is well known that such operators can be expressed as a sum of grasping operators [109]. In the holomorphic context, these operators are due to the insertions of the $SU(N)$ operators [79], from which all geometrical operators are made. The insertion of Wilson loops and the action of $SU(N)$ operators are two sides of the same coin [90] – they are constructed from the same type of gauge-invariant observables, which in our language are the products $[z|w\rangle$ and $\langle z|w\rangle$. The operators we get for the 4–2 and 5–1 moves can be thus thought as an exponentiated combination of $SU(N)$ grasping operators and Wilson loops. Iteration of 5-1 moves leads to a new kind of loop expansion, reminiscent of higher order diagrams in perturbative quantum field theory. Graphically, this would seem to define a sort of geometric series of operators made out of the “diamonds” in Fig. 6.11. Putting five of these together, and dealing with the loops again would give us a large diamond with smaller ones on the vertices, leading to some sort of fractal geometry.

We leave the analysis of this geometric expansion for future work and will instead try a different approach to understanding these operators.

6.2 Necessity for truncation

In the previous section we have seen that the mixing of strands could be understood as the insertion of a $SU(N)$ grasping operator. In this section we mainly focus on the 5–1 move. This Pachner move alone can be understood as a coarse graining move which maps one choice of the vertex amplitude to another one obtained after coarse graining. All the other coarse graining moves have to be built out of non-trivial combinations of 3–3, 4–2 and 5–1 moves. As we have shown that 5–1 move generates non-local couplings via the mixing terms, similarly to what happens in Real Space Renormalization Group calculations. Remarkably it will turn out that the mixing terms are clearly subdominant. This motivates a truncation scheme in which we keep only the non-mixing terms in the 5–1 move leading to a specific renormalization flow for the vertex amplitude, which we will show in the next chapter to be indeed restricted to the space of 4-simplices.

A truncation scheme in the study of RG flows is usually associated with a choice of the relevant and irrelevant couplings. In the usual setting this choice is tied up with the assumptions of locality but also has to be compatible with the symmetries like Lorentz invariance and eventually should be compatible with unitarity. These concepts need to be replaced by others in the case of Spin Foam renormalization. The current Spin Foam models, including the holomorphic one we study here, are defined in such a way that they possess the correct leading semi-classical behavior at the level of a single 4-simplex. In hopes of defining a continuum theory down the line, the requirement of correct asymptotics should be kept unchanged at each step of truncation in the coarse graining procedure. Apart from this requirement, the only other one that is obvious is the preservation of gauge symmetries. In the next subsection, we will see that a natural truncation scheme does seem to exist for the Pachner moves already at the level of the constrained loop identity and it preserves the above requirements.

In order to successfully coarse grain the non-local operators in the Pachner moves, we need to understand and deal with their divergences, which we study in section 6.4. It is important to appreciate that the divergences in the 5–1 move are welcomed in Spin Foam models, since ultimately we would like to understand them as coming from a vertex translation symmetry, which is expected to be related to diffeomorphism invariance. This would have to be removed by some appropriately defined Fadeev-Popov gauge-fixing procedure, similarly to what has been achieved in 3d [102]. It is natural in our context, to control the presence of potential divergences by introducing parameters like η determining the strength of the face weights, or a coupling constant for each vertex, and try to absorb the divergence into them (and perhaps into the other coupling constants already present, like ρ , the Newton constant G_N together with a cosmological constant Λ , or even the τ

parameters that we treated so far as book-keeping parameters).

Once we have understood the truncation and divergences, we can perform the renormalization step. We will suggest at the end of this chapter that this could be done by absorbing the relevant part of the operator into the definition of the constrained propagator. This would define for us a flow $P_\rho \rightarrow \tilde{P}_\rho$ in the space of constrained propagators. We will see however in the next chapter that things are a bit more complicated than that.

It is interesting to note that besides the truncation we perform, we could also study the effect of the insertion of the mixing terms which are subleading contributions. For the 5–1 Pachner move, we could in principle integrate out the non-local operator. Once the divergence is removed the effect of the mixing terms leaves us with an amplitude that is more involved than a simple 4-simplex. It corresponds to a more general structure of all strands being mixed in the middle of the vertex, giving rise to higher-valent intertwiners. This suggests that the additional contributions would lead to flow towards a theory of higher-valent vertex amplitudes.

6.3 Truncation of the loop identity

In this section we introduce a truncation scheme for the Pachner moves, that will ultimately allow us to define the renormalization flow. The expression for the 5–1 Pachner move in Eq.(6.4) is very compact, but requires us to perform many extra integrations over spinors, each of which in itself is straightforward, but the resulting answer is rather long. To simplify the discussion, let us drop the dependence on the external spinors, which corresponds to setting the boundary spins to zero. As we will discuss in the next section, this selects out the most divergent part of the Pachner move. With this simplification, we can use the techniques introduced in [98] and perform all of the spinor integrals immediately, with the result being again the inverse of a determinant. The power series expansion is however very large, depending on the order of $\mathcal{O}(150)$ sums over integers. Nonetheless, its structure is simple – it is a large summation of a product of six functions $N(J, A, B, J', \rho)$ defined in the constrained loop identity in Eq.(5.11). Thus, instead of trying to truncate the whole 5–1 Pachner move, which is a daunting task, first we can simplify the problem by just studying the properties of a single constrained loop identity – a much more tractable problem.

Let us then take a look at the constrained loop identity. Recall that in section 5.2, after we integrated out the loop, additional mixing terms appeared, which were not there in BF theory and which seem to be non-geometrical. We can analyze Eq.(5.11) to see how much these extra terms contribute to the amplitude. The mixing terms are characterized by their

total spin J' in Eq.(5.11). The larger J' is, the higher order polynomials of complicated mixings appear. The mixed strands disappear only when $J' = 0$.

Let us look at the large spin behavior first. As an illustration, the Fig. 6.12 presents logarithmic plots for the coefficient function $N(J, A, B, J', \rho)$ when J, A, B are universally large (as an example, we set them to 100, but it can be any large enough number), while J' picks small values $J' \in \{0, 1, 2\}$. We can observe that for any $\rho \in [0, 1]$, $N(J' = 0)$ is at least

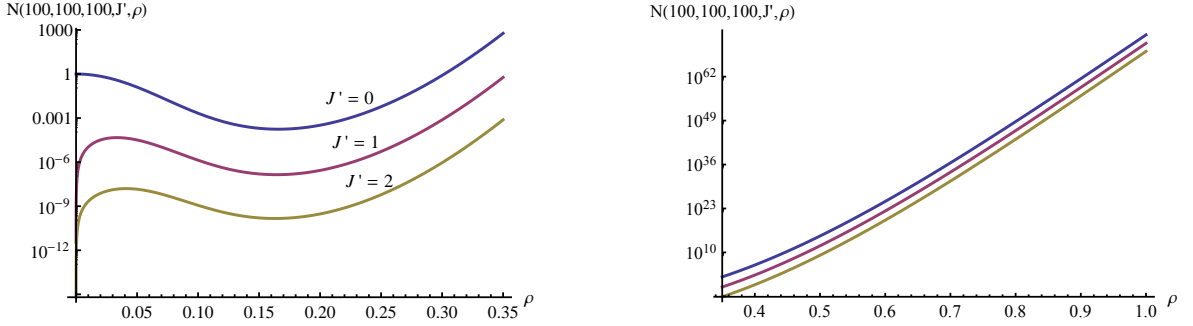


Figure 6.12: Logarithmic plots for the coefficient N when $J = A = B = 100$ and face weight scaling is $\eta = 1$. The blue, red, yellow lines correspond to $J' = 0, 1, 2$ respectively.

more than J times larger than the next order $N(J' = 1)$, which is also approximately more than J times larger than the next order $N(J' = 2)$. Actually, we can plot the ratio between the coefficient of the first term $N(J' = 0)$ and the sum of a few subleading coefficients $\sum_{J'=1}^{10} N(J')$ in Fig.6.13 as a function of ρ . When $\rho = 0$, the expression converges to the behavior of BF theory, $N(J, A, B, 0, 0) = 1$ and $N(J, A, B, J', 0) = 0$ for any $J' \neq 0$, as desired. For $\rho \neq 0$, we get a smooth deformation of the BF result, with a similar behavior, in the sense that the constrained loop identity is dominated by the $J' = 0$ term. The smaller the ρ , the more dominating the unmixed term is. The same behavior holds when spins are large but not uniformly large – the constrained loop identity is always dominated by the terms of $J' = 0$.

What about the case when the spins are not large? The plots in Fig.6.14 illustrate that actually the $J' = 0$ terms are still dominating even when the spins J, A, B are small. This means that the dominance of $J' = 0$ terms surprisingly holds not only for large spins, but also for the small ones, even though the suppression is less pronounced compared with large spins cases. For small spins with the value of $\rho \rightarrow 1$, the dominance of $J' = 0$ term is the least pronounced but still valid. To prove that we this term dominates, it suffices to see that the sum over the remaining $J' \neq 0$ converges quickly to a value much smaller than the $J' = 0$ term. This is indeed true and can be seen in Fig. 6.15.

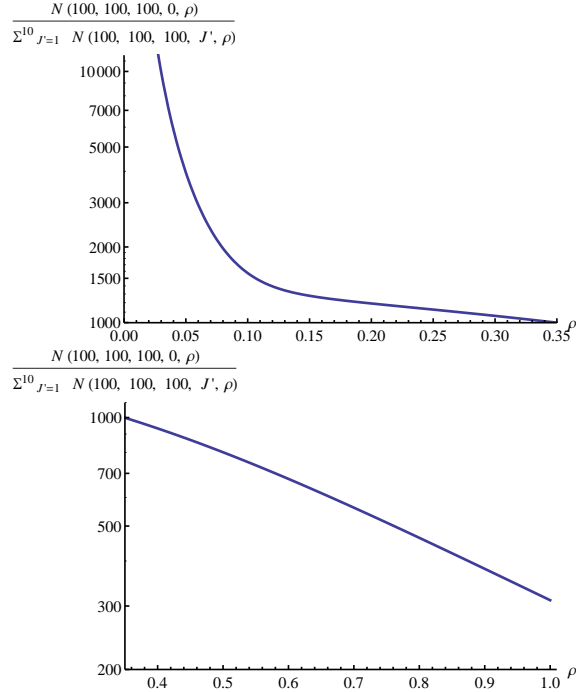


Figure 6.13: Plots of the ratio between $N(J' = 0)$ and the sum of subleading coefficients $\sum_{J'=1}^{10} N(J')$ with $J = A = B = 100$ and face weight scaling $\eta = 1$.

All of these results so far have been for the choice of face weight corresponding to $\eta = 1$. One could worry that perhaps the dominance of $J' = 0$ fails for bigger face weights. We find however that the increasing of the face weight η makes the effect stronger, as it is illustrated for small spins in the Fig.6.16.

In general, for a fixed choice of J, A and B , the leading term is given by $J' = 0$.

We thus propose a natural truncation of keeping just the $J' = 0$ terms and throwing away all the mixing terms $J' \neq 0$:

$$\begin{aligned}
 N(J, A, B, J', \rho) &\approx N(J, A, B, 0, \rho) \\
 &= \frac{(J+1)^{\eta-1}}{(1+\rho^2)^{A+B+7J}} F_\rho^2(J) F_\rho^2\left(\frac{A+J}{2}\right) F_\rho^2\left(\frac{B+J}{2}\right). \quad (6.8)
 \end{aligned}$$

This truncation dramatically simplifies the expression of N , making all the mixing and non-geometrical terms disappear. The reason why this is sensible is because after integrating out all the spinors, the amplitudes are a summation of a product of N s from different

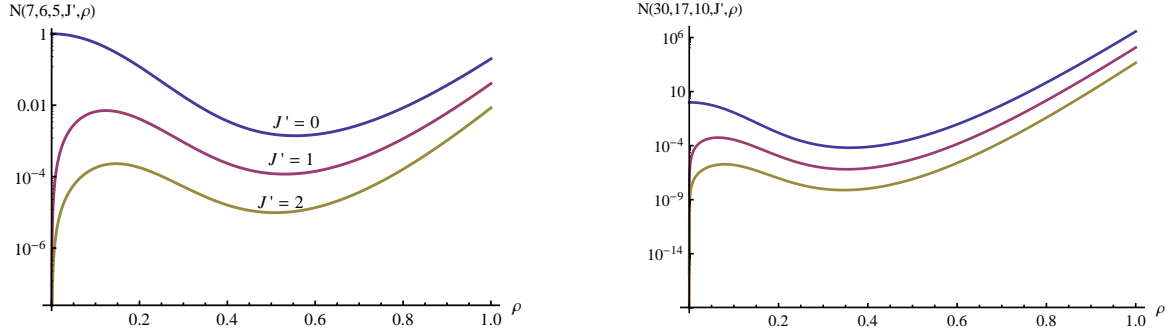


Figure 6.14: Logarithmic plots for the coefficient N when $J = 7, A = 6, B = 5$, and $J = 30, A = 17, B = 10$. The blue, red, yellow lines correspond to $J' = 0, 1, 2$ respectively.

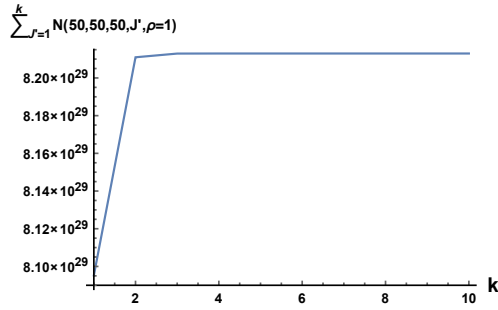


Figure 6.15: Partial sum of $\sum_{J'=1}^k N$ for $J = A = B = 50$ and $\rho = 1$. The $J' = 0$ term is dominant with $N(J' = 0) \approx 7.1 \times 10^{31}$. The subdominant terms converge very rapidly.

loops, and as such the dominant contribution is from the $J' = 0$ terms. The truncation scheme can be graphically expressed as

$$\begin{aligned}
 & \text{Diagram of a loop with vertices GF 1 and GF 2} \\
 & = \sum_{A,B,J} N(J' = 0) \begin{array}{c} \parallel \\ \parallel \\ \parallel \\ \text{A} \end{array} \begin{array}{c} \parallel \\ \parallel \\ \parallel \\ \text{B} \end{array} + \sum_{A,B,J,J'} N(J' \neq 0) \begin{array}{c} \parallel \\ \parallel \\ \parallel \\ \text{A} \end{array} \begin{array}{c} \parallel \\ \parallel \\ \parallel \\ \text{B} \end{array} \\
 & \hspace{15em} (6.9)
 \end{aligned}$$

Note that the left over strands will have to be integrated over in a calculation of a Spin Foam amplitude. The contractions of these spinors give additional factors of $1/(1 + \rho^2)$, see the Appendix A.1. These factors will lead to additional suppression of amplitude for bigger ρ , making it more convergent. This however does not spoil the truncation. We will see the effect of this suppression in calculating the degree of divergence of Pachner moves

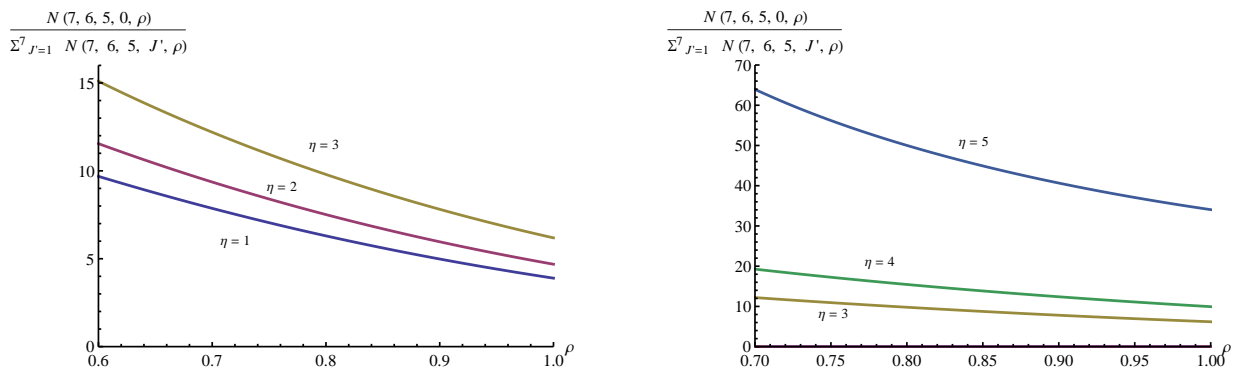


Figure 6.16: Plots of the dependence of the ratio between $N(J' = 0)$ and the sum of subleading coefficients with face weight η when $J = 7, A = 6, B = 5$ and ρ is close to 1.

in the coming section.

6.4 Counting the degree of divergence

Before we write out the truncated Pachner moves, let us first calculate how divergent the 5–1 move is as a function of face weight. The question of divergence is closely related to the one of symmetries. Indeed it is expected that in a physical model divergences of the partition function should be related to symmetries. This has been only shown exactly in 3 dimensions [102] so far.

In a model describing 4d gravity we would expect the 5–1 move to be invariant up to a divergence coming from the freedom of translation of the added vertex inside the 4-simplex. Hence we would expect that for gravity the divergence should scale as $(length)^4$. Of course at this stage this is a naive guess but it would be harder to argue for a diffeomorphism symmetry otherwise. In the case of translational symmetry this divergence is due to the possibility of moving the internal vertex outside the geometrical simplex. It can be tamed by incorporating orientation dependent factors as shown in 3 dimensions [104]. The Spin Foam models at our disposal do not yet incorporate orientation dependence so it is unlikely that this phenomenon can be used in our context.

The easiest way to count the degree of divergence is to set the external spins to 0, so that only the internal loops contribute. The calculation for the mixed 4 loops in the 5–1 move is rather involved, but thanks to the natural truncation discussed in the previous section we can do the calculation. Let us however first try to estimate the degree of divergence arising

from a single loop in the 4–2 move. It is important to stress here that in this case we do not need to do the truncation, as setting the external spins to 0 corresponds to dropping all the products of spinors that contain the external ones in Eq. (6.2), and hence naturally makes all the mixing terms drop out². This allows us to write the amplitude for the single loop in 4–2 move as

$$\mathcal{A}_\tau^{4-2}(0) = \int d\mu_\rho(w) e^{\frac{\tau_N^{AB} \tau_N^{AD} \tau_N^{BD} \tau'}{(1+\rho^2)^2} \langle w|w \rangle} = \frac{1}{\left(1 - \frac{\tau_N^{AB} \tau_N^{AD} \tau_N^{BD} \tau'}{(1+\rho^2)^3}\right)^2} = \sum_j (2j+1) \left(\frac{\tau_N^{AB} \tau_N^{AD} \tau_N^{BD} \tau'}{(1+\rho^2)^3}\right)^{2j}, \quad (6.10)$$

where, recall we have labeled the three loops, on which we applied the loop identity, by $\{AB, AD, BD\}$. Using the homogeneity map defined in Eq. (6.7), we can reintroduce the factors of face weight and the functions of ρ from loop identities. Regularizing the expression by putting a cut-off of Λ on spins, we get that a single loop in the 4–2 move is given by

$$D_{4-2}(\Lambda, \rho, \eta) = \sum_{j=0}^{\Lambda} \frac{(2j+1)^{4\eta-2}}{(1+\rho^2)^{24 \times 2j}} [{}_2F_1(-2j-1, -2j; 2; \rho^4)]^{12}. \quad (6.11)$$

It is easy to see that, since ${}_2F_1(-2j-1, -2j; 2; 0) = 1$, for $\rho = 0$ and $\eta = 1$ we recover the SU(2) BF theory's divergence of a delta function $\delta_{SU(2)}(\mathbb{1})$. It may seem surprising that the exact result is this simple. For the purpose of analyzing the divergence let us write $D_{4-2}(\Lambda, \rho, \eta) = \sum_{j=0}^{\Lambda} X_{4-2}(2j, \rho, \eta)$.

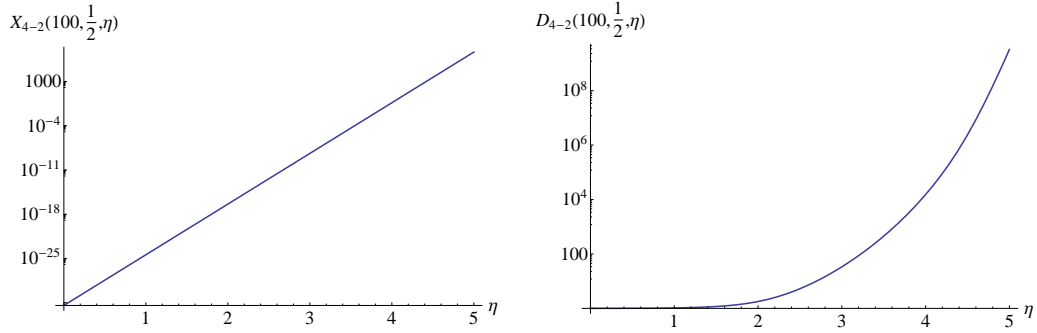


Figure 6.17: X_{4-2} has an obvious dependence on η on a logarithmic plot. The sum diverges a lot faster with increasing η .

Let us start with analyzing the behavior of X_{4-2} and D_{4-2} as a function of η . This is shown in Fig. 6.17. Quite obviously, at fixed spin, both X_{4-2} and D_{4-2} are diverging

²This is another reason for seeing that the mixing terms might not be important.

with increasing η . We get the opposite behavior for increasing ρ – both X_{4-2} and D_{4-2} are heavily suppressed for increasing ρ , as can be seen in Fig. 6.18. This is the effect of the additional suppression by factors of $1/(1 + \rho^2)$ that we mentioned in the previous section. We can thus expect interesting competition between ρ and η in concerning divergences.

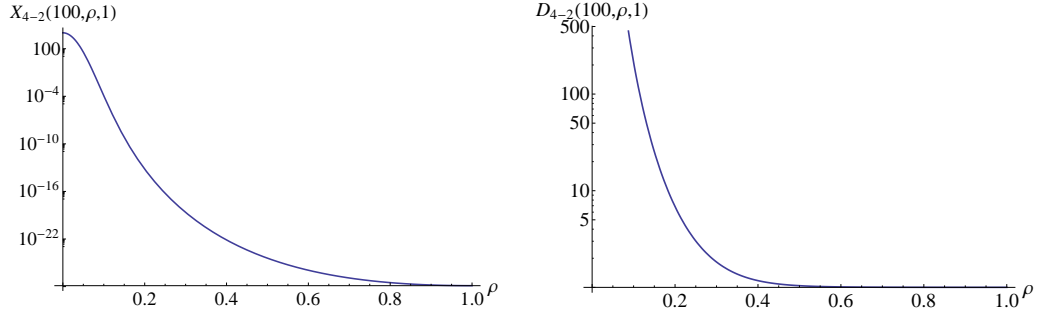


Figure 6.18: X_{4-2} gets suppressed with increasing ρ , with $\rho = 0$ being the limit of SU(2) BF divergence. The sum is even more suppressed with increasing ρ .

Fixing ρ to a specific value, we can analyze now the divergence of X_{4-2} for different values of η , as a function of spin. We numerically find that X_{4-2} is suppressed with increasing spin, but around $\eta = 5$ there is a transition to divergence, see Fig. 6.19. This seems to be independent of the value of ρ , and indeed in [101] Chen used the asymptotic expansion of the hypergeometric functions (3.12) to show that the exact degree of divergence is $D_{4-2} = \Lambda^{4\eta-19}$.

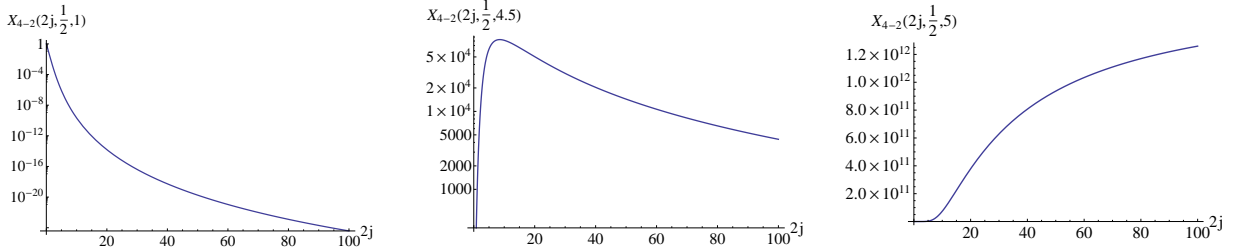


Figure 6.19: For small values of η , X_{4-2} gets suppressed with increasing spin. There seems to be a transition in the behavior around $\eta = 5$.

Let us now move onto the calculation of the degree of divergence for the 5–1 Pachner move. Truncating the loop identities in the 5–1 move allows us to perform the Gaussian

integrals easily and write the four remaining loops as

$$\mathcal{A}_\tau^{5-1} \text{ truncated}(0) = \frac{1}{\left(1 + \frac{\tau_N^{AC} \tau_N^{AD} \tau_N^{CD} \tau'_y}{(1+\rho^2)^3}\right)^2 \left(1 + \frac{\tau_N^{AB} \tau_N^{AD} \tau_N^{BD} \tau'_b}{(1+\rho^2)^3}\right)^2 \left(1 + \frac{\tau_N^{AB} \tau_N^{AC} \tau_N^{BC} \tau'_g}{(1+\rho^2)^3}\right)^2 \left(1 + \frac{\tau_N^{BC} \tau_N^{BD} \tau_N^{CD} \tau'_r}{(1+\rho^2)^3}\right)^2}, \quad (6.12)$$

where, similarly as in the 4-2 move, the six loops that we have integrated out were labeled by the set $\{AB, AC, AD, BC, BD, CD\}$ and the left over four loops are labeled by $\{y, g, b, r\}$. Comparing this to the 4-2 move expression (6.10), we see that clearly we have 4 loops, that are not connected by any strands, but which are nonetheless coupled by sharing the τ s, and hence functions of spin and ρ . We can now expand this in a power series for the four spins j_y, j_g, j_b, j_r and reintroduce the factors of the hypergeometric functions and face weights by using the homogeneity map from Eq. (6.7). Letting $a, b, c \in \{y, g, b, r\}$ we can write the full expression for the degree of divergence as

$$D_{5-1} = \sum_{j_y, j_g, j_b, j_r} \frac{\prod_a (2j_a + 1)^{\eta+1}}{(1+\rho^2)^{24 \sum_a 2j_a}} \left(\prod_{a < b} F_\rho(2j_a + 2j_b)^2 (2j_a + 2j_b + 1)^{\eta-1} \right) \left(\prod_{a < b < c} F_\rho(2j_a + 2j_b + 2j_c)^2 \right), \quad (6.13)$$

where, recall, we have previously defined $F_\rho(J) = {}_2F_1(-J-1, -J; 2; \rho^4)$ for simplification. Let us define $D_{5-1} = \sum_{\{j\}} X_{5-1}(j)$.

This general expression is rather long when expanded, but numerically it turns out that it is peaked around all the spins being equal. Hence for all spins equal to j , we have a nice simplification

$$X_{5-1}(\{j\}) = \frac{(2j+1)^{4(\eta+1)} (4j+1)^{6(\eta-1)}}{(1+\rho^2)^{96 \times 2j}} F_\rho(4j)^{12} F_\rho(6j)^8. \quad (6.14)$$

Again, it is easy to see that for $\rho = 0$ and $\eta = 1$ we recover the result of $\delta_{SU(2)}(\mathbb{1})^4$ for the SU(2) BF theory. We can now analyze the behavior of X_{5-1} as a function of ρ . The results are qualitatively similar to those of 4-2 move, in the sense that the expression is suppressed for increasing ρ , see Fig. 6.20.

Quite obviously X_{5-1} has similar behavior to X_{4-2} as a function of η , so we will not present plots for this. The interesting difference is in the transition from convergence to divergence of each X_{5-1} term in the summation. The point of transition numerically seems to be around $\eta = 3.2$, see Fig. 6.21. Note, that the expression of D_{5-1} includes four summations, so it actually becomes divergent even before $\eta = 3.2$. Again, Chen showed in [101] that the exact degree of divergence is given by $D_{5-1} = \Lambda^{10\eta-28}$. This means that the

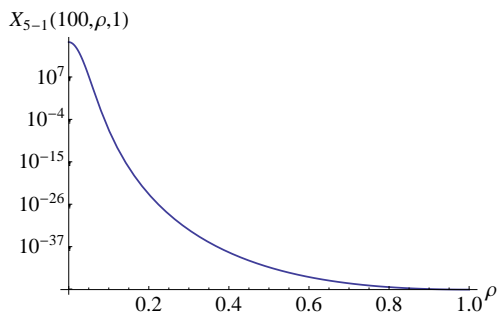


Figure 6.20: X_{5-1} is suppressed with increasing ρ for all values of η and spin. This plot is evaluated at $2j = 100$ and $\eta = 1$.

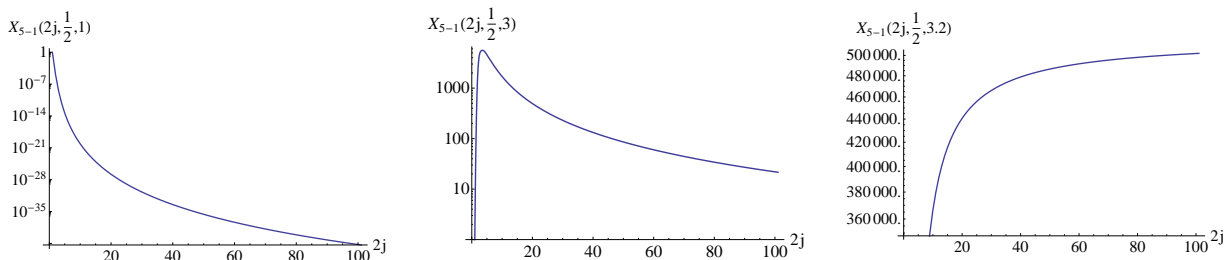


Figure 6.21: For small values of η , X_{5-1} gets suppressed with increasing spin. There seems to be a transition in the behavior for $\eta = 3.2$, but the overall the summation is divergent for $\eta \geq 2.8$.

5-1 Pachner move is divergent for $\eta \geq 2.8$, while it has the possibly desired divergence of Λ^2 at $\eta = 3$. Interestingly, we thus find that there is a range of the parameters η for which 4-2 Pachner move is finite and 5-1 move is divergent.

Somewhat disappointingly however, the face weight of $(2j + 1)^3$ is not one that is naturally motivated. One could just accept this and move forward, which is actually what we will do. There is however a pretty natural explanation for this value – our imposition of constraints on the inside of the 4-simplices quite naturally might have resulted in more suppressed amplitudes. Indeed, if at each edge we multiplied the factor of $\frac{F_\rho(J)^2}{(J+1)!(1+\rho^2)^{2J}}$ by a simple factor of J , then the ten internal edges in the 5-1 move would conspire to give us a divergence of Λ^{10} . Combining this with our result, we would get that this simple modification would give us the correct divergence at $\eta = 2$! This inclusion of the factor of J for each edge would also increase the divergence of the 4-2 move, but it would still be convergent at $\eta = 2$. We should be also careful to not spoil the truncation scheme we

introduced in the previous section. One could justify this additional factor by suggesting a non-trivial edge weight $\mathcal{A}_e(j_e)$ in the model, but unfortunately there is no guiding principle for choosing it to be anything else than 1 naturally, apart from the artificial fine-tuning of divergences. This however lets us keep in mind that the exact value of the coupling constants might not be that relevant, if we allow arbitrary edge weights.

6.5 Truncated Pachner moves

Now that we have already studied their divergence properties, we can write down the full expression for the 4-dimensional Pachner moves after truncation of the loop identities. As we will see, even though the loops in the moves are no longer mixed, there is still non-local coupling by spins.

Let us start with the simple observation, that the truncation does not change the non-invariance of the 3–3 Pachner move. The loop inside does decouple, but the truncation of the constrained loop identity does not change the fact that the hypergeometric functions of ρ depend on different boundary spins in the two configurations. Thus even after the truncation, the 3–3 Pachner move is obviously not invariant, unless one considers very fine-tuned boundary spins.

Since the amplitude for the 4–2 and 5–1 moves look formally very similar, let us focus on the most interesting case of the 5–1 Pachner move. After truncation, the amplitude in Eq. (6.4) becomes

$$\begin{aligned} \mathcal{A}_{\tau \text{ truncated}}^{5-1}(z_{\gamma}^{\alpha f}) &= \int \prod_{\text{all}} d\mu_{\rho}(v, w) \prod_{\alpha} P_{\rho}(z_{\gamma}^{\alpha f}; w_{\gamma}^{\alpha f}) \cdot e^{\sum_{\sigma} \tilde{\tau}_{E\sigma} [\tilde{v}^{E\sigma} | \tilde{w}^{E\sigma}] + \sum_{\mu\kappa i} \tau_N^{\mu\nu} \beta_i^{\mu\nu} [v_i^{\mu\nu} | w_i^{\nu\mu}]} \\ &= \int \prod_{\text{left over}} d\mu_{\rho}(v, w) \prod_{\alpha} P_{\rho}(z_{\gamma}^{\alpha f}; w_{\gamma}^{\alpha f}) \cdot e^{\sum_{\sigma} \tilde{\tau}_{E\sigma} [\tilde{v}^{E\sigma} | \tilde{w}^{E\sigma}] + \sum_{\mu\nu} \tau_N^{\mu\nu} [v_f^{\mu\nu} | w_f^{\nu\mu}]} \mathcal{A}_{\tau \text{ truncated}}^{5-1}(0), \end{aligned} \tag{6.15}$$

where recall that indices run over $\sigma \in \{A, B, C, D\}$, $\mu\nu \in \{AB, AC, AD, BD, BC, CD\}$, $i \in \{f, b, r, y, g\}$, $\alpha, \gamma \in \{A, B, C, D, E\}$. We have also defined the amplitude with boundary spins set to zero, $\mathcal{A}_{\tau \text{ truncated}}^{5-1}(0)$, in the previous section in Eq. (6.12) to be given by

$$\mathcal{A}_{\tau \text{ truncated}}^{5-1}(0) = \frac{1}{\left(1 + \frac{\tau_N^{AC} \tau_N^{AD} \tau_N^{CD} \tau_y'}{(1+\rho^2)^3}\right)^2 \left(1 + \frac{\tau_N^{AB} \tau_N^{AD} \tau_N^{BD} \tau_b'}{(1+\rho^2)^3}\right)^2 \left(1 + \frac{\tau_N^{AB} \tau_N^{AC} \tau_N^{BC} \tau_g'}{(1+\rho^2)^3}\right)^2 \left(1 + \frac{\tau_N^{BC} \tau_N^{BD} \tau_N^{CD} \tau_r'}{(1+\rho^2)^3}\right)^2}.$$

It is imperative now to notice that this does not trivially factorize, as we still have to apply the homogeneity map to obtain the final expression. The map defined in Eq. (6.7) tells us that the τ_N s are actually functions of the $\tilde{\tau}$ s from the partially gauge-fixed propagators. The homogeneity map for the truncated 5–1 Pachner move is $H_{5-1}[\mathcal{A}_\tau^{5-1} \text{ truncated}] = \mathcal{A}_{\text{truncated}}^{5-1}$ and is given by

$$H_{5-1} : \tau_N^{\mu\nu J} \mapsto F_\rho(J)^2 (J+1)^{\eta-1} \left(\frac{\tilde{\tau}_{E\mu} \tilde{\tau}_{E\nu}}{(1+\rho^2)^5} \right)^J, \quad \tilde{\tau}_{E\sigma}^J \mapsto \frac{F_\rho(J/2)^2}{(1+\rho^2)^J}, \quad \tau_i^{2j} \mapsto (2j+1)^\eta. \quad (6.16)$$

Before applying this homogeneity map, we need to first integrate out the extra spinors on the internal strands – because of the previously inserted propagators, each strand now has two spinors, instead of one. This is a simple Gaussian integration that we have performed many times before. This however requires us to contract the boundary propagators P_ρ with functions of τ_N and $\tilde{\tau}$. If these integrations could be performed in a symmetric manner, we then could define new boundary propagators \tilde{P}_ρ after applying the homogeneity map (6.16). The amplitude (6.15) in that case would become

$$\mathcal{A}_{\text{truncated}}^{5-1}(z_\gamma^{\alpha f}) = \tilde{D}_{5-1} \int \prod_\gamma d\mu_\rho(w_\gamma) \prod_\alpha \tilde{P}_\rho(z_\gamma^{\alpha f}; w_\gamma^{\alpha f}). \quad (6.17)$$

This is the form of an amplitude for a 4-simplex with the modified propagators \tilde{P}_ρ weighted by an overall, possibly divergent, factor \tilde{D}_{5-1} which we would expect to have the same degree of divergence as the function D_{5-1} we studied in the previous section. The exchange $P_\rho \rightarrow \tilde{P}_\rho$ would then be proposal for a renormalization flow in the space of propagators. We will however show in the next chapter that the situation is not this simple.

Chapter 7

Towards vertex renormalization

The story so far:

In the beginning the Universe was created.

*This has made a lot of people very angry and
been widely regarded as a bad move.*

Douglas Adams

The Restaurant at the End of the Universe

At the end of the last chapter, we came to the expectation that the amplitude after the 5–1 move could be rewritten as a product of five new propagators. We will however show in the second section of this chapter that this is impossible, due to the non-local structure of the result. It turns out however that it is possible to write this expression in terms of a renormalized 15j symbol. To see this, we will first rewrite the amplitude back from spinorial basis into the more usual spin basis. It turns out that in this basis, the result of the 5–1 Pachner move factorizes. We will then study the result in a symmetric case to reduce the parameter space.

7.1 Current state of Spin Foam renormalization

Before we dive in to studying what the 5–1 move tells us about renormalization, let us quickly review some of the previous work towards renormalization in Spin Foams. While the Spin Foam approach has naive similarity to lattice gauge theories, since both are defined on a discretization, there are very important differences that make renormalization

in our case non-trivial. The main difference is that Spin Foams are background independent. What this means in practice is that the discretization does not have a global spacing parameter. Moreover, the simplicial decomposition of spacetime is highly irregular, so the usual techniques do not apply.

In one of the earliest stabs at the problem, Markopoulou [31] suggested that a single block transformation could increase the Planck length l_P to a multiple of it as a definition of a scale transformation. She then proposed an interesting renormalization procedure based on local block transformations based on a Hopf group construction à la Kreimer. The crucial idea that would allow this was a notion of the possibility to nest more fine sub-foams in more coarser foams. Foams that have no such sub-foams are then called *primitive*, and in our notation would correspond to various types of loops. An interesting point raised in Markopoulou's work was that there was no natural notion of an inverse of a Spin Foam, but that one could define an *antipode*, which is the equivalent of the inverse for the *coproduct*, which can be defined as the unfolding of the nesting structure. The antipode then can be seen as an iteration over the sub-foams until one reaches a primitive foam.

The work of Oeckl [32, 33] provided another local framework, which changed the Renormalization Group to a cellular groupoid. The interesting point of the proposal was that one could dispense with the notion of a lattice spacing in favor of a more local notion of arrows defined by changing of cellular decomposition, with a fixed initial and final decomposition. The collection of arrows, which allow the definition of an inverse define the renormalization groupoid. The big difference of Oeckl's construction to our work lies in his use of cellular moves, which are all coarse-graining, unlike the Pachner moves. As we are however mostly interested in the 5–1 Pachner move, some of the ideas in his work are relevant.

The notion of using the embedding of Spin Foams to define scale has been crystallized in the notion of cylindrical consistency and embedding maps [17, 34, 35, 36, 37, 38]. As in the above constructions, one starts with the notion of embedding finer 2-complexes within more coarse ones. Since general 2-complexes form only a partially ordered, but directed, hierarchy, the Renormalization flow runs not over a linear sequence, but along a partially ordered filter. To define this embedding, we consider the Spin Foam amplitudes as transitions between boundary spin network states ψ in a Hilbert space \mathcal{H}_Γ , where Γ is the graph on the boundary of the 2-complex. If a boundary graph Γ' can be embedded in a finer graph Γ , then we can define a partial ordering $\Gamma' \preceq \Gamma$. The *embedding map* is then an isometry

$$\iota_{\Gamma\Gamma'} : \mathcal{H}_{\Gamma'} \rightarrow \mathcal{H}_\Gamma \tag{7.1}$$

that satisfies the compositions $\iota_{\Gamma\Gamma'}\iota_{\Gamma'\Gamma''} = \iota_{\Gamma\Gamma''}$. The *cylindrical consistency* condition for

the amplitudes is then defined by requiring that the amplitudes satisfy

$$\mathcal{A}_{\Gamma'} = \mathcal{A}_{\Gamma \wr \Gamma'}. \tag{7.2}$$

In this framework one then would study the flow of coupling constants $g \rightarrow g'$, and consider a theory to be renormalizable if the amplitudes can be parametrized by a finite number of these coupling constants, same as in perturbative QFT.

This scheme has been implemented in the series of works by Dittrich et al. on using Tensor Network Renormalization [39, 40, 41] applied to simplified analogues of Spin Foam models, known as Spin Nets [42, 43, 44, 45, 46, 47, 48]. These models are dimensionally reduced in the sense of being defined on a regular lattice of an arbitrary dimension, rather than a 2-complex. The partition function of these models can be expressed as a contraction of a tensor network, which allow local changes into a coarser network – in this sense one defines an RG flow of tensors. The numerical studies of these models in case of finite groups (including $SU(2)_k$, which is related to imposition of a cosmological constant in LQG) have discovered very rich phase structures. Recently, these methods have been also applied to 4d Spin Net analogues of the EPRL-FK model with the finite $SU(2)_k \times SU(2)_k$ group and revealed complex dynamics resulting from the imposition of the simplicity constraints [49]. It is however unclear how these results on regular lattices with finite groups (with the cutoff on spins set to the rather small value of $k = 12$ to make the numerical computations feasible) exactly relate to the full 4d Spin Foam models. The first such attempts have been made in [50]

Interestingly, the framework of cylindrical consistency and embedding maps has been recently applied to the EPRL-FK model restricted to hypercuboidal configurations by Bahr and Steinhaus [110, 111, 112]. While the restriction to summing only over the hypercuboidal foams is quite restrictive one, as these configurations do not capture any curvature (the Regge action always vanishes for hypercuboids [110], because all the dihedral angles are $\pi/2$ with four hypercuboids meeting at each square), it does nonetheless describe some of the configurations of the full theory. In this regime, the RG flow truncated to the space of hypercuboids was studied and showed the existence of a phase transition in the power of face weight η related to hypercuboid vertex translation symmetry (in the context of subdividing a hypercuboid into two parts). These results however are not applicable to our study of the simplicial case for several reasons. The first one is that the notion of vertex translation symmetry in the simplicial case is much more complicated, as one has to sum over many spins rather than one. More importantly, while the amplitude of a single hypercuboid depends on the face weight, while a single 4-simplex does not. As such, we come to the conclusion that a single 5–1 Pachner move cannot define a flow in the power

of the face weight η . The results in the hypercuboidal case are nonetheless an important step forward in understanding renormalization of 4d Spin Foams.

Finally, no discussion of Spin Foam renormalization would be complete without mentioning Group Field Theories [52]. GFTs are a generalization of matrix models very similar to ordinary QFTs, with the difference that one integrates over group manifolds G , rather than \mathbb{R}^4 . The partition function of a general GFT for G^D -valued fields $\phi(g_1, \dots, g_D) \equiv \phi(g_i)$ can be written as

$$Z_{GFT} = \int \mathcal{D}\phi e^{-\frac{1}{2} \int dg_i dh_i \phi(g_i) \mathcal{K}(g_i h_i^{-1}) \phi(h_i) - \lambda \int \prod_{i \neq j} dg_{ij} \mathcal{V}(g_{ij} g_{ji}^{-1}) \phi(g_{1j}) \cdots \phi(g_{D+1j})}, \quad (7.3)$$

where \mathcal{K} and \mathcal{V} are arbitrary kinetic and potential kernels respectively and λ is a vertex coupling constant. The evaluations of the Feynman diagrams of GFTs are Spin Foam amplitudes. For example, the choice of

$$\mathcal{K}(x_i) = \int_G dg \prod_i \delta(x_i g), \quad \mathcal{V}(x_{ij}) = \int_G \prod_i dg_i \prod_{i < j} \delta(g_i x_{ij} g_j^{-1}) \quad (7.4)$$

results in a GFT whose Feynman diagrams correspond to BF amplitudes. With recent progress in large N limit and colored Group Field Theories [113, 114, 115], the renormalization of these models can be finally studied. Technicalities aside, the renormalization of GFTs is very similar to that of standard perturbative QFT. The models studied so far [53, 54, 55, 56, 57, 58, 59, 60, 61, 62, 63, 64, 65, 66, 67] however have not been of direct relevance to 4d Quantum Gravity. As such, the lessons of GFT renormalization will not be directly applicable to our situation, though we will borrow the notion of a coupling constant λ for a vertex.

7.2 Non-locality with spinors

We will now show that the expectation that the amplitude after the 5–1 Pachner move could be written as a product of renormalized propagators is actually false. This actually could have been simply predicted already before the truncation, where we made the observation that the effect of the move could be seen as an insertion of an operator that mixed strands. The truncation of loop identity removed the additional mixing in spinors, but did not completely take away mixing of spins.

The technical reason for why we can make this statement is that the overall product of τ_s in the amplitude (6.15) restores hypergeometric functions, which depend on sums of spins belonging to different propagators.

While the above statement is conceptually rather clear, proving it in the case of the 5–1 move is quite lengthy. We will thus show why it cannot work in a simpler case that nonetheless captures the main difficulty. Namely, we will consider the 4–1 Pachner move in a theory constructed from the same constrained propagators P_ρ as in the 4-dimensional model, but with one strand less. The loop identity and all the other methods follow in exactly the same way, with the only difference being the smaller number of spinors.

First of all, recall from Chapter 4 the 4–1 move results in a single loop. There are also six strands, each carrying a factor of $\exp(\tilde{\tau}[\tilde{v}|\tilde{w}])$ or the corresponding one for τ_N . These factors can be easily integrated, and their effect is to rescale the spinors at the end of the strands. For each strand we can symmetrically split each τ into two factors of $\sqrt{\tau}$ and absorb these into the spinors on the boundary propagators. We will label the strands $1, \dots, 6$ and the propagators as A, B, C, D as in Fig. 7.1.

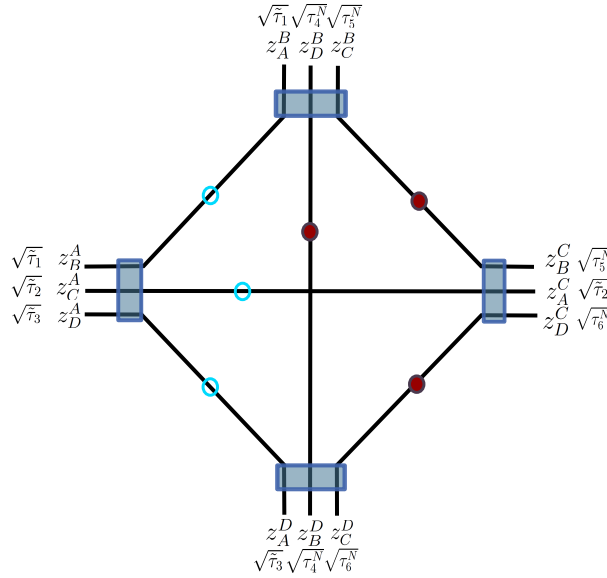


Figure 7.1: Moving the τ s onto edges after the 4–1 Pachner move. The open circles denote gauge-fixed contributions to the nonlocal factor, while dots denote the un-gauge-fixed ones.

To show what the amplitude looks like as a product of spinors, we will use the methods developed by Hnybida and Freidel in [98] for exact evaluation of $SU(2)$ spin networks. It was shown in that work that an arbitrary $SU(2)$ amplitude is given by

$$\mathcal{A}_\Gamma(z_e) = \frac{1}{(1 + \sum_C \mathcal{A}_C(z_e))^2}, \quad (7.5)$$

where $C = \{c_1, \dots, c_k\}$ is a cycle union in the graph Γ where a cycle is a collection of edges $c = (e_1, \dots, e_n)$. The cycle union amplitude is then $\mathcal{A}_C(z_e) = \mathcal{A}_{c_1}(z_e) \cdots \mathcal{A}_{c_k}(z_e)$, where \mathcal{A}_c is a product of spinors for each cycle given by

$$\mathcal{A}_c(z_e) = (-1)^{|e|} [z_{e_1}^{-1} | z_{e_2} \rangle [z_{e_2}^{-1} | z_{e_3} \rangle \cdots [z_{e_n}^{-1} | z_{e_1} \rangle, \quad (7.6)$$

where $|e|$ is the number of edges with orientation same as Γ .

What this means is that in the specific case of the tetrahedron, we have

$$\mathcal{A}_{3S} = \frac{1}{(1 - \mathcal{A}_{ABC} - \mathcal{A}_{ABD} - \mathcal{A}_{ACD} - \mathcal{A}_{BCD} + \mathcal{A}_{ABCD} - \mathcal{A}_{ABDC} - \mathcal{A}_{ACBD})^2}, \quad (7.7)$$

where for example $\mathcal{A}_{ABC} = [z_C^A | z_B^A \rangle [z_A^B | z_C^B \rangle [z_B^C | z_A^C \rangle$ and so on. Note that this result only holds true for $SU(2)$ BF theory. However, since we can use the homogeneity map, we can hide the $F_\rho(J)$ for each propagator in a τ_a for $a \in \{A, B, C, D\}$ and absorb these factors into the external spinors $|z\rangle$. We thus can write the amplitude for the constrained tetrahedron in terms of τ s as

$$\mathcal{A}_{3S}^\tau = \sum_{n_1, \dots, n_7} \frac{(n_1 + \cdots + n_z + 1)!}{n_1! \cdots n_7!} \mathcal{A}_{ABC}^{n_1} \cdots \mathcal{A}_{ACBD}^{n_7} \times f_{\tau_A \tau_B \tau_C \tau_D}(n_1, \dots, n_7) \quad (7.8)$$

with

$$f_{\tau_A \tau_B \tau_C \tau_D}(n_1, \dots, n_7) = \tau_A^{n_1+n_2+n_3} \tau_B^{n_1+n_2+n_4} \tau_C^{n_1+n_3+n_4} \tau_D^{n_2+n_3+n_4} (\tau_A \tau_B \tau_C \tau_D)^{n_5+n_6+n_7}, \quad (7.9)$$

where each τ_a^J carries a factor of $F_\rho(J)$. We can also write this for the amplitude of the 4-1 move by absorbing the additional τ s into the spinors as discussed above and shown in Fig. 7.1. Before we do this, note that each τ^N depends on some $\tilde{\tau}$ s. We can factor these out by defining

$$\tau_4^N = \tilde{\tau}_1 \tilde{\tau}_3 \tau_4, \quad \tau_5^N = \tilde{\tau}_1 \tilde{\tau}_2 \tau_5, \quad \tau_6^N = \tilde{\tau}_2 \tilde{\tau}_3 \tau_6, \quad (7.10)$$

where now the homogeneity maps are given by $\tau^J \mapsto F_\rho(J)^2 (J+1)^{\eta-1} (1+\rho^2)^{-5J}$ and $\tilde{\tau}^{2J} \mapsto F_\rho(J)^2 (1+\rho^2)^{-2J}$. Since the single loop in the 4-1 move gives an additional factor of

$$\left(1 - \frac{\tau_4^N \tau_5^N \tau_6^N \tau'}{(1+\rho^2)^3}\right)^{-2} = \sum_L (L+1)^{\eta+1} \left(\frac{\tau_4^N \tau_5^N \tau_6^N \tau'}{(1+\rho^2)^3}\right)^L, \quad (7.11)$$

we find that the amplitude for the constrained 4-1 move can be written as

$$\begin{aligned} \mathcal{A}_{4-1}^\tau &= \sum_{n_1, \dots, n_7, L} \frac{(n_1 + \cdots + n_z + 1)!}{n_1! \cdots n_7!} \mathcal{A}_{ABC}^{n_1} \cdots \mathcal{A}_{ACBD}^{n_7} \frac{(L+1)^{\eta+1}}{(1+\rho^2)^3} f_{\tau_A \tau_B \tau_C \tau_D}(n_1, \dots, n_7) \\ &\times (\tilde{\tau}_1^2)^{n_1+n_2+n_4} (\tilde{\tau}_2^2)^{n_1+n_3+n_4} (\tilde{\tau}_3^2)^{n_2+n_3+n_4} (\tilde{\tau}_1^2 \tilde{\tau}_2^2 \tilde{\tau}_3^2)^{n_5+n_6+n_7+L} \\ &\times \tau_4^{n_2+n_4+n_6+n_7+L} \tau_5^{n_1+n_4+n_5+n_7+L} \tau_6^{n_3+n_4+n_5+n_6+L}. \end{aligned} \quad (7.12)$$

Comparing the coefficients in $f_{\tau_A \tau_B \tau_C \tau_D}(n_1, \dots, n_7)$ and those of the additional factor above, we can readily see that the *different* nonlinear functions carried by τ and $\tilde{\tau}$ cannot be absorbed in any symmetric way into the τ_A, \dots, τ_D . The main reason for this failure are the properties of the hypergeometric functions in that they do not factorize nicely and that a product of two different hypergeometric functions is no longer the same type of a hypergeometric function. For some more justification, see the Appendix. This rather anti-climactic remark proves the statement that we cannot write the 4–1 amplitude as a product of a same type of propagators. Similar reasoning can be carried out for the case of 5–1 move, though with quite a bit more parameters floating about.

The fact that the amplitude cannot be written as a local product of propagators seems to be a Spin Foam realization of the result in quantum linearized Regge Calculus, where Dittrich et al. [70, 72] showed that while the Regge action was invariant under the 5–1 move, the measure attained a non-local factor.

7.3 4-simplex amplitude in terms of spins

Let us now try the alternative approach of rewriting the amplitude in the spin basis. This goes against the spirit of using the spinor basis to simplify calculations, but as we will see, it makes the structure of the result more clear in this case.

We can start by remembering that we can rewrite a propagator as a summation over intertwiners

$$\begin{array}{c} \dot{j}_1 \\ \dot{j}_2 \\ \dot{j}_3 \\ \dot{j}_4 \end{array} \left[\begin{array}{c} \dot{j}_1 \\ \dot{j}_2 \\ \dot{j}_3 \\ \dot{j}_4 \end{array} \right] = \sum_{\iota} \begin{array}{c} \dot{j}_1 \\ \dot{j}_2 \\ \dot{j}_3 \\ \dot{j}_4 \end{array} \begin{array}{c} \iota \\ \iota \end{array} \begin{array}{c} \dot{j}_1 \\ \dot{j}_2 \\ \dot{j}_3 \\ \dot{j}_4 \end{array} \quad (7.13)$$

Recall, that the intertwiner basis we use in this thesis is labeled by integers k_{ij} and was introduced in [99]. From our definition of the propagator in Eq. (3.14), we have that the propagator written in terms of k_{ij} s is given by

$$\begin{array}{c} \text{---} \\ \text{---} \\ \text{---} \\ \text{---} \end{array} \left[\begin{array}{c} \text{---} \\ \text{---} \\ \text{---} \\ \text{---} \end{array} \right] = \sum_J \frac{F_\rho(J)}{(J+1)!} \sum_{[k]} \prod_{i < j} \frac{([z_i | z_j][w_i | w_j])^{k_{ij}}}{k_{ij}!}.$$

A natural splitting of this expression presents itself, since it is already a neat product of

$[z_i|z_j\rangle$ and $[w_i|w_j\rangle$. We find that a 4-valent intertwiner can be simply expressed as

$$\begin{array}{c} \diagup \\ \diagdown \\ \diagup \\ \diagdown \end{array} = \sqrt{\frac{F_\rho(J)}{(J+1)!}} \prod_{i<j} \frac{([z_i|z_j\rangle)^{k_{ij}}}{\sqrt{k_{ij}!}} \quad (7.14)$$

In a 4-simplex amplitude, we have in total 20 integers k . This naturally leads to a definition of a 20j symbol. To see the structure, let us first explore this in the case of BF theory, where it is given by

$$\{20j\}_{BF} \equiv \frac{1}{\sqrt{\prod_a (J_a + 1)! \prod_{a \neq i < j} k_{ij}^a!}} \int \prod_{i \neq j} \frac{d^2 z_j^i}{\pi^2} e^{\sum_{i < j} [z_j^i | z_i^j] + \sum_a \sum_{i < j} k_{ij}^a \ln [z_i^a | z_j^a]}, \quad (7.15)$$

where $|z_j^i\rangle$ is a spinor from vertex i to vertex j . To connect this to the usual definition in terms of 15j symbols, we need a parametrization of the integers k .

In [99] a useful parametrization of the basis of 4-valent intertwiners labeled by integers k_{ij} was introduced in terms of Mandelstam variables S, T and U . Recall that

$$\sum_{j \neq i} k_{ij} = 2j_i.$$

We then can express the Mandelstam variables in terms of the 4 spins and k_{ij} s as

$$S = j_1 + j_2 - k_{12}, \quad T = j_1 + j_3 - k_{13}, \quad U = j_1 + j_4 - k_{14}. \quad (7.16)$$

They can be expressed also in terms of other spins due to the overcompleteness. Overall the Mandelstam variables satisfy the constraint

$$S + T + U = J. \quad (7.17)$$

The usual 15 j symbol is expressed in terms of 10 spins j and a single intertwiner label. In [99] it was shown that for example in terms of the labels S , we have simply

$$\{15j\}_{S_a} = \sum_{T_a} \{20j\}_{S_a, T_a} \quad (7.18)$$

We are now ready to express the 20j symbol in the constrained case. The only two differences are the extra weights $F_\rho(J)$ in the 4-valent intertwiner and the different measure of integration $d_\mu(z)$. Looking at the expression in BF theory, we see that clearly

the hypergeometric functions are going to factorize, so the only non-triviality lies in the integration measure. However, a simple change of variables and the property of logarithms makes the additional factors of $(1 + \rho^2)$ also factorize. We thus find that the contraction of five constrained intertwiners is given by

$$\begin{aligned}
\{20j\}_\rho &= \sqrt{\frac{\prod_a F_\rho(J_a)}{\prod_a (J_a + 1)! \prod k_{ij}^a}} \int \prod_{i \neq j} \frac{d^2 z_j^i}{\pi^2 (1 + \rho^2)^{-2}} e^{\sum_{i < j} (1 + \rho^2) [z_j^i | z_i^j] + \sum_a \sum_{i < j} k_{ij}^a \ln [z_i^a | z_j^a]} \\
&\stackrel{\sqrt{1 + \rho^2} z = z'}{=} \sqrt{\frac{\prod_a F_\rho(J_a)}{\prod_a (J_a + 1)! \prod k_{ij}^a}} \int \prod_{i \neq j} \frac{d^2 z_j^i}{\pi^2} e^{\sum_{i < j} [z_j^i | z_i^j] + \sum_a \sum_{i < j} k_{ij}^a \ln \frac{[z_i^a | z_j^a]}{(1 + \rho^2)}} \\
&= \left(\prod_a \sqrt{F_\rho(J_a)} \right) e^{-\sum_a \sum_{i < j} k_{ij}^a \ln(1 + \rho^2)} \{20j\}_{BF} \\
&= \{20j\}_{BF} \prod_{a=1}^5 \sqrt{F_\rho(J_a)} (1 + \rho^2)^{-J_a}
\end{aligned} \tag{7.19}$$

Just as we expected above, the additional functions of the Barbero-Immirzi parameter factorized.

Since the additional factors only depend on total spins on each of the vertices, we can again sum over the T labels to get finally

$$\{15j\}_\rho = \prod_{a=1}^5 \frac{\sqrt{F_\rho(J_a)}}{(1 + \rho^2)^{J_a}} \times \{15j\}_{BF} \tag{7.20}$$

This result is perhaps surprising in its simplicity, but as we have shown in Chapter 3, it seems to lead to the correct semi-classical limit. Having already integrated out the group elements and identified the left and right spinors with the simplicity constraints, it is no easy task to get intuition for the asymptotics.

7.4 Renormalizing the 15j symbol

Now that we have rewritten the 4-simplex amplitude in our model in terms of a 15j symbol, let us rewrite the 5–1 amplitude in terms of the spins as well. Before we jump into the details of the calculation, let us try to schematically see what the calculation will look like.

For each strand in the diagram we have effectively an additional factor of $d\mu_\rho(w)e^{\tau_i\tau_j[w_i|w_j]}$ after the 5–1 move, as well as the factor $\mathcal{A}_\tau^{5-1}{}_{\text{truncated}}(0)$. We can split this additional factor by inserting a trivial $SU(2)$ projector in the middle and changing the variables to $|w'_i\rangle = \tau_i|w_i\rangle$. This split allows us to pull the two factors into the opposing ends of the strands, and hence into two different boundary propagators. What this effectively means is that the boundary propagators change as $P_\rho(z, w) \rightarrow P_\rho(z, \tau w)$. For the whole Pachner move we would then have something along the lines of

$$\begin{aligned} \{20j\}_\rho^{5-1} &= \sqrt{\frac{\prod_a F_\rho(J_a)}{\prod_a (J_a + 1)! \prod_{i \neq j} k_{ij}^a}} \prod_{i \neq j} \int \frac{d^2w}{\pi^2(1 + \rho^2)^{-2}} e^{\sum(1+\rho^2)[w_i|w_j] + \sum k_{ij} \ln \tau_i \tau_j [w_i|w_j]} \mathcal{A}_\tau^{5-1}{}_{\text{truncated}}(0) \\ &= \sqrt{\prod_a F_\rho(J_a)} \{20j\}_{BF} e^{\sum k_{ij}^a \ln \frac{\tau_i \tau_j}{(1+\rho^2)}} \mathcal{A}_\tau^{5-1}{}_{\text{truncated}}(0) \\ &= \{20j\}_\rho \prod (\tau_i \tau_j)^{k_{ij}} \mathcal{A}_\tau^{5-1}{}_{\text{truncated}}(0) \end{aligned}$$

Assuming that such a product of τ s does not depend on the S, T intertwiner labels, we could then transform this into an equation for 15j symbols. Let us see now explore the 5–1

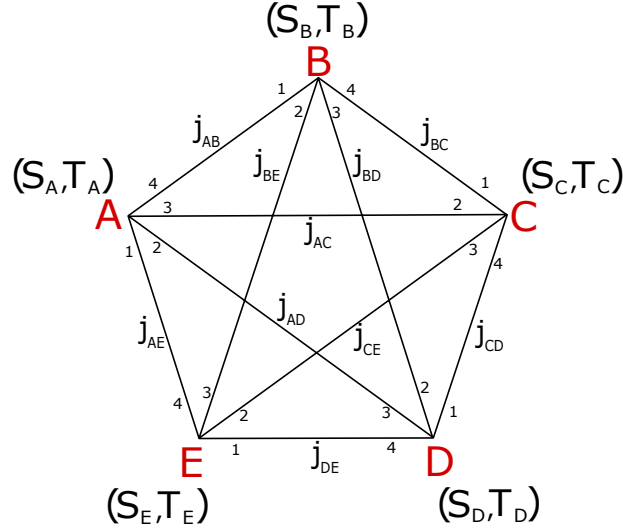


Figure 7.2: Spin labels in a 20j symbol, together with ordering of strands for each vertex.

amplitude in more detail. Comparing the above to the Eq. (6.15), we see that each internal strand carries either a factor of τ_N or $\tilde{\tau}$. Each vertex would then get half a contribution from the given strand, for example a $\sqrt{\tau_N}$. To get these factors correct, let us first label the 4-simplex carefully. See Fig. 7.2 for the choices we make here.

For concreteness, let us see how the k_{ij}^A depend on spins at the vertex A, and what the τ s associated with them are. From the condition $\sum_{j \neq i} k_{ij} = 2j_i$ and Eqs. (7.16) and (7.17) we have

$$\begin{aligned} k_{12}^A &= j_{AE} + j_{AD} - S_A, & k_{13}^A &= j_{AE} + j_{AC} - T_A, & k_{14}^A &= S_A + T_A - j_{AD} - j_{AC}, \\ k_{23}^A &= S_A + T_A - j_{AE} - j_{AB}, & k_{24}^A &= j_{AD} + j_{AB} - T_A, & k_{34}^A &= j_{AB} + j_{AC} - S_A. \end{aligned} \quad (7.21)$$

Similar relations can be obtained for all five tetrahedra. Notice that this defines 30 integers k, only 20 of which are independent.

Let us now look at the product of τ on each vertex. We will only do this again explicitly for vertex A. Following the labelling in Fig. 7.2, these are simply

$$\tau_1^A = \sqrt{\tilde{\tau}_{AE}}, \quad \tau_2^A = \sqrt{\tau_N^{AD}}, \quad \tau_3^A = \sqrt{\tau_N^{AC}}, \quad \tau_4^A = \sqrt{\tau_N^{AB}}. \quad (7.22)$$

Putting these two above results together means that the overall product of τ s for the vertex A is given simply by

$$\begin{aligned} \prod_{i < j} (\tau_i^A \tau_j^A)^{k_{ij}^A} &= \tau_1^{A(k_{12}^A + k_{13}^A + k_{14}^A)} \tau_2^{A(k_{12}^A + k_{23}^A + k_{24}^A)} \tau_3^{A(k_{13}^A + k_{23}^A + k_{34}^A)} \tau_4^{A(k_{14}^A + k_{24}^A + k_{34}^A)} \\ &= \left(\sqrt{\tilde{\tau}_{AE}} \right)^{2j_{AE}} \left(\sqrt{\tau_N^{AD}} \right)^{2j_{AD}} \left(\sqrt{\tau_N^{AC}} \right)^{2j_{AC}} \left(\sqrt{\tau_N^{AB}} \right)^{2j_{AB}} \end{aligned} \quad (7.23)$$

This can be repeated for all the vertices. As we see, the careful analysis indeed shows that each τ is only raised to the spin of the strand it is attached to. Since each strand appears in two vertices, we arrive at the pretty obvious, in hindsight, result that the overall product of τ s is

$$\begin{aligned} \prod_a \prod_{i < j} (\tau_i^a \tau_j^a)^{k_{ij}^a} &= (\tau_N^{AB})^{2j_{AB}} (\tau_N^{AC})^{2j_{AC}} (\tau_N^{AD})^{2j_{AD}} (\tilde{\tau}_{AE})^{2j_{AE}} (\tau_N^{BC})^{2j_{BC}} (\tau_N^{BD})^{2j_{BD}} \times \\ &\quad \times (\tilde{\tau}_{BE})^{2j_{BE}} (\tau_N^{CD})^{2j_{CD}} (\tilde{\tau}_{CE})^{2j_{CE}} (\tilde{\tau}_{DE})^{2j_{DE}} \end{aligned} \quad (7.24)$$

It's pretty important to note here that this does not depend on any S or T labels, but only on the spins. This means that we can safely sum over the S or T labels to work with the 15j symbol, rather than the more unusual 20j.

Before we assemble all the pieces, we cannot forget that these τ s have been absorbed into propagators through integration, which will give us additional factors of $(1 + \rho^2)$. For example, we have

$$\int d\mu_\rho(v) P_\rho(z, w) e^{\tilde{\tau}[v|w]} = P_\rho \left(z, \frac{\tilde{\tau}}{1 + \rho^2} w \right) \quad (7.25)$$

Hence, we have to divide every τ by a factor of $(1 + \rho^2)$, which gives us an overall factor of $(1 + \rho^2)^{-\sum_a J_a}$. To obtain our desired result, we now only have to expand the $\mathcal{A}_\tau^{5-1} \text{truncated}(0)$ factor into a power series and use the homogeneity maps from Eq. (6.16). Notice that this factor depends on the same τ s as the $\prod_a \prod_{i < j} (\tau_i^a \tau_j^a)^{k_{ij}^a}$ we just calculated. Recall that, crucially, the τ_N depend on $\tilde{\tau}$ s. In the homogeneity map (6.16) we have

$$\tau_N^{\mu\nu J} \rightarrow F_\rho(J)^2 (J+1)^{\eta-1} \left(\frac{\tilde{\tau}_{E\mu} \tilde{\tau}_{E\nu}}{(1+\rho^2)^5} \right)^J,$$

so it seems quite natural and useful to redefine it as

$$\tau_N^{\mu\nu J} = \tau_{\mu\nu}^J \tilde{\tau}_{E\mu}^J \tilde{\tau}_{E\nu}^J, \quad \text{with} \quad \tau_{\mu\nu}^J \rightarrow \frac{F_\rho(J)^2 (J+1)^{\eta-1}}{(1+\rho^2)^{5J}}. \quad (7.26)$$

Now that we have dealt with the τ factors on the strands, we need to deal with the terms coming from the remaining loops. To express $\mathcal{A}_\tau^{5-1} \text{truncated}(0)$ in terms of spins, we will use the power expansion of the square of the geometric series

$$\frac{1}{(1-x)^2} = \sum_j (2j+1)x^{2j}. \quad (7.27)$$

Expanding all the τ_N into the $\tilde{\tau}$ and τ s, we can finally write down the extra series expansion of τ after the 5–1 Pachner move. For sake of brevity, let us define the function of τ s that we need to evaluate as

$$\mathcal{N}([\tau], [k]) \equiv (1 + \rho^2)^{-\sum_a J_a} \prod_a \prod_{i < j} (\tau_i^a \tau_j^a)^{k_{ij}^a} \mathcal{A}_\tau^{5-1} \text{truncated}(0) \quad (7.28)$$

Using the expansion above together with the Eq. (7.24), we find that \mathcal{N} is given by the not too lengthy expression:

$$\begin{aligned} \mathcal{N}([\tau], [j]) = & (1 + \rho^2)^{-\sum_a J_a} \sum_{j_b, j_g, j_r, j_y} \left(\prod_{l=b, g, r, y} \frac{(2j_l + 1)^{\eta+1}}{(1 + \rho^2)^{6j_l}} \right) \tau_{AB}^{2j_{AB} + 2j_b + 2j_g} \times \\ & \times \tau_{AC}^{2j_{AC} + 2j_y + 2j_g} \tau_{AD}^{2j_{AD} + 2j_y + 2j_b} \tau_{BC}^{2j_{BC} + 2j_r + 2j_g} \tau_{BD}^{2j_{BD} + 2j_b + 2j_r} \tau_{CD}^{2j_{CD} + 2j_y + 2j_r} \times \\ & \times \tilde{\tau}_{EA}^{2j_{EA} + 4(j_b + j_g + j_y)} \tilde{\tau}_{EB}^{2j_{EB} + 4(j_b + j_g + j_r)} \tilde{\tau}_{EC}^{2j_{EC} + 4(j_r + j_g + j_y)} \tilde{\tau}_{ED}^{2j_{ED} + 4(j_b + j_r + j_y)}. \end{aligned} \quad (7.29)$$

As is often the case with gauge theories, the truncation we have chosen is clearly visible in this expression, but hopefully the dominant contribution is independent of this choice.

This was actually shown to be true in [101] at least when the external spins vanish – the choice of the gauge-fixing tree does not impact the degree of divergence.

All that is now left is to apply the homogeneity map (6.16) to \mathcal{N} to get the renormalization factor after the 5–1 Pachner move. We define

$$\mathcal{N}_{5-1}([j]) \equiv H_{5-1}[\mathcal{N}([\tau], [j])] \quad (7.30)$$

The full expression for $\mathcal{N}_{5-1}([j])$ is a rather lengthy, but still manageable, monstrosity. To simplify the expression, we will label the loops not by their colors, but by the edges they originally touched before the loop identities. As such, we let

$$j_b = j_{ABD}, \quad j_g = j_{ABC}, \quad j_r = j_{BCD}, \quad j_y = j_{ACD} \quad (7.31)$$

With this notation, we can get also get rather clearer understanding of each of the terms. We obtain

$$\begin{aligned} \mathcal{N}_{5-1}([j]) = & \sum_{j_b, j_g, j_r, j_y} \left(\prod_{l=b, g, r, y} \frac{(2j_l + 1)^{\eta+1}}{(1 + \rho^2)^{48j_l}} \right) (1 + \rho^2)^{-3 \sum_a J_a + 2J_E - 10 \sum_{\mu < \nu \in \{A, B, C, D\}} j_{\mu\nu}} \\ & \times \left[\prod_{\mu < \nu \in \{A, B, C, D\}} F_\rho \left(2j_{\mu\nu} + 2 \sum_{\sigma > \mu, \nu} j_{\mu\nu\sigma} \right)^2 \left(2j_{\mu\nu} + 2 \sum_{\sigma > \mu, \nu} j_{\mu\nu\sigma} + 1 \right)^{\eta-1} \right] \\ & \times \prod_{\mu \in \{A, B, C, D\}} F_\rho \left(2 \sum_{\nu < \sigma \neq \mu} j_{\mu\nu\sigma} + J_\mu \right)^2 \end{aligned} \quad (7.32)$$

We can see immediately that this is a minor modification of the expression (6.13) for degree of divergence of the 5–1 move, with additional external spins inserted in the hypergeometric functions and some additional factors of $(1 + \rho^2)$.

Introducing a coupling constant λ_v for each 4-simplex, the above calculation allows us to write down the equation for the flow of the vertex amplitude under the 5–1 Pachner move as

$$\sum_{\text{internal } j} \{15j\}_\rho^5 \lambda_v^5 = \{15j\}_\rho \times \mathcal{N}_{5-1}([j]) \lambda_v^5 \equiv \lambda'_v \{15j\}'_\rho. \quad (7.33)$$

This shows that our truncation scheme has successfully truncated the flow to the space of 4-simplices.

The ten external spins are all independent, which complicates the analysis of the general case of this flow equation. We will consider the simpler case where all the spins are set

equal to the same j . This is well motivated, since the symmetric configurations have the highest contribution in the large spin limit¹. The non-trivial function $\mathcal{N}_{5-1}([j])$ in this limit becomes

$$\begin{aligned} \mathcal{N}_{5-1}(j) = & \sum_{j_b, j_g, j_r, j_y} \frac{\prod_{l=b,g,r,y} (2j_l + 1)^{\eta+1}}{(1 + \rho^2)^{48 \sum_l j_l + 112j}} \prod_{l_1 < l_2 < l_3 \in \{b,g,r,y\}} F_\rho \left(2 \sum_{i=1}^3 j_{l_i} + 4j \right)^2 \\ & \times \left[\prod_{l_1 < l_2 \in \{b,g,r,y\}} F_\rho \left(2j + 2 \sum_{i=1}^2 j_{l_i} \right)^2 \left(2j + 2 \sum_{i=1}^2 j_{l_i} + 1 \right)^{\eta-1} \right] \end{aligned} \quad (7.34)$$

where we went back to the shorter notation for the loops. We expect this to diverge as D_{5-1} , but note that the external spins are now mixed up with the internal loops through the hypergeometric functions. To understand this structure better, let us study it in the large spin limit approximation. Since we are interested in \mathcal{N}_{5-1} as a function of both ρ and η , we can use the asymptotic expression for $F_\rho(J)$ in Eq. (3.12), which is valid for $0 < \rho < 1$ strictly. Note that the contribution from the internal summed over loops is purely divergent, so we can also approximate them to be large. Thus letting all spins be large, we have to leading order

$$\mathcal{N}_{5-1}(j) \sim N_\rho \sum_{j_b, j_g, j_r, j_y} \frac{\prod_l (2j_l + 1)^{\eta+1} \prod_{l_1 < l_2} (2j + 2 \sum_{i=1}^2 j_{l_i} + 1)^{\eta-1}}{\prod_{l_1 < l_2} (2j + 2 \sum_{i=1}^2 j_{l_i})^3 \prod_{l_1 < l_2 < l_3} (4j + 2 \sum_{i=1}^3 j_{l_i})^3}, \quad (7.35)$$

where the normalization factor is given by

$$N_\rho = \frac{(1 + \rho^2)^{60}}{(4\pi)^{10} \rho^{60}}. \quad (7.36)$$

If we impose a cutoff Λ on spins, rescale the external spins to $\tilde{\Lambda} j$ and the summed over ones to $\tilde{\Lambda} \tilde{j}_l$, with $\Lambda \rightarrow \infty$, and approximate the summations by integrations, we get

$$\mathcal{N}_{5-1}(j) \sim N_\rho D_{5-1} \int_\epsilon^1 \prod_{l=b,g,r,y} d\tilde{j}_l \frac{\prod_l 2\tilde{j}_l^{\eta+1} \prod_{l_1 < l_2} (2\tilde{j} + 2 \sum_{i=1}^2 \tilde{j}_{l_i})^{\eta-4}}{\prod_{l_1 < l_2 < l_3} (4\tilde{j} + 2 \sum_{i=1}^3 \tilde{j}_{l_i})^3}, \quad (7.37)$$

where we introduced a small regulating cutoff ϵ due to our expressions for $F_\rho(J)$ being only valid for large spins, and recall the divergence of 5-1 move is $D_{5-1} = \Lambda^{10\eta-28}$. This

¹Note critically though that neglecting the off-diagonal terms results in greatly underestimated value of the amplitude.

integral is now a finite function of $\tilde{j} = j/\Lambda$, which we can study numerically. Before we do so, notice that we have roughly $\mathcal{N}_{5-1}(j) \sim \tilde{j}^{6(\eta-6)}$, so we expect some phase transition from a decreasing to an increasing function of j .

Numerically integrating the above expression gives us the behavior of $\mathcal{N}_{5-1}(j)$ as both a function of spin and face weight power η . Let us first see what happens when the 5–1 move has the divergence of Λ^2 , which is the one we would expect it naively to have if it corresponded purely to the freedom of translating a vertex in 3d space. The results in this case can be seen in Fig. 7.3. As we can see, in this case $\mathcal{N}_{5-1}(j)$ is a rapidly decreasing function of the boundary spins.

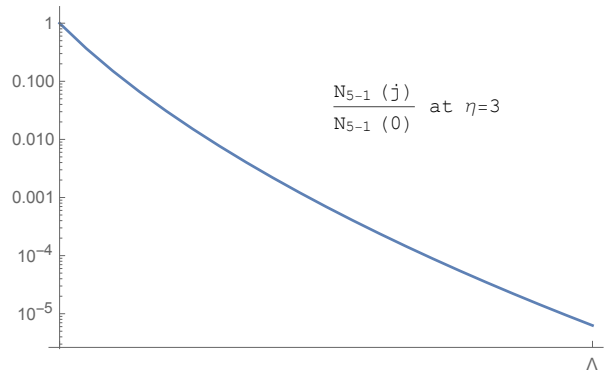


Figure 7.3: Plot of $\frac{\mathcal{N}_{5-1}(j)}{\mathcal{N}_{5-1}(0)}$ at $\eta = 3$, where the 5–1 move has Λ^2 divergence.

Let us now investigate the "phase transition" when boundary spins start contributing towards the divergence of the amplitude. It turns out that our naive expectation was not exactly right, as at $\eta = 6$ we still have the same behavior, though a much slower decrease with j . However, we find that around $\eta = 6.5$ we do indeed get a transition from a rapidly decreasing to an increasing function of spin. Interestingly, around the transition point there seems to be a range of η for which the function is first decreasing and then increasing, but extremely slowly - to the extent that it is approximately flat. In this regime we have nearly no spin dependence and one could wonder whether this could be a good candidate for a fixed point for the renormalization of the vertex. Note however that here the 5–1 move is very divergent, namely it scales like Λ^{37} . It is thus not clear what to make of this point. See Fig. 7.4 for the behavior of $\mathcal{N}_{5-1}(j)$ around this transition.

If we follow the discussion at the end of Section 6.4, then the above results change slightly by introducing an edge weight. If we would introduce a factor of $\mathcal{A}_e(J) = (J+1)^\alpha$, then the divergence of the 5–1 move becomes $\Lambda^{10(\eta+\alpha)-28}$, while the scaling of \mathcal{N}_{5-1} as

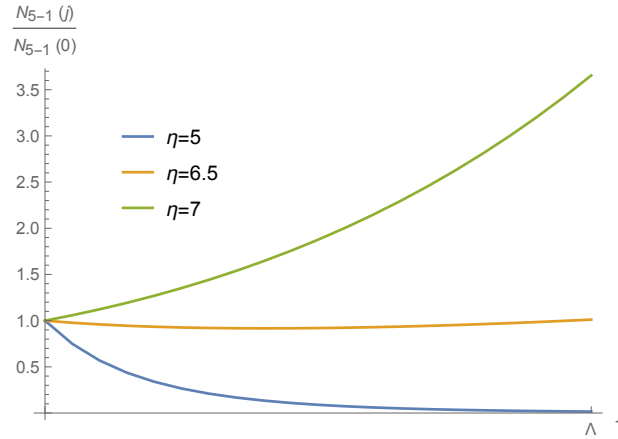


Figure 7.4: Plot of $\frac{\mathcal{N}_{5-1}(j)}{\mathcal{N}_{5-1}(0)}$ for 3 different values of η around the transition point.

a function of spin becomes something along the lines of $\tilde{j}^{6(\eta-6)+10\alpha}$. Since these scale differently, we could in principle have the transition point coincide with the Λ^2 divergence of the 5–1 move. A rough estimate in which we exchange $\eta \rightarrow \eta + \frac{10}{6}\alpha$, gives us that this would happen around the point $(\eta = -\frac{9}{4}, \alpha = \frac{21}{4})$. The negative power of the face weight makes this however an even more bizarre suggestion than the above.

It is now very important to note that each of the hypergeometric functions in $\mathcal{N}_{5-1}([j])$ depends in part on spins in the 4 loops that we sum over. This means that whenever the 5–1 move is divergent (i.e. for $\eta > 2.8$ without the inclusion of the arbitrary edge weights), we do not need the external spins to be necessarily large for the validity of asymptotic expansion of $F_\rho(J)$ – even for small external spins Eq. (7.35) is an excellent approximation! Moreover, we can even allow the external spins to be all different and still not worry about butchering the final answer. This means that as far as the renormalization factor $\mathcal{N}_{5-1}([j])$ is concerned, we can effectively work with the greatly simplified expression in terms of simple ratios of polynomials of spin, rather than the gnarly hypergeometric functions!

7.5 Proposal for a new amplitude

The factorization of the result of the 5–1 move into a $15j$ symbol and a nonlocal function of spins suggests that while we cannot write the amplitude in terms of renormalized propagators, we could nonetheless proceed by embracing this nonlocality. The factor $\mathcal{N}_{5-1}([j])$

depends only on the 10 boundary spins (and 4 summed over spins), but not on the intertwiner labels. This would suggest that we could try to rescale each strand separately, but recall that the hypergeometric functions and the face weight factors do not factorize in any neat way. The only option then is to include this nonlocal function into the vertex amplitude itself. Recall that in Eq. (3.13) we defined the partition function of our model as a product of face weights for each face and propagators at fixed spins for each edge of the Spin Foam 2-complex. Our results in this chapter suggest that while there is no clear rewriting of the model in terms of new propagators after the RG step, what is naturally generated is a non-trivial operator for each vertex. After the 5–1 Pachner move then, we suggest that the amplitude can be written in terms of non-trivial edge, face *and* also vertex amplitudes. We would have then

$$Z^{\Delta^*} = \sum_{j_f} \sum_{k_{f,f'}^e \in K_j} \prod_{f \in \Delta^*} \mathcal{A}_f(j_f) \prod_{e \in \Delta^*} \int \left\{ \prod_{all} d\mu_\rho(z^e, w^e) \right\} P_\rho^{k_{ij}^e}(z_i^e; w_i^e) \prod_{v \in \Delta^*} \lambda_v \mathcal{N}(j_{v_1}, \dots, j_{v_{10}}), \quad (7.38)$$

where we have normalized each vertex by a factor of λ_v , which absorbs the divergence D_{5-1} of the 5–1 Pachner move. Based on the previous discussion, one might also want to include an arbitrary edge weight $\mathcal{A}_e(j_{e_1}, \dots, j_{e_4})$ for each pair of propagators. For calculation purposes, one might find it useful to re-express this additional vertex term in terms of spinors. We can do so by inserting trivial connections to all the spinors. Inserting a factor of

$$\frac{(1 + \rho^2)^{2j}}{(2j)!} [z|w]^{2j}$$

for each spin in the expression for $\mathcal{N}_{5-1}([j])$ and contracting with the spinors from the boundary propagators does not change the expression. Note that the additional factor of $(1 + \rho^2)^{2j}$ cancels the contribution from the measure of integration. We can then re-exponentiate the whole expression using the homogeneity map technique.

The continued iteration of 5^n-5^{n-1} Pachner moves then generates a flow in the $\mathcal{N}([j])$ only, without modifying any of the edge or face amplitudes. While we could in principle try modifying the edge propagators at each step there is still always the nonlocal vertex factor. As for the face amplitude, as we have discussed earlier in the chapter, there is no well-defined flow for η , since the original configuration of a single 4-simplex does not have any faces to sum over.

To see what kind of divergences we generate at each RG step, let us investigate what happens in the 25–1 move. In [101] it was shown that the degree of divergence of an arbitrary amplitude is $\Lambda^{(\eta+2)|F|-6|E|+3|V|-3}$, where $|E|$, $|F|$ and $|V|$ are the number of edges,

faces and vertices in the 2-complex respectively. The symmetric configuration of 25 4-simplices has $|E| = |F| = 60$ and obviously $|V| = 25$. We thus find that the 25–1 Pachner move has divergence of $(D_{5-1})^6$. This means that at each RG step we get exactly the same type of divergences, all of which can be absorbed into the single parameter λ_v . The model is thus renormalizable under the iterated Pachner moves, as we do not need to add any further coupling constants.

Following the suggestion in the previous chapter, we could consider $\mathcal{N}([j])$ as a geometrical operator. The flow under the iterated RG steps could then be expressed in terms of the interesting graphical series, which as we suggested before introducing the truncation scheme. Namely, if we represent $\mathcal{N}_{5-1}([j])$ by a diamond with six vertices, then after a 25–5 Pachner move we get a larger diamond, at the vertices of which there are the smaller diamonds representing the divergences of the original 5–1 moves, which seems to converge to some sort of fractal geometry.

The main open question now is how to obtain a model that is invariant under the vertex translation symmetry. If the above graphical series for \mathcal{N} converges for the 5^n-1 Pachner move in the $n \rightarrow \infty$ limit, then we are done. This sounds like a daunting task, but with the methods of this thesis should in principle be doable. Due to the unforgiving nature of the hypergeometrical functions, we might however arrive at expressions that are difficult to deal with. This can be avoided by either working with $\rho = 1$, where $F_\rho(J)$ is simplified into a ratio of factorials, or using the large spin limit. However, as we noticed at the end of the last section, whenever the 5–1 move is divergent, then working with the asymptotic expression for $\mathcal{N}_{5-1}([j])$ is valid even for small external spins. While the analysis of the general case is somewhat complicated due to the ten arbitrary external spins, the numerical results of the previous section suggest that in the symmetric case, there is a phase transition of $\mathcal{N}_{5-1}([j])$ as a function of j around $\eta = 6.5$ (if we do not include the edge weights). At the transition point $\mathcal{N}_{5-1}(j)$ is a very slowly varying function of spin, so in some sense we could speak of having an approximate translation invariance. If this fixed point persists after iterated Pachner moves, then we could have invariance at least for the symmetric vertex.

Chapter 8

Summary & Concluding remarks

There is no real ending. It's just the place where you stop the story.

Frank Herbert

Reaching the end of this thesis, let us look back at what was achieved and where the paths onward lead. The starting point we took was choosing to work with the newly developed spinor representation for Spin Foams, rather than working with the traditionally challenging spin representation. This rewriting allowed us to consider an alternative imposition of the holomorphic simplicity constraints, resulting in a definition of a new Riemannian Spin Foam model. Instead of constraining the boundary spin networks, we imposed the constraints directly on the topological BF propagators. We then compared this new model to the more traditional imposition of the simplicity constraints by expressing the Dupuis-Livine model (which is a rewriting of the EPRL-FK models in terms of spinors) also in terms of propagators. This comparison clearly showed that the alternative model results in greatly simplified expressions. One could worry that we have over-constrained the dynamics, but we showed that surprisingly both models are given by Regge Calculus in the semi-classical limit.

The power of the holomorphic representation lies in the fact that difficult integrals of SU(2) Wigner D-matrices can be recast into much simpler spinor Gaussian integrals. We have used this fact to define a *homogeneity map*, which allows us to recast all integrations of interest into Gaussians, thus making it possible to perform integrations that were previously deemed too difficult to evaluate exactly. Hoping that these results would allow us to study

coarse graining in our 4-dimensional model, we then turned to studying the lessons of 3d quantum gravity. The coarse graining procedure in the 3d case depends on two Pachner moves: the 3–2 move and the 4–1 move. The results for these have been long known: the 3–2 move is exactly invariant, while 4–1 move is invariant up to a factor of an $SU(2)$ delta function, which results from not fixing the vertex translation symmetry. The calculation of the 3d Pachner moves relies on a single identity for summation of spins in a closed loop.

In order to study the coarse graining, we thus had to evaluate this *loop identity* for the constrained models. We showed that in the case of our alternative model we obtained additional mixing of spinors that is not present in the topological case. We then attempted to derive this for the DL model. While this was still in principle possible, we found the resulting expression to be quite difficult to manage, and decided to only proceed with the simpler model. Using the techniques we developed, we then proceeded to evaluate the 4-dimensional Pachner moves: the 3–3, 4–2 and 5–1 moves. We found that the 3–3 move was invariant only in the very symmetric case of all spins being equal. While the naive expectation, at least at the level of the classical action, was that the model should be invariant under the 4–2 and 5–1 Pachner moves, we found it to not be true for the exact evaluation. For both the 4–2 and 5–1 moves, we obtained an additional insertion of a non-local combination of $SU(N)$ grasping operators in the final coarse grained simplices, with a mixing of strands leading to a non-geometrical and non-local configuration.

Recalling however that in real-space renormalization group flows it is natural to generate additional couplings at each RG step, we found a natural truncation scheme for each loop identity that removes the mixing of strands and seems to restrict the flow to the space of 4-simplices. This removal of mixing allowed us to show that both 4–2 and 5–1 moves are invariant up to a weight depending on the boundary spins. We then studied the degree of divergence of both of these moves and found that it depends on the choice of the power of the face weight η . The 5–1 move turns out to be much more divergent than the 4–2 move. Indeed, when the 5–1 move has the divergence of Λ^2 that was in the past suggested as relating to diffeomorphism invariance, the 4–2 move is finite. We then conjectured that the divergent factor of the 5–1 move that also depends on boundary spins could be absorbed into a renormalized definition of new edge propagators.

In our last chapter however, we showed that this rewriting is impossible – in fact there is no way of writing the amplitude after the 5–1 move as a symmetric local product of propagators. This seems to be a Spin Foam realization of the result in linearized quantum Regge Calculus, where the measure of integration picks up a non-local factor after the 5–1 move [72]. In order to understand what we can extract out of our result, we decided to rewrite the result in terms of the more traditional 15j symbols. Expanding our result in a power series, we showed that we do have a renormalization equation that relates five 15j

symbols with a single $15j$ multiplied by the divergent function $\mathcal{N}_{5-1}(j_1, \dots, j_{10})$ depending on boundary spins. Interestingly, this function coupled the external spins with the summed over spins from the remaining divergent loops in the 5–1 move. This allowed us to use the asymptotic expansions for the hypergeometric functions even for small boundary spins. We then showed that in the symmetric case the factor $\mathcal{N}_{5-1}(j)$ had a transition from a decreasing function of j to an increasing one around $\eta = 6.5$, at which point the function is very slowly varying with spin. It is now important to note that in our RG step given by the 5–1 move there can be no flow in either ρ or η . This is because the dependence on the Barbero-Immirzi parameter simply drops out in the large spin limit, so it does not appear in conjunction with divergences. The reason why there can be no flow in η is simple – a single 4-simplex does not depend on a face weight, so the renormalized vertex should not either. For this reason we introduced the coupling λ_v for a vertex.

These results suggest that we can perhaps have to redefine the amplitude to not only have a product of propagators at each edge, but also this non-local factor at each vertex. We argue that iterated 5–1 Pachner moves only change this factor, and do not generate any more complicated couplings. Since there is already a range of parameters for which $\mathcal{N}_{5-1}(j)$ is nearly constant, we have hopes that the iterated application of 5^n – 5^{n-1} moves can converge to an expression that has exact vertex translation symmetry. The reason we say that this would constitute a vertex translation symmetry is that embedding the vertex amplitude after the 5–1 move or before in a bigger graph that would require us to sum over the spins, would only result in a difference up to an overall divergent factor. The question of whether the iterated Pachner moves lead to such an expression is one we leave for future research.

On a related note, it is interesting to consider whether our requirement for symmetry might not be too strong. Rather than requiring that the RG flow makes $\mathcal{N}(j)$ spin-independent, maybe it is enough to enforce the weaker condition that only after the summation over the spins do we get something that is easy to deal with. Technically, we could try to evaluate the 5^n – 5^{n-1} move, express $\mathcal{N}(j)$ as a function of n , close up the boundary by contracting all the strands and see whether we can obtain an expression that does not finally depend on n . For such closed diagrams, the methods developed by Chen in [101] would be immediately applicable.

Apart from the iteration of the Pachner moves, the work in this thesis suggests several interesting avenues of continued research. First of all, it would be interesting to study the validity of adding the additional edge weights that we suggested during the study of the divergences, as they seem to allow the more natural choice of face weight η . It would be crucial to see whether the truncation of the loop identity is still valid with this modification however. Another interesting path forward lies in seeing whether we could obtain similar

results without the necessity for gauge fixing, which would give us a more symmetric expression for $\mathcal{N}_{5-1}(j)$. This would require us to recalculate the loop identity with three full propagators. The results in the 2d case suggest that the result might not be too unwieldy. The non-trivial question then is whether the truncation scheme we found would still work, or whether an alternative truncation would be necessary. Of slightly higher difficulty would be the attempt at calculating the Pachner moves with the DL model. The greatly increased number of variables would make the evaluation more tiresome, but possible in principle. Again, some truncation would be probably needed in this case as well. We leave this project for some brave individuals who really dislike the construction of our simplified model.

The big open problem here is whether we could generalize these results to the Lorentzian case. The biggest obstacle is the non-existence of the holomorphic representation with the nice Gaussian measure of integration for the $SL(2, \mathbb{C})$ group. While our construction relied quite heavily on the Gaussian integrations, the main trick of the homogeneity map was not crucially reliant on that – we could use it with some other basis functions that integrate nicely. Of special interest are the results of Speziale in [\[116\]](#), where it was shown that $SL(2, \mathbb{C})$ results can be obtained by boosting $SU(2)$ expressions. It would be interesting to see if these techniques could be applied to our results to make some statements about the Lorentzian theory.

Bibliography

- [1] A. Banburski, L. Q. Chen, L. Freidel and J. Hnybida, “Pachner moves in a 4d Riemannian holomorphic Spin Foam model,” *Phys. Rev. D* **92**, no. 12, 124014 (2015) doi:10.1103/PhysRevD.92.124014 [arXiv:1412.8247 [gr-qc]].
- [2] A. Banburski and L. Q. Chen, “Simpler way of imposing simplicity constraints,” *Phys. Rev. D* **94**, no. 10, 104003 (2016) doi:10.1103/PhysRevD.94.104003 [arXiv:1512.05331 [gr-qc]].
- [3] M. B. Green, J. H. Schwarz and E. Witten, “Superstring Theory. Vol. 1: Introduction,” Cambridge, Uk: Univ. Pr. (1987) 469 P. (Cambridge Monographs On Mathematical Physics)
- [4] M. B. Green, J. H. Schwarz and E. Witten, “Superstring Theory. Vol. 2: Loop Amplitudes, Anomalies And Phenomenology,” Cambridge, Uk: Univ. Pr. (1987) 596 P. (Cambridge Monographs On Mathematical Physics)
- [5] T. Thiemann, “Modern canonical quantum general relativity,” gr-qc/0110034.
- [6] C. Rovelli, “Quantum gravity,” Cambridge University Press (2007)
- [7] C. Rovelli, “Zakopane lectures on loop gravity,” *PoS QGQGS* **2011**, 003 (2011) [arXiv:1102.3660 [gr-qc]].
- [8] A. Perez, “The Spin Foam Approach to Quantum Gravity,” *Living Rev. Rel.* **16**, 3 (2013) [arXiv:1205.2019 [gr-qc]].
- [9] J. F. Plebanski, “On the separation of Einsteinian substructures,” *J. Math. Phys.* **18**, 2511 (1977).
- [10] E.R. Livine and S. Speziale, “A new spinfoam vertex for quantum gravity”, *Phys.Rev.D76* (2007) 084028 [arXiv:0705.0674]

- [11] E. R. Livine and S. Speziale, “Consistently Solving the Simplicity Constraints for Spinfoam Quantum Gravity,” *Europhys. Lett.* **81**, 50004 (2008) [arXiv:0708.1915 [gr-qc]].
- [12] J. Engle, E. Livine, R. Pereira and C. Rovelli, “LQG vertex with finite Immirzi parameter,” *Nucl. Phys. B* **799**, 136 (2008) [arXiv:0711.0146 [gr-qc]].
- [13] J. Engle, R. Pereira and C. Rovelli, “The Loop-quantum-gravity vertex-amplitude,” *Phys. Rev. Lett.* **99**, 161301 (2007) [arXiv:0705.2388 [gr-qc]].
- [14] J. Engle, R. Pereira and C. Rovelli, “Flipped spinfoam vertex and loop gravity,” *Nucl. Phys. B* **798**, 251 (2008) [arXiv:0708.1236 [gr-qc]].
- [15] L. Freidel and K. Krasnov, “A New Spin Foam Model for 4d Gravity,” *Class. Quant. Grav.* **25**, 125018 (2008) [arXiv:0708.1595 [gr-qc]].
- [16] M. Dupuis and E. R. Livine, “Holomorphic Simplicity Constraints for 4d Spinfoam Models,” *Class. Quant. Grav.* **28**, 215022 (2011) [arXiv:1104.3683 [gr-qc]].
- [17] B. Bahr, “On background-independent renormalization of spin foam models,” arXiv:1407.7746 [gr-qc].
- [18] D. Mamone and C. Rovelli, “Second-order amplitudes in loop quantum gravity,” *Class. Quant. Grav.* **26**, 245013 (2009) [arXiv:0904.3730 [gr-qc]].
- [19] A. Riello, “Self-energy of the Lorentzian Engle-Pereira-Rovelli-Livine and Freidel-Krasnov model of quantum gravity,” *Phys. Rev. D* **88**, no. 2, 024011 (2013) [arXiv:1302.1781 [gr-qc]].
- [20] B. Dittrich, S. Mizera and S. Steinhaus, “Decorated tensor network renormalization for lattice gauge theories and spin foam models,” arXiv:1409.2407 [gr-qc].
- [21] M. H. Goroff and A. Sagnotti, “The Ultraviolet Behavior of Einstein Gravity,” *Nucl. Phys. B* **266**, 709 (1986). doi:10.1016/0550-3213(86)90193-8
- [22] H. Nicolai, “Quantum Gravity: the view from particle physics,” *Fundam. Theor. Phys.* **177**, 369 (2014) doi:10.1007/978-3-319-06349-2-18 [arXiv:1301.5481 [gr-qc]].
- [23] S. Weinberg, “Critical Phenomena for Field Theorists,” HUTP-76-160.
- [24] D. Dou and R. Percacci, “The running gravitational couplings,” *Class. Quant. Grav.* **15**, 3449 (1998) doi:10.1088/0264-9381/15/11/011 [hep-th/9707239].

- [25] M. Reuter and F. Saueressig, “Renormalization group flow of quantum gravity in the Einstein-Hilbert truncation,” *Phys. Rev. D* **65**, 065016 (2002) doi:10.1103/PhysRevD.65.065016 [hep-th/0110054].
- [26] O. Lauscher and M. Reuter, “Fractal spacetime structure in asymptotically safe gravity,” *JHEP* **0510**, 050 (2005) doi:10.1088/1126-6708/2005/10/050 [hep-th/0508202].
- [27] I. Donkin and J. M. Pawłowski, “The phase diagram of quantum gravity from diffeomorphism-invariant RG-flows,” arXiv:1203.4207 [hep-th].
- [28] P. Don, A. Eichhorn and R. Percacci, “Matter matters in asymptotically safe quantum gravity,” *Phys. Rev. D* **89**, no. 8, 084035 (2014) doi:10.1103/PhysRevD.89.084035 [arXiv:1311.2898 [hep-th]].
- [29] C. Rovelli and L. Smolin, “Discreteness of area and volume in quantum gravity,” *Nucl. Phys. B* **442**, 593 (1995) Erratum: [*Nucl. Phys. B* **456**, 753 (1995)] doi:10.1016/0550-3213(95)00150-Q, 10.1016/0550-3213(95)00550-5 [gr-qc/9411005].
- [30] I. Montvay and G. Münster, “Quantum fields on a lattice,” Cambridge, UK: Univ. Pr. (1994) 491 p. (Cambridge monographs on mathematical physics)
- [31] F. Markopoulou, “Coarse graining in spin foam models,” *Class. Quant. Grav.* **20**, 777 (2003) [gr-qc/0203036].
- [32] R. Oeckl, “Renormalization of discrete models without background,” *Nucl. Phys. B* **657**, 107 (2003) [gr-qc/0212047].
- [33] R. Oeckl, “Renormalization for spin foam models of quantum gravity,” In *Rio de Janeiro 2003, Recent developments in theoretical and experimental general relativity, gravitation, and relativistic field theories, pt. C* 2296-2300 [gr-qc/0401087].
- [34] A. Ashtekar and J. Lewandowski, “Projective techniques and functional integration for gauge theories,” *J. Math. Phys.* **36**, 2170 (1995) [gr-qc/9411046].
- [35] A. Ashtekar and J. Lewandowski, “Differential geometry on the space of connections via graphs and projective limits,” *J. Geom. Phys.* **17**, 191 (1995) [hep-th/9412073].
- [36] A. Baratin, B. Dittrich, D. Oriti and J. Tambornino, “Non-commutative flux representation for loop quantum gravity,” *Class. Quant. Grav.* **28**, 175011 (2011) [arXiv:1004.3450 [hep-th]].

- [37] B. Dittrich, “From the discrete to the continuous: Towards a cylindrically consistent dynamics,” *New J. Phys.* **14**, 123004 (2012) [arXiv:1205.6127 [gr-qc]].
- [38] B. Dittrich, “The continuum limit of loop quantum gravity - a framework for solving the theory,” arXiv:1409.1450 [gr-qc].
- [39] M. Levin, C. P. Nave, “Tensor renormalization group approach to 2D classical lattice models,” *Phys. Rev. Lett.* **99** (2007) 120601.
- [40] S. Singh and G. Vidal, “Tensor network states and algorithms in the presence of a global SU(2) symmetry,” *Phys. Rev. B* **86**, 195114 (2012) [arXiv:1208.3919 [cond-mat.str-el]].
- [41] Z. C. Gu and X. G. Wen, “Tensor-Entanglement-Filtering Renormalization Approach and Symmetry Protected Topological Order,” *Phys. Rev. B* **80**, 155131 (2009) [arXiv:0903.1069 [cond-mat.str-el]].
- [42] B. Dittrich, F. C. Eckert and M. Martin-Benito, “Coarse graining methods for spin net and spin foam models,” *New J. Phys.* **14**, 035008 (2012) [arXiv:1109.4927 [gr-qc]].
- [43] B. Dittrich and F. C. Eckert, “Towards computational insights into the large-scale structure of spin foams,” *J. Phys. Conf. Ser.* **360**, 012004 (2012) [arXiv:1111.0967 [gr-qc]].
- [44] B. Bahr, B. Dittrich, F. Hellmann and W. Kaminski, “Holonomy Spin Foam Models: Definition and Coarse Graining,” *Phys. Rev. D* **87**, 044048 (2013) [arXiv:1208.3388 [gr-qc]].
- [45] B. Dittrich, M. Martin-Benito and E. Schnetter, “Coarse graining of spin net models: dynamics of intertwiners,” *New J. Phys.* **15**, 103004 (2013) [arXiv:1306.2987 [gr-qc]].
- [46] B. Dittrich and W. Kaminski, “Topological lattice field theories from intertwiner dynamics,” arXiv:1311.1798 [gr-qc].
- [47] B. Dittrich, M. Martin-Benito and S. Steinhaus, “Quantum group spin nets: refinement limit and relation to spin foams,” *Phys. Rev. D* **90**, 024058 (2014) [arXiv:1312.0905 [gr-qc]].
- [48] B. Dittrich, S. Mizera and S. Steinhaus, “Decorated tensor network renormalization for lattice gauge theories and spin foam models,” *New J. Phys.* **18**, no. 5, 053009 (2016) doi:10.1088/1367-2630/18/5/053009 [arXiv:1409.2407 [gr-qc]].

- [49] B. Dittrich, E. Schnetter, C. J. Seth and S. Steinhaus, “Coarse graining flow of spin foam intertwiners,” *Phys. Rev. D* **94**, no. 12, 124050 (2016) doi:10.1103/PhysRevD.94.124050 [arXiv:1609.02429 [gr-qc]].
- [50] C. Delcamp and B. Dittrich, “Towards a phase diagram for spin foams,” arXiv:1612.04506 [gr-qc].
- [51] E. R. Livine and D. Oriti, “Coupling of spacetime atoms and spin foam renormalisation from group field theory,” *JHEP* **0702**, 092 (2007) [gr-qc/0512002].
- [52] L. Freidel, R. Gurau and D. Oriti, “Group field theory renormalization - the 3d case: Power counting of divergences,” *Phys. Rev. D* **80**, 044007 (2009) [arXiv:0905.3772 [hep-th]].
- [53] J. Ben Geloun and V. Rivasseau, “A Renormalizable 4-Dimensional Tensor Field Theory,” *Commun. Math. Phys.* **318**, 69 (2013) [arXiv:1111.4997 [hep-th]].
- [54] V. Rivasseau, “Quantum Gravity and Renormalization: The Tensor Track,” *AIP Conf. Proc.* **1444**, 18 (2011) [arXiv:1112.5104 [hep-th]].
- [55] J. Ben Geloun and D. O. Samary, “3D Tensor Field Theory: Renormalization and One-loop β -functions,” *Annales Henri Poincare* **14**, 1599 (2013) [arXiv:1201.0176 [hep-th]].
- [56] J. Ben Geloun and E. R. Livine, “Some classes of renormalizable tensor models,” *J. Math. Phys.* **54**, 082303 (2013) [arXiv:1207.0416 [hep-th]].
- [57] S. Carrozza, D. Oriti and V. Rivasseau, “Renormalization of Tensorial Group Field Theories: Abelian U(1) Models in Four Dimensions,” *Commun. Math. Phys.* **327**, 603 (2014) [arXiv:1207.6734 [hep-th]].
- [58] D. O. Samary and F. Vignes-Tourneret, “Just Renormalizable TGFT’s on $U(1)^d$ with Gauge Invariance,” *Commun. Math. Phys.* **329**, 545 (2014) [arXiv:1211.2618 [hep-th]].
- [59] S. Carrozza, D. Oriti and V. Rivasseau, “Renormalization of a SU(2) Tensorial Group Field Theory in Three Dimensions,” *Commun. Math. Phys.* **330**, 581 (2014) [arXiv:1303.6772 [hep-th]].
- [60] J. Ben Geloun, “Renormalizable Models in Rank $d \geq 2$ Tensorial Group Field Theory,” arXiv:1306.1201 [hep-th].

- [61] S. Carrozza, “Discrete Renormalization Group for SU(2) Tensorial Group Field Theory,” arXiv:1407.4615 [hep-th].
- [62] V. Lahoche, D. Oriti and V. Rivasseau, “Renormalization of an Abelian Tensor Group Field Theory: Solution at Leading Order,” JHEP **1504**, 095 (2015) doi:10.1007/JHEP04(2015)095 [arXiv:1501.02086 [hep-th]].
- [63] V. Lahoche and D. Oriti, “Renormalization of a tensorial field theory on the homogeneous space SU(2)/U(1),” J. Phys. A **50**, no. 2, 025201 (2017) doi:10.1088/1751-8113/50/2/025201 [arXiv:1506.08393 [hep-th]].
- [64] V. Rivasseau, “Why are tensor field theories asymptotically free?,” Europhys. Lett. **111**, no. 6, 60011 (2015) doi:10.1209/0295-5075/111/60011 [arXiv:1507.04190 [hep-th]].
- [65] D. Benedetti and V. Lahoche, “Functional Renormalization Group Approach for Tensorial Group Field Theory: A Rank-6 Model with Closure Constraint,” Class. Quant. Grav. **33**, no. 9, 095003 (2016) doi:10.1088/0264-9381/33/9/095003 [arXiv:1508.06384 [hep-th]].
- [66] J. Ben Geloun, R. Martini and D. Oriti, “Functional Renormalisation Group analysis of Tensorial Group Field Theories on \mathbb{R}^d ,” Phys. Rev. D **94**, no. 2, 024017 (2016) doi:10.1103/PhysRevD.94.024017 [arXiv:1601.08211 [hep-th]].
- [67] S. Carrozza, “Flowing in Group Field Theory Space: a Review,” SIGMA **12**, 070 (2016) doi:10.3842/SIGMA.2016.070 [arXiv:1603.01902 [gr-qc]].
- [68] U. Pachner, “P.L. homeomorphic manifolds are equivalent by elementary shellings,” European Journal of Combinatorics **12** (2), 129145 (1991)
- [69] T. Regge, “General Relativity Without Coordinates,” Nuovo Cim. **19**, 558 (1961).
- [70] B. Dittrich and S. Steinhaus, “Path integral measure and triangulation independence in discrete gravity,” Phys. Rev. D **85**, 044032 (2012) [arXiv:1110.6866 [gr-qc]].
- [71] C. Perini, C. Rovelli and S. Speziale, “Self-energy and vertex radiative corrections in LQG,” Phys. Lett. B **682**, 78 (2009) [arXiv:0810.1714 [gr-qc]].
- [72] B. Dittrich, W. Kaminski and S. Steinhaus, “Discretization independence implies non-locality in 4D discrete quantum gravity,” arXiv:1404.5288 [gr-qc].

- [73] G Ponzano and T Regge, “Semiclassical limit of racah coefficients,” Spectroscopic and group theoretical methods in physics, ed. F. Bloch, North-Holland Publ. Co., Amsterdam, 1968
- [74] J. W. Barrett and L. Crane, “Relativistic spin networks and quantum gravity,” J. Math. Phys. **39**, 3296 (1998) doi:10.1063/1.532254 [gr-qc/9709028].
- [75] V. Bargmann, “On the Representations of the Rotation Group,” Rev. Mod. Phys. **34**, 829 (1962).
- [76] J. Schwinger, “On Angular Momentum,” U.S. Atomic Energy Commission. (unpublished) NYO-3071, (1952).
- [77] L. Freidel, K. Krasnov and E. R. Livine, “Holomorphic Factorization for a Quantum Tetrahedron,” Commun. Math. Phys. **297**, 45 (2010) [arXiv:0905.3627 [hep-th]].
- [78] L. Freidel and E. R. Livine, “The Fine Structure of SU(2) Intertwiners from U(N) Representations,” J. Math. Phys. **51**, 082502 (2010) [arXiv:0911.3553 [gr-qc]].
- [79] L. Freidel and E. R. Livine, “U(N) Coherent States for Loop Quantum Gravity,” J. Math. Phys. **52**, 052502 (2011) [arXiv:1005.2090 [gr-qc]].
- [80] E. F. Borja, L. Freidel, I. Garay and E. R. Livine, “U(N) tools for Loop Quantum Gravity: The Return of the Spinor,” Class. Quant. Grav. **28**, 055005 (2011) [arXiv:1010.5451 [gr-qc]].
- [81] E. R. Livine and J. Tambornino, “Spinor Representation for Loop Quantum Gravity,” J. Math. Phys. **53**, 012503 (2012) [arXiv:1105.3385 [gr-qc]].
- [82] M. Dupuis, S. Speziale and J. Tambornino, “Spinors and Twistors in Loop Gravity and Spin Foams,” PoS QGQGS **2011**, 021 (2011) [arXiv:1201.2120 [gr-qc]].
- [83] M. Dupuis and E. R. Livine, “Revisiting the Simplicity Constraints and Coherent Intertwiners,” Class. Quant. Grav. **28**, 085001 (2011) [arXiv:1006.5666 [gr-qc]].
- [84] M. Dupuis and E. R. Livine, “Holomorphic Simplicity Constraints for 4d Riemannian Spinfoam Models,” J. Phys. Conf. Ser. **360**, 012046 (2012) [arXiv:1111.1125 [gr-qc]].
- [85] M. Dupuis, L. Freidel, E. R. Livine and S. Speziale, “Holomorphic Lorentzian Simplicity Constraints,” J. Math. Phys. **53**, 032502 (2012) [arXiv:1107.5274 [gr-qc]].

- [86] B. S. DeWitt, Quantum Theory of Gravity. I. The Canonical Theory, *Phys. Rev.*, Vol. 160, No. 5, 1967, pp. 1113-1148
- [87] M. Visser, “Lorentzian wormholes: From Einstein to Hawking,” Woodbury, USA: AIP (1995) 412 p
- [88] A. Ashtekar and J. Lewandowski, “Representation theory of analytic holonomy C-algebras”, *Knots and quantum gravity* (Riverside, CA, 1993), Oxford Lecture Ser. Math. Appl., vol. 1, Oxford Univ. Press, New York, 1994, pp. 21-61. MR1309913 (95j:58021).
- [89] T. Thiemann, “Quantum spin dynamics (QSD),” *Class. Quant. Grav.* **15**, 839 (1998) doi:10.1088/0264-9381/15/4/011 [gr-qc/9606089].
- [90] E. R. Livine and J. Tambornino, “Holonomy Operator and Quantization Ambiguities on Spinor Space,” *Phys. Rev. D* **87**, no. 10, 104014 (2013) [arXiv:1302.7142 [gr-qc]].
- [91] M. Assanioussi, J. Lewandowski and I. Mkinen, “New scalar constraint operator for loop quantum gravity,” *Phys. Rev. D* **92**, no. 4, 044042 (2015) doi:10.1103/PhysRevD.92.044042 [arXiv:1506.00299 [gr-qc]].
- [92] J. Roberts, “Classical 6j-symbols and the tetrahedron,” *Geom. Topol.* **3**, 21 (1999) doi:10.2140/gt.1999.3.21 [math-ph/9812013].
- [93] V. G. Turaev and O. Y. Viro, “State sum invariants of 3 manifolds and quantum 6j symbols,” *Topology* **31**, 865 (1992). doi:10.1016/0040-9383(92)90015-A
- [94] Y. Neiman, “A look at area Regge calculus,” arXiv:1308.1012 [gr-qc].
- [95] F. Conrady and L. Freidel, “On the semiclassical limit of 4d spin foam models,” *Phys. Rev. D* **78**, 104023 (2008) [arXiv:0809.2280 [gr-qc]].
- [96] J. W. Barrett, R. J. Dowdall, W. J. Fairbairn, H. Gomes and F. Hellmann, “Asymptotic analysis of the EPRL four-simplex amplitude,” *J. Math. Phys.* **50**, 112504 (2009) [arXiv:0902.1170 [gr-qc]].
- [97] B. Dittrich and S. Speziale, “Area-angle variables for general relativity,” *New J. Phys.* **10**, 083006 (2008) doi:10.1088/1367-2630/10/8/083006 [arXiv:0802.0864 [gr-qc]].
- [98] L. Freidel and J. Hnybida, “On the exact evaluation of spin networks,” arXiv:1201.3613 [gr-qc].

- [99] L. Freidel and J. Hnybida, “A Discrete and Coherent Basis of Intertwiners,” arXiv:1305.3326 [math-ph].
- [100] M. X. Han and M. Zhang, “Asymptotics of Spinfoam Amplitude on Simplicial Manifold: Euclidean Theory,” *Class. Quant. Grav.* **29**, 165004 (2012) [arXiv:1109.0500 [gr-qc]].
- [101] L. Q. Chen, “Bulk amplitude and degree of divergence in 4d spin foams,” *Phys. Rev. D* **94**, no. 10, 104025 (2016) doi:10.1103/PhysRevD.94.104025 [arXiv:1602.01825 [gr-qc]].
- [102] L. Freidel and D. Louapre, “Diffeomorphisms and spin foam models,” *Nucl. Phys. B* **662**, 279 (2003) [gr-qc/0212001].
- [103] L. Freidel and E. R. Livine, “Spin networks for noncompact groups,” *J. Math. Phys.* **44**, 1322 (2003) [hep-th/0205268].
- [104] M. Christodoulou, M. Langvik, A. Riello, C. Roken and C. Rovelli, “Divergences and Orientation in Spinfoams,” *Class. Quantum Grav.* **30**, 055009 (2013) [arXiv:1207.5156 [gr-qc]].
- [105] L. Freidel and D. Louapre, “Ponzano-Regge model revisited II: Equivalence with Chern-Simons,” gr-qc/0410141.
- [106] J. W. Barrett and I. Naish-Guzman, “The Ponzano-Regge model and Reidemeister torsion,” gr-qc/0612170.
- [107] V. Bonzom and M. Smerlak, “Bubble divergences from cellular cohomology,” *Lett. Math. Phys.* **93**, 295 (2010) [arXiv:1004.5196 [gr-qc]].
- [108] V. Bonzom and M. Smerlak, “Bubble divergences: sorting out topology from cell structure,” *Annales Henri Poincare* **13**, 185 (2012) [arXiv:1103.3961 [gr-qc]].
- [109] L. Freidel and K. Krasnov, “Spin foam models and the classical action principle,” *Adv. Theor. Math. Phys.* **2**, 1183 (1999) [hep-th/9807092].
- [110] B. Bahr and S. Steinhaus, “Investigation of the Spinfoam Path integral with Quantum Cuboid Intertwiners,” *Phys. Rev. D* **93**, no. 10, 104029 (2016) doi:10.1103/PhysRevD.93.104029 [arXiv:1508.07961 [gr-qc]].

- [111] B. Bahr and S. Steinhaus, “Numerical evidence for a phase transition in 4d spin foam quantum gravity,” *Phys. Rev. Lett.* **117**, no. 14, 141302 (2016) doi:10.1103/PhysRevLett.117.141302 [arXiv:1605.07649 [gr-qc]].
- [112] B. Bahr and S. Steinhaus, “Hypercuboidal renormalization in spin foam quantum gravity,” arXiv:1701.02311 [gr-qc].
- [113] R. Gurau, “The $1/N$ expansion of colored tensor models,” *Annales Henri Poincare* **12**, 829 (2011) doi:10.1007/s00023-011-0101-8 [arXiv:1011.2726 [gr-qc]].
- [114] R. Gurau and V. Rivasseau, “The $1/N$ expansion of colored tensor models in arbitrary dimension,” *Europhys. Lett.* **95**, 50004 (2011) doi:10.1209/0295-5075/95/50004 [arXiv:1101.4182 [gr-qc]].
- [115] R. Gurau, “The complete $1/N$ expansion of colored tensor models in arbitrary dimension,” *Annales Henri Poincare* **13**, 399 (2012) doi:10.1007/s00023-011-0118-z [arXiv:1102.5759 [gr-qc]].
- [116] S. Speziale, “Boosting Wigner’s n_j -symbols,” *J. Math. Phys* **58**, no. 3, 032501 (2017) doi:10.1063/1.4977752 [arXiv:1609.01632 [gr-qc]].

APPENDICES

Appendix A

A.1 Gaussian Integration Techniques

In this appendix we compile a list of useful Gaussian spinor integrals. Consider first a standard Gaussian integral over the complex line \mathbb{C}

$$\int_{\mathbb{C}} \frac{d^2\alpha}{\pi^2} e^{-|\alpha|^2 + \bar{x}\alpha + y\bar{\alpha}} = e^{\bar{x}y}. \quad (\text{A.1})$$

This easily generalizes to a Gaussian integration over spinors on \mathbb{C}^2 with the Bargmann measure $d\mu(z) = \pi^{-2} e^{-\langle z|z \rangle} d^4z$ giving us the integral that allows us to contract strands on cable graphs

$$\int_{\mathbb{C}^2} d\mu(z) e^{\langle x|z \rangle + \langle z|y \rangle} = e^{\langle x|y \rangle}. \quad (\text{A.2})$$

It is interesting to note that this contraction also works with anti-holomorphic spinors $|z]$, since $[x|y] = \langle y|x \rangle$. We have thus

$$\int_{\mathbb{C}^2} d\mu(z) e^{\langle x|z \rangle + [z|y]} = e^{\langle x|y \rangle}. \quad (\text{A.3})$$

As with usual Gaussian integrations, we can calculate Gaussian spinor integrals of arbitrary polynomials. The special case worth mentioning is of course how delta function acts on holomorphic functions

$$\int_{\mathbb{C}^2} d\mu(z) f(z) e^{\langle z|w \rangle} = f(w). \quad (\text{A.4})$$

Let us now consider the integrals that are crucial to the computations in this thesis – integrals with a matrix A . First consider the more familiar case of integrals over vectors of n complex numbers

$$\int_{\mathbb{C}^n} \prod_{i=1}^n \frac{d^2\alpha_i}{\pi^2} e^{-\sum_{i,j} \bar{\alpha}_i A_{ij} \alpha_j} = \frac{1}{\det(A)} \quad (\text{A.5})$$

This again trivially extends to the integrals over spinors. The expression useful for our thesis is

$$\int_{\mathbb{C}^{2n}} \prod_{i=1}^n d\mu(z_i) e^{\sum_{i,j} \langle z_i | A_{ij} | z_j \rangle} = \frac{1}{\det(\mathbb{1} - A)}. \quad (\text{A.6})$$

Recall that for the constrained model we had to change the measure of integration over spinors to $d\mu_\rho(z) = (1 + \rho^2)^2 \pi^{-2} e^{-(1+\rho^2)\langle z|z \rangle} d^4z$. It is easy to check that this is normalized properly as

$$\int_{\mathbb{C}^2} \frac{(1 + \rho^2)^2 d^4z}{\pi^2} e^{-(1+\rho^2)\langle z|z \rangle} = 1. \quad (\text{A.7})$$

This change of measure leads to very simple changes to the above integrals. In particular, for a contraction we have

$$\int_{\mathbb{C}^2} d\mu_\rho(z) e^{\langle x|z \rangle + \langle z|y \rangle} = e^{(1+\rho^2)^{-1}\langle xy \rangle}. \quad (\text{A.8})$$

Hence for every contraction of spinors we pick up a factor of $1/(1 + \rho^2)$. Thus for a loop on which we have three spinors we get the factor of $(1 + \rho^2)^{-3}$ – this appears all the time in loop identity and Pachner moves calculations.

A.2 Mapping $SU(2)$ to spinors

Lemma A.2.1. *Let $f \in L^2(SU(2))$ be homogeneous of degree $2J$, i.e. $f(\lambda g) = \lambda^{2J} f(g)$. Given a spinor by $|z\rangle$ define $g(z) = (|0\rangle\langle 0| + |0\rangle[0|)g(z) = |0\rangle\langle z| + |0\rangle[z|$ where $|0\rangle = (1, 0)^t$. Then*

$$\int_{\mathbb{C}^2} d\mu(z) f(g(z)) = \Gamma(J + 2) \int_{SU(2)} dg f(g). \quad (\text{A.9})$$

Proof. We can relate the inner product (2.69) to the standard $L^2(SU(2))$ inner product by parameterizing the spinor as

$$|z\rangle = \begin{pmatrix} r \cos \theta e^{i\phi} \\ r \sin \theta e^{i\psi} \end{pmatrix}, \quad (\text{A.10})$$

where $r \in (0, \infty)$, $\theta \in [0, \pi/2)$, $\phi \in [0, 2\pi)$, $\psi \in [0, 2\pi)$. The Lebesgue measure in these coordinates is $d^4z = r^3 \sin \theta \cos \theta dr d\phi d\theta d\psi$. Now using the homogeneity property $f(g(z)) = r^{2J} f(\tilde{g}(z))$ we have

$$\int_{\mathbb{C}^2} d\mu(z) f(g(z)) = \int_0^\infty dr r^{3+2J} e^{-r^2} \int_0^{\pi/2} d\theta \sin \theta \cos \theta \int_0^{2\pi} d\phi \int_0^{2\pi} d\psi f(\tilde{g}(z)), \quad (\text{A.11})$$

where $\tilde{g}(z) \in \text{SU}(2)$. Performing the integral over r we get

$$\int dr r^{3+2J} e^{-r^2} = \frac{1}{2} \Gamma(J+2) \quad (\text{A.12})$$

and so

$$\int_{\mathbb{C}^2} d\mu(z) f(g(z)) = \Gamma(J+2) \int_{\text{SU}(2)} dg f(g), \quad (\text{A.13})$$

where dg is the normalized Haar measure on $\text{SU}(2)$. In our case J is an integer so $\Gamma(J+2) = (J+1)!$. \square

A.3 Group averaging the $\text{SU}(2)$ projector

In this appendix we recall the calculation in [98] which shows that we can perform the integration over g explicitly for the BF projector (2.80), which we prove in the following theorem.

Theorem A.3.1. *The projector (2.80) can be expressed as a power series in the holomorphic spinor invariants as*

$$P(z_i; w_i) = \sum_{[k]} \frac{1}{(J+1)!} \prod_{i < j} \frac{([z_i | z_j][w_i | w_j])^{k_{ij}}}{k_{ij}!}. \quad (\text{A.14})$$

where the sum is over sets of $n(n-1)/2$ non-negative integers k_{ij} with $1 \leq i < j \leq n$.

Proof. Expanding (2.80) in a power series

$$\int_{\text{SU}(2)} dg e^{[z_i | g | w_i]} = \sum_{j_i} \int dg \prod_i \frac{[z_i | g | w_i]^{2j_i}}{(2j_i)!}, \quad (\text{A.15})$$

we see that each term in the sum is homogeneous of degree $2J = \sum_i (2j_i)$. This fact allows us to use Lemma A.2.1 detailed in Appendix A.2 which says that we can replace the integral over $SU(2)$ with a Gaussian integral paying a factor of $1/(J+1)!$ as in

$$(J+1)! \int dg \prod_i \frac{[z_i|g|w_i]^{2j_i}}{(2j_i)!} = \int d\mu(\alpha) \prod_i \frac{([z_i|0]\langle\alpha|w_i\rangle + [z_i|0][\alpha|w_i])^{2j_i}}{(2j_i)!}. \quad (\text{A.16})$$

Now resum over j_i to get

$$\sum_{j_i} (J+1)! \int dg \prod_i \frac{[z_i|g|w_i]^{2j_i}}{(2j_i)!} = \int d\mu(\alpha) e^{\sum_i ([z_i|0]\langle\alpha|w_i\rangle + [z_i|0][\alpha|w_i])} = e^{\sum_{i,j} [z_i|0][0|z_j][w_i|w_j]}, \quad (\text{A.17})$$

where we've performed the Gaussian integration in the second equality. Using the anti-symmetry $[w_i|w_j] = -[w_j|w_i]$ and recognizing the identity $1 = |0\rangle\langle 0| + |0][0|$ in

$$\sum_{i,j} [z_i|0][0|z_j][w_i|w_j] = \sum_{i<j} [z_i(|0\rangle\langle 0| + |0][0|) |z_j\rangle[w_i|w_j] = \sum_{i<j} [z_j|z_i][w_i|w_j]. \quad (\text{A.18})$$

Finally we have

$$\sum_{j_i} (J+1)! \int dg \prod_i \frac{[z_i|g|w_i]^{2j_i}}{(2j_i)!} = e^{\sum_{i<j} [z_j|z_i][w_i|w_j]} = \sum_{[k]} \prod_{i<j} \frac{([z_i|z_j][w_i|w_j])^{k_{ij}}}{k_{ij}!} \quad (\text{A.19})$$

and since $J = \sum_{i<j} k_{ij}$ is just the total homogeneity of each term we can move the $(J+1)!$ to the RHS and complete the proof. \square

A.4 Proof of Lemma (4.4.1)

Proof. For a 2×2 matrix $2 \det M = \text{Tr}(M)^2 - \text{Tr}(M^2)$. If one consider $M = \mathbb{1} - \sum_i C_i |A_i\rangle[B_i|$, we have

$$\text{Tr}(M^2) = 2 - 2 \sum_i C_i [B_i|A_i] + \sum_{i,j} C_i C_j [B_i|A_j][B_j|A_i]$$

and

$$\text{Tr}(M)^2 = 4 - 4 \sum_i C_i [B_i|A_i] + \sum_{i,j} C_i C_j [B_i|A_i][B_j|A_j],$$

therefore

$$2 \det(M) = 2 - 2 \sum_i C_i [B_i|A_i] + \sum_{i,j} C_i C_j ([B_i|A_i][B_j|A_j] - [B_i|A_j][B_j|A_i])$$

and using $[A_i|B_i][B_j|A_j] - [A_i|B_j][B_i|A_j] = [A_i|A_j][B_j|B_i]$ gives the result. \square

A.5 The 4-simplex amplitude for the constrained propagator model

This appendix shows that in the constrained propagator model, the amplitude for a 4-simplex can be indeed written as (3.49). Starting from the constrained propagators (3.47), we can straightforwardly get that the spin foam amplitude for a single 4-simplex in the constrained propagator model is given by

$$\tilde{A}_\sigma = \int \prod_a d\mu_\rho(w_b^a) dg_a^{L,R} e^{\tau_{bR}^a [w_b^a | g_a^R | z_b^a] + \tau_{aR}^b \langle w_b^a | g_b^R | z_a^b \rangle + \tau_{bL}^a \rho^2 [w_b^a | g_a^L | z_b^a] + \tau_{aL}^b \rho^2 \langle w_b^a | g_b^L | z_a^b \rangle} \quad (\text{A.20})$$

where we have added a collection of τ 's which all have trivial values 1. However, under Taylor expansion, the power of τ gives the homogeneity of the corresponding term. For example, the first term in the exponent becomes

$$\sum_{j_a^R} \frac{(\tau_{bR}^a [w_b^a | g_a^R | z_b^a])^{2j_a^R}}{(2j_a^R)!}. \quad (\text{A.21})$$

We get similar expressions for all the different τ 's, which are raised to the appropriate powers in their series expansions,

$$(\tau_{bR}^a)^{2j_a^R}, (\tau_{bL}^a)^{2j_a^L}, (\tau_{aL}^b)^{2j_b^L}, (\tau_{aR}^b)^{2j_b^R}. \quad (\text{A.22})$$

The reason for temporarily introducing these factors of τ is that before we continue with the asymptotics, we have to reduce the action to the same number of variables, as in the DL model's one. To do this we have to integrate out the auxiliary contracting spinors w_a^b . We will see however, that this produces a mixing between the different spins, so the factors of τ keep track of the spin information. After the $|w\rangle$ integration, the amplitude becomes

$$\tilde{A}_\sigma = \int \prod_a dg_a^{L,R} e^{(1+\rho^2)^{-1} [z_b^a | (\tau_{bR}^a g_a^{R-1} + \rho^2 \tau_{bL}^a g_a^{L-1}) (\tau_{aR}^b g_b^R + \rho^2 \tau_{aL}^b g_b^L) | z_a^b]}. \quad (\text{A.23})$$

Expanding this expression in a power series we get again four terms, but with different expansion coefficients:

$$\begin{aligned} \tilde{A}_\sigma = & \int \prod_a dg_a^{L,R} \sum_{j_i} ([z_b^a | \tau_{bR}^a \tau_{aR}^b g_a^{R-1} g_b^R | z_a^b]^{2j_1} (\rho^4 [z_b^a | \tau_{bL}^a \tau_{aL}^b g_a^{L-1} g_b^L | z_a^b])^{2j_2} \times \\ & \times (\rho^2 [z_b^a | \tau_{bR}^a \tau_{aL}^b g_a^{R-1} g_b^L | z_a^b])^{2j_3} (\rho^2 [z_b^a | \tau_{aR}^b \tau_{bL}^a g_a^{L-1} g_b^R | z_a^b])^{2j_4}) / \prod_i (2j_i)! (1 + \rho^2)^{2j_i}. \end{aligned} \quad (\text{A.24})$$

By comparing the coefficients of the power expansion of the different τ 's in Eqs. (A.22) and (A.24), we find that j_i and $j_{a,b;L,R}$ are related by the following set of equations:

$$\begin{cases} j_1 + j_3 = j_a^R \\ j_1 + j_4 = j_b^R \\ j_2 + j_4 = j_a^L \\ j_2 + j_3 = j_b^L. \end{cases} \quad (\text{A.25})$$

Note now that in the large z limit the holomorphic simplicity constraints imply that we have $(j_a^L, j_b^L) = \rho^2(j_a^R, j_b^R)$, which allows us to eliminate one of the spins and leads to an important relation for the asymptotic analysis:

$$j_3 = j_4, \quad j_a^R = j_b^R := j_{ab}^R, \quad j_a^L = j_b^L := j_{ab}^L \quad (\text{A.26})$$

In the main text we define $J_{ab} \equiv j_3$. After the τ 's have completed their mission, we can discard them by setting their values back to 1. Thus we have proved that the amplitude is indeed (3.49).

A.6 Explicit calculation of the Constrained Loop Identity

In this appendix we explicitly show how to calculate the constrained loop identity (5.11). Let us consider the loop composed of two pairs of partially gauge-fixed propagators $\mathbb{1}_\rho \circ \mathbb{1}_\rho$ and one pair of propagators $P_\rho \circ P_\rho$. To calculate this loop, let us use the homogenized propagators $\mathbb{1}_{\tilde{\tau}} \circ \mathbb{1}_{\tilde{\tau}}$ and $G_\tau \circ G_\tau$ instead and at the end of the calculation use the homogeneity maps (5.9) and (5.10), which we recall are given by

$$\mathbb{1}_{\tilde{\tau}} \circ \mathbb{1}_{\tilde{\tau}} = e^{\tilde{\tau} \sum_i [\tilde{z}_i | \tilde{w}_i]} \quad \text{with} \quad \tilde{\tau}^J \rightarrow \frac{F_\rho(J/2)^2}{(1 + \rho^2)^J} \quad \text{for} \quad \mathbb{1}_{\tilde{\tau}} \circ \mathbb{1}_{\tilde{\tau}} \rightarrow \mathbb{1}_\rho \circ \mathbb{1}_\rho$$

for a pair of gauge-fixed propagators and by

$$G_\tau \circ G_\tau = e^{\tau \sum_{i < j} [z_i | z_j] [w_i | w_j]} \quad \text{with} \quad \tau^J \rightarrow \frac{F_\rho(J)^2}{(1 + \rho^2)^{2J} (J + 1)!} \quad \text{for} \quad G_\tau \circ G_\tau \rightarrow P_\rho \circ P_\rho.$$

for the pair of propagators P_ρ . We will also insert a face weight by tracking the homogeneity of spin in the loop by a factor of τ' . The contractions of the spinors around the loop are as follows: $|w_4\rangle = |\tilde{w}_4^2\rangle$, $|\tilde{z}_4^2\rangle = |\tilde{z}_4^1\rangle$ and $|\tilde{w}_4^1\rangle = |z_4\rangle$. The cable diagram with all the labels is shown in Fig. A.1.

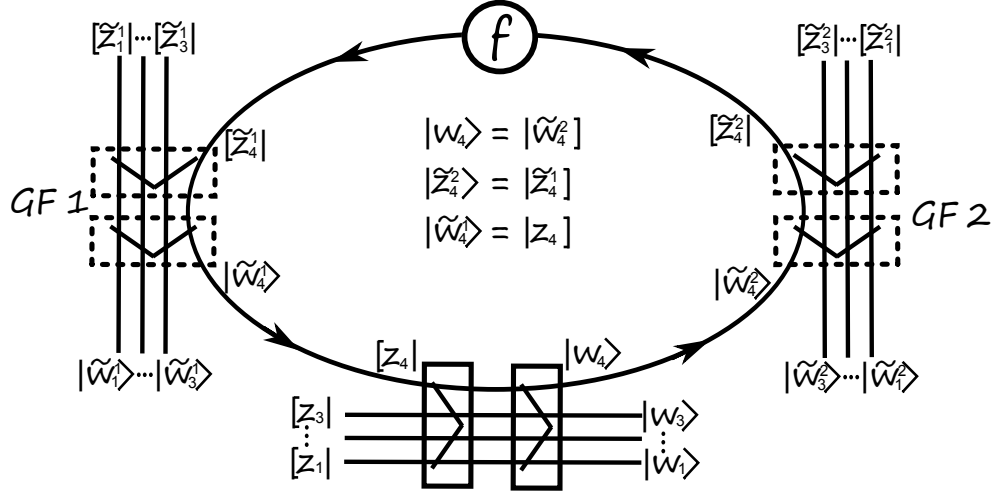


Figure A.1: Cable diagram with all the labels for the constrained loop identity.

We can thus finally calculate the loop identity:

$$\begin{aligned}
& \int d\mu_\rho(z_4, w_4, \tilde{z}_4^1) G_\tau^2(z_1, \dots, \tau' z_4; w_1, \dots, \tilde{w}_4^2) \mathbb{1}_{\tilde{\tau}_1}^2(\tilde{z}_1^1, \dots, \tilde{z}_4^1; \tilde{w}_1^1, \dots, \tilde{z}_4) \mathbb{1}_{\tilde{\tau}_2}^2(\tilde{z}_1^2, \dots, \tilde{z}_4^1; \tilde{w}_1^2, \dots, \tilde{w}_4^2) \\
&= \frac{e^{\tau \sum_{i<j<4} [z_i|z_j]\langle w_i|w_j\rangle + \sum_{i<4} \tilde{\tau}_1 [\tilde{z}_i^1|\tilde{w}_i^1] + \tilde{\tau}_2 [\tilde{z}_i^2|\tilde{w}_i^2]}}{1 - \frac{\tau \tilde{\tau}_1 \tilde{\tau}_2 \tau'}{(1+\rho^2)^3} \sum_{i<4} [z_i|w_i] + \left(\frac{\tau \tilde{\tau}_1 \tilde{\tau}_2 \tau'}{(1+\rho^2)^3}\right)^2 \sum_{i<j<4} [z_i|z_j]\langle w_i|w_j\rangle} \\
&= \exp\left(\tau \sum_{i<j<4} [z_i|z_j]\langle w_i|w_j\rangle + \sum_{i<4} \tilde{\tau}_1 [\tilde{z}_i^1|\tilde{w}_i^1] + \tilde{\tau}_2 [\tilde{z}_i^2|\tilde{w}_i^2]\right) \times \\
&\quad \times \sum_{N,M} \frac{(N+M)!}{N!M!} \left(\frac{\tau \tilde{\tau}_1 \tilde{\tau}_2 \tau'}{(1+\rho^2)^3}\right)^{N+2M} \left(\sum_{i<4} [z_i|w_i]\right)^N \left(-\sum_{i<j<4} [z_i|z_j]\langle w_i|w_j\rangle\right)^M.
\end{aligned}$$

The factor of $1/(1+\rho^2)^3$ arises from the three spinor integrations. Compared to the toy loop, the result is thus an exchange of $\frac{\tau\tau'}{1+\rho^2} \rightarrow \frac{\tau\tilde{\tau}_1\tilde{\tau}_2\tau'}{(1+\rho^2)^3}$ and the addition of the trivial propagation of the gauge-fixed strands. Before we can use the homogeneity maps we have

to expand the exponentials in a power series. Doing this we arrive at

$$\sum_{A,B,C,M,N} \frac{(-1)^M (N+M)!}{A!B!C!M!N!} \left(\frac{\tau \tilde{\tau}_1 \tilde{\tau}_2 \tau'}{(1+\rho^2)^3} \right)^{N+2M} \tilde{\tau}_1^A \tilde{\tau}_2^B \tau^C \times$$

$$\times \left(\sum_{i<4} [\tilde{z}_i^1 | \tilde{w}_i^1] \right)^A \left(\sum_{i<4} [\tilde{z}_i^2 | \tilde{w}_i^2] \right)^B \left(\sum_{i<4} [z_i | w_i] \right)^N \left(\sum_{i<j<4} [z_i | z_j] [w_i | w_j] \right)^{M+C}.$$

Relabeling $N \rightarrow J$ and $M+C \rightarrow J'$ and using the above homogeneity maps for $\tau, \tilde{\tau}_1, \tilde{\tau}_2$ and $\tau'^{2j} \rightarrow (2j+1)^\eta$, we recover the result for the constrained loop identity (5.11).

A.7 Mixing of spins in DL model

Here we prove the statement that in the DL propagator left and right spins mix. To see this, let us take the gauge fixed DL propagator (5.15) and write it as

$$\int \left\{ \prod_{i=1}^4 d\mu_\rho(z_i) \right\} \prod_i \tau_{w_i L}^{2j_L^{w_i}} \frac{[w_i^L | z_i]^{2j_L^{w_i}}}{(2j_L^{w_i})!} \tau_{w_i R}^{2j_R^{w_i}} \frac{[w_i^R | z_i]^{2j_R^{w_i}}}{(2j_R^{w_i})!} \tau_{v_i L}^{2j_L^{v_i}} \frac{\langle z_i | v_i^L \rangle^{2j_L^{v_i}}}{(2j_L^{v_i})!} \tau_{v_i R}^{2j_R^{v_i}} \frac{\langle z_i | v_i^R \rangle^{2j_R^{v_i}}}{(2j_R^{v_i})!} \quad (\text{A.27})$$

We have inserted τ 's in front of every term to keep track of the all the spins. Now, performing the integrals over the $|z_i\rangle$ spinors, we get the following (rather easy to guess) exponentiated expression for the gauge-fixed propagator

$$e^{(1+\rho^2)^{-1} \sum_i \tau_{w_i L} \tau_{v_i L} [w_i^L | v_i^L] + \rho (\tau_{w_i L} \tau_{v_i R} [w_i^L | v_i^R] + \tau_{w_i R} \tau_{v_i L} [w_i^R | v_i^L]) + \rho^2 \tau_{w_i R} \tau_{v_i R} [w_i^R | v_i^R]}. \quad (\text{A.28})$$

To see the relations between spins, let us now yet again expand this in a power series. Each of the terms in the expansion can be written as

$$\prod_i \frac{(\tau_{w_i L} \tau_{v_i L} [w_i^L | v_i^L])^{2j_i^1}}{(2j_i^1)!} \frac{(\rho \tau_{w_i L} \tau_{v_i R} [w_i^L | v_i^R])^{2j_i^2}}{(2j_i^2)!} \frac{(\rho \tau_{w_i R} \tau_{v_i L} [w_i^R | v_i^L])^{2j_i^3}}{(2j_i^3)!} \frac{(\rho^2 \tau_{w_i R} \tau_{v_i R} [w_i^R | v_i^R])^{2j_i^4}}{(2j_i^4)!} \quad (\text{A.29})$$

Comparing now the powers of τ 's from Eq. (A.27) and Eq. (A.29), we get the following relations between the spins

$$\begin{cases} j_L^{w_i} &= j_i^1 + j_i^2 \\ j_R^{w_i} &= j_i^3 + j_i^4 \\ j_L^{v_i} &= j_i^1 + j_i^3 \\ j_R^{v_i} &= j_i^2 + j_i^4 \end{cases} \quad (\text{A.30})$$

It is easy to see that we cannot solve for $(j_i^1, j_i^2, j_i^3, j_i^4)$ in terms of $(j_L^{w_i}, j_R^{w_i}, j_L^{v_i}, j_R^{v_i})$. Also obviously we have $j_{L,R}^{w_i} \neq j_{L,R}^{v_i}$. It is true however that $j_L^{w_i} + j_R^{w_i} = j_L^{v_i} + j_R^{v_i}$ is always satisfied.

A.8 Arbitrary face weight in DL model

In order to have a face weight in the DL model that depends on arbitrary combinations of j^L and j^R , we need to introduce four τ s into the Eq. (5.23) as follows:

$$\begin{aligned}
& \int d\mu(w_4^L) d\mu(w_4^R) e^{\tau_1[w_4^L|M_L|w_4^L] + \tau_2[w_4^R|M_R|w_4^R] + \tau_3[w_4^L|\rho M_L|w_4^R] + \tau_4[w_4^R|\frac{M_R}{\rho}|w_4^L]} \\
&= \left\{ 1 - \tau_1 \left(\text{Tr}(M_L) - \tau_1 \det(M_L) \right) - \tau_2 \left(\text{Tr}(M_R) - \tau_2 \det(M_R) \right) + \tau_3^2 \tau_4^2 \det(M_L) \det(M_R) \right. \\
&\quad + \tau_1 \tau_2 \left(\text{Tr}(M_L) - \tau_1 \det(M_L) \right) \left(\text{Tr}(M_R) - \tau_2 \det(M_R) \right) - \tau_3 \tau_4 \left(\text{Tr}(M_L M_R) - \right. \\
&\quad \left. \left. - \tau_1 \det(M_L) \text{Tr}(M_R) - \tau_2 \det(M_R) \text{Tr}(M_L) + 2\tau_1 \tau_2 \det(M_L) \det(M_R) \right) \right\}^{-1}.
\end{aligned} \tag{A.31}$$

This is rather complicated, but allows for insertions of arbitrary face weights.

A.9 Justification for the nonlocality

Here we explain a bit more the reason why the amplitude after the 4–1 Pachner move (and by extension the 5–1 move) cannot be written as a local product of propagators. Let us compare the powers of τ s in the expression for $f_{\tau_A \tau_B \tau_C \tau_D}(n_1, \dots, n_7)$ in Eq. (7.9) to the additional factor for the amplitude after the Pachner move in Eq. (7.12). To simplify this, let us perform some relabelling. Let

$$\begin{cases} n_1 + n_2 + n_3 = A \\ n_1 + n_2 + n_4 = B \\ n_1 + n_3 + n_4 = C \\ n_2 + n_3 + n_4 = D \\ n_5 + n_6 + n_7 = X \end{cases} \tag{A.32}$$

We then have that

$$f_{\tau_A \tau_B \tau_C \tau_D}(n_1, \dots, n_7) = \tau_A^{A+X} \tau_B^{B+X} \tau_C^{C+X} \tau_D^{D+X}. \tag{A.33}$$

The additional factor from the Pachner move is on the other hand given by

$$\left((\tilde{\tau}_1^2)^{B+X} (\tilde{\tau}_2^2)^{C+X} (\tilde{\tau}_3^2)^{D+X} \tau_4^{\frac{2B+2D-A-C}{3}+X-n_5} \tau_5^{\frac{2B+2C-A-D}{3}+X-n_6} \tau_6^{\frac{2C+2D-A-B}{3}+X-n_7} \right)^L. \quad (\text{A.34})$$

If the amplitude could be rewritten into a product of four propagators, we would have to absorb these additional three $\tilde{\tau}$ s and three τ s into the τ_A, \dots, τ_D . While the $\tilde{\tau}$ s look promising, the τ_4, τ_5, τ_6 each depend on an additional parameter n_5, n_6 and n_7 respectively. If these τ s carried nice multiplicative functions, like an exponential, then we could absorb their combination, since $n_5 + n_6 + n_7 = X$. Alas, we have $\tau^J \mapsto F_\rho(J)^2 (J+1)^{\eta-1} (1+\rho^2)^{-5J}$ and both the $(J+1)^{\eta-1}$ and the hypergeometric function do not factorize nicely. This is even true in the large spin limit.

There are simply not enough free parameters in the propagators to absorb this additional factor in a symmetric way. The only alternative could be to allow each strand carry its own τ and allow for asymmetric results.